Morphological modelling of ebb and flood channel systems in estuaries

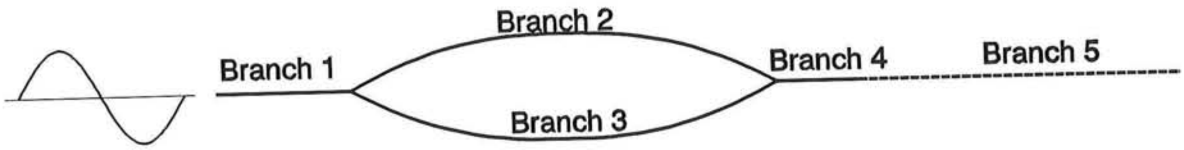

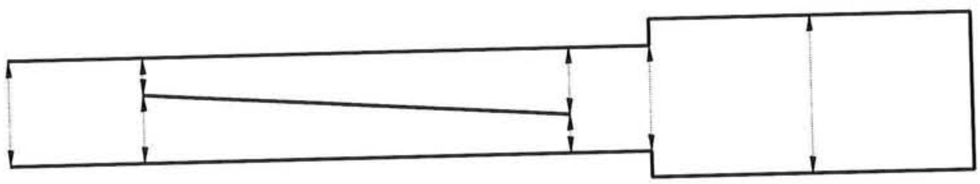

by

J.D.M. van Kerckhoven

Supervisors: Prof.dr.ir. M. de Vries
Dr.ir. Z.B. Wang
Ir. A. Langerak
Dr. R.J. Fokkink

Preface

This report is a presentation of the research done for the completion of my MSc. thesiswork at the Delft University of Technology, Department of Civil Engineering.
The topic involved is the problem of the morphological behaviour of ebb and flood channel systems. The problem is closely associated with the problem of bifurcations in rivers, a subject that has been studied in previous research e.g. Fokkink & Wang, 1993, Dekker & Voorthuizen, 1994 and Roosjen & Zwanenburg, 1995.

I would like to express my gratitude to all who supported me and especially the members of my examination committee. First of all Prof.dr.ir. M. de Vries and Dr.ir. Z.B. Wang of the Delft University and ir. A. Langerak of the Ministry of Public Works and Transport (RWS, RIKZ). Further I would like to thank Dr. R.J. Fokkink for this help with the SOBEK computations.

Delft, December 1995
Jos van Kerckhoven

Summary

Introduction

The morphological behaviour of estuaries is complex and at present (1995) not well understood. Ebb and flood channels play an important role in the morphological behaviour of an estuary.
In order to get more insight in the morphological behaviour of such systems it is studied whether a 1-D morphodynamic network model gives insight in this problem. This insight can be important for e.g. maintenance dredging, river training, and the design of navigation channels.

Approach

As in estuaries a static equilibrium profile cannot be defined, first a condition for a dynamic equilibrium profile is derived. Next the dynamic equilibrium of a short basin is analysed with a single-channel and a simple two-channel model on an analytical base. Subsequently the ebb and flood channel system 'Pas van Terneuzen - Everingen' of the Western Scheldt is taken as a reference case and the available data is gathered.
Finally the reference case is schematised to a numerical model. In this model the morphological development is considered.
In the numerical model the following scenarios are worked out.

1. The gradual change in width of the ebb and flood channels along the channels
2. A constant width of the ebb and flood channels
3. A Chézy coeffcient which depends on the flow direction
4. Different lengths of the ebb and flood channels
5. Combination of scenarios 1 and 3
6. As scenario 5 with a different phase difference between the M_2 and M_4 component at the seaside boundary

Conclusions

<u>dynamic equilibrium profile:</u>

- As the bed profile is continuously in motion, a static equilibrium profile cannot be defined. However, a bed profile is a dynamic equilibrium profile when the net sediment transport is equal for every cross-section.

About the short basin as single-channel model and a two-channel model:

<u>single-channel model:</u>

- In the single-channel model only a net sediment transport occurs when a number of small factors are taken into account. The most important factor is the seaside boundary condition which contains at least the M_2 and M_4 component.

- The single-channel model will only lead to a trivial solution, viz. a filled basin as result of the closed boundary condition at the end of the basin. However, a quasi-dynamic equilibrium can be defined.

two-channel model:

- The two channel model leads to a well defined dynamic equilibrium profile. The closed boundary condition does not influence the equilibrium as a result of horizontal circulation.
- The two channel model leads to a well defined dynamic equilibrium profile without taking into account a number of small factors. At the seaside boundary only the M_2 component is required.

available data of the reference case 'Pas van Terneuzen - Everingen':

- The net volume of water over a tidal period can not be determined as a result of the errors in the measurements.
- The net sediment transport is even more difficult to determine.
- To schematise a specific ebb and flood channel is difficult as the geometry is very complex.

computational results:

- The change of width of the ebb and flood channels is an important parameter for the morphological development of the channel system. For a flood channel with an increasing width from seaside to landside a linear inclining bed profile develops. For an ebb channel with a decreasing width from seaside to landside a nearly horizontal bed profile develops.
- As a result of the Chézy coefficient, which depends on the flow direction, the bed slope of the flood channel becomes smaller and the bed slope of the ebb channel becomes larger. The volumes of water that pass through the ebb and flood channels change significantly.
  When the difference between the Chézy coefficients during ebb and flood is large compared to the convective term in the momentum equation the M_2 component at the seaside boundary generates M_4.
- The phase difference between the M_2 and M_4 components at the seaside boundary is an important parameter as this determines the magnitude and direction of the net sediment transport. This net sediment transport can be split up in a symmetric and an asymmetric part over the ebb and flood channels. When the asymmetric part is larger than the symmetric part circulation of net sediment transport occurs.
- The length of the channels is another important parameter. The longest channel becomes shallow.

Contents

1 Introduction

1.1 General

The morphological behaviour of estuaries is complex and at present (1995) not well understood. Within the complex system of estuaries ebb and flood channels (always) occur.
In contrast to many river problems an equilibrium bottom profile is hard to define for estuary problems. In estuaries a dynamic equilibrium profile can be defined as the averaged bed profile over a long period, providing the net sediment transport over the tidal period for that profile is the same for every cross-section. Within this equilibrium profile ebb and flood channels play an important role.
In order to get more insight in this phenomenon, the morphological behaviour of a simple ebb and flood channel system is analysed.

1.2 Description of the problem

In the Western Scheldt many ebb and flood channels are found. This estuary is an important entrance to the Antwerp harbour (Belgium), see Figure 1-1.
Insight where bars and shallows occur can be important e.g. for maintenance dredging, river training and design of navigation channels.
The relevance of the present study is thus illustrated.

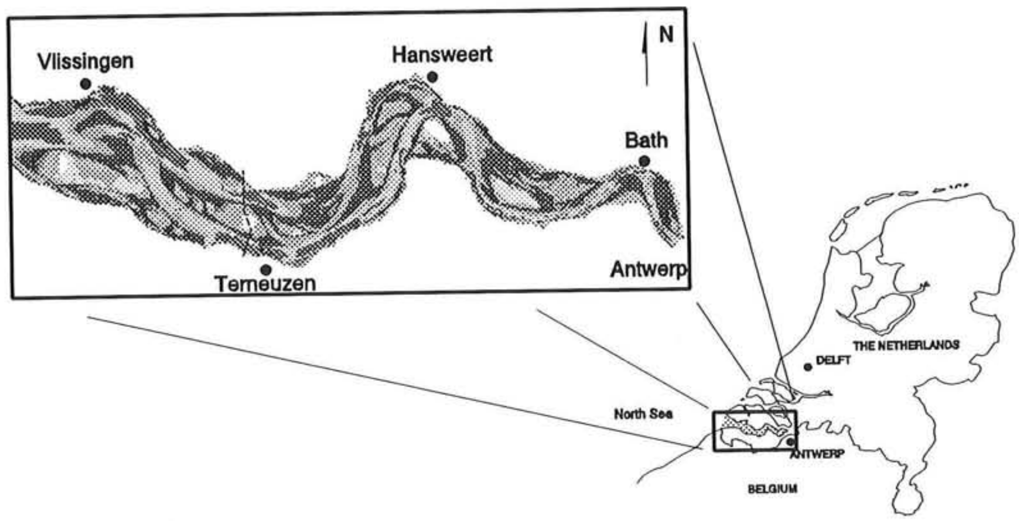

Figure 1-1: Western Scheldt

1.3 Goal of the study

In this study an existing ebb and flood channel system is schematised. The morphological behaviour of this schematised system is studied by changing several factors which influence the morphological processes. Studied factors are: change of the width, a Chézy coefficient that depends on the flow direction, the combination of the M_2- and M_4-tides at the open boundary and different lengths of the channels.

1.4 Restrictions of the study

In this study a number of important assumptions are made, viz.:

1. profile averaged parameters are used (1-D model).
2. the estuary is assumed to be well mixed, no density currents are taken into account.
3. the morphological development is current driven. There is no influence of wind or waves.
4. only M_2 and higher frequency components are taken into account (no neap-spring tides).
5. non-erodible banks, morphological changes only effect the bed level.
6. sediment transport depends on the local hydraulic conditions only.
7. Coriolis acceleration is neglected.
8. effects of bends are not taken into account.

1.5 Outline of the report

In Chapter 2 of this report a condition for a dynamic equilibrium profile is derived. Chapter 3 is concerned with a dynamic equilibrium profile for a simple single-channel model, whilst Chapter 4 deals with the dynamic equilibrium profile of a simple two-channel model. Chapter 5 describes an ebb and flood channel system in the Western Scheldt viz., 'Pas van Terneuzen - Everingen'. In Chapter 6 this ebb and flood channel system is schematised into a simple model. Chapter 7 deals with morphodynamic computations with SOBEK. In Chapter 8 conclusions and recommendations are given.

2 Condition for a dynamic equilibrium profile

2.1 General

The profile of the bed in a tidal or non-tidal river is continuously in motion. As a consequence a static equilibrium profile cannot be defined.
However, if a bed profile is defined as the averaged bed profile over a long time P, the averaged profile can be considered as a dynamic equilibrium profile.

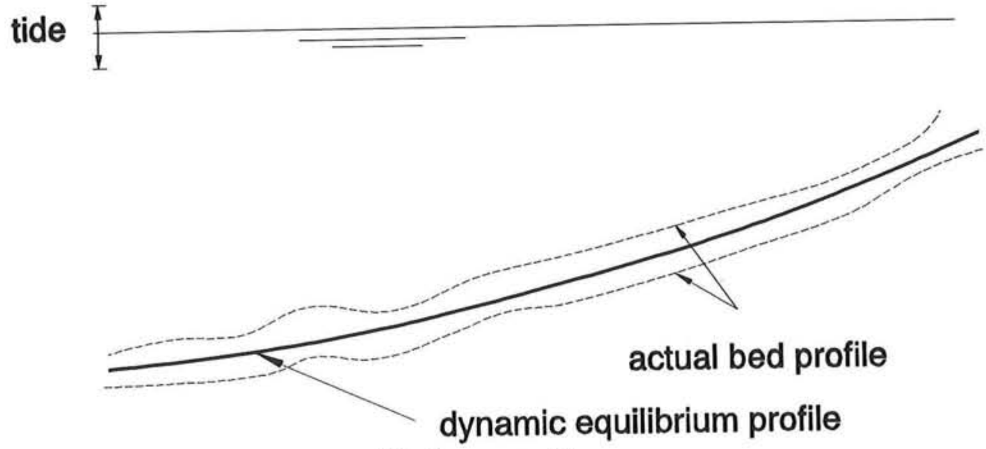

Figure 2-1: Dynamic equilibrium profile

In a period of less sediment supply (less sediment supply from upstream), erosion will occur and the actual bed profile is situated under the dynamic equilibrium profile. In a period of much sediment supply (much sediment supply from upstream), sedimentation will occur and the actual bed profile is situated above the dynamic equilibrium profile. Van Velzen (1986) derived along these lines a condition for a dynamic equilibrium profile, which is presented in the following Sections.

2.2 Basic equations

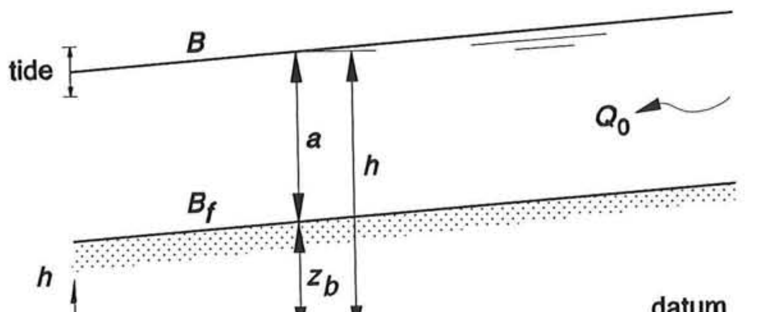

Figure 2-2: Definition sketch

The equilibrium profile is determined by four equations.
For a one-dimensional system the water motion is described mathematically by the following two equations:

continuity: $$B\frac{\partial h}{\partial t} + \frac{\partial Q}{\partial x} = 0 \tag{2.1}$$

momentum: $$\frac{\partial Q}{\partial t} + \frac{\partial Qu}{\partial x} + gaB_f\frac{\partial h}{\partial x} + g\frac{Q|Q|}{C^2a^2B_f} = 0 \tag{2.2}$$

The sediment motion is described mathematically by the following two equations:

mass-balance: $$B_f\frac{\partial z_b}{\partial t} + \frac{\partial S}{\partial x} = 0 \tag{2.3}$$

transport: $$S = B_f f(u,\ C,\ a,\ D_{50},\ ....) \tag{2.4}$$

herein:

a = water depth	[m]
t = time	[s]
u = flow velocity	[m/s]
Q = discharge	[m³/s]
x = horizontal spatial coordinate	[m]
g = acceleration of gravity	[m/s²]
z_b = bed level	[m]
C = Chézy-coefficient	[m½/s]
S = sediment transport	[m³/s]
f = a function representing a sediment transport formula	[m²/s]
B = storage width	[m]
B_f = flow width	[m]

2.3 Condition for dynamic equilibrium

This system of four partial differential equations (2.1) ... (2.4) describes the actual morphodynamic development.
To obtain a dynamic equilibrium profile the mass-balance equation for sediment, equation (2.3), has to be integrated over a long time P.

$$B_f\int_0^P\frac{\partial z_b}{\partial t}\,\mathrm{d}t + \frac{\partial}{\partial x}\int_0^P S\,\mathrm{d}t = 0 \tag{2.5}$$

The sediment transport S is a function of the flow velocity (u). The flow velocity (u) itself contains two components, the tidal motion and the river discharge. The river discharge generally depends on the season and the tide depends on the lunar and solar motion. Both can be represented by a probability density function.

Thus the sediment transport S can be represented by a probability density function (*cf.* Section 2.4).
If the sediment transport S is regarded as a stochastic variable and the time P is long enough then equation (2.5) reads:

$$B_f \int_0^P \frac{\partial z_b}{\partial t}\,\mathrm{d}t + \frac{\partial}{\partial x}\,\bar{S}P = 0 \tag{2.6}$$

Where $\bar{S}$ is the averaged sediment transport. The averaged sediment transport in turn is defined as:

$$\bar{S} = \int_{-\infty}^{+\infty} S\,\mathrm{f}\{S\}\mathrm{d}S \tag{2.7}$$

herein: $\mathrm{f}\{S\}$ = probability density function

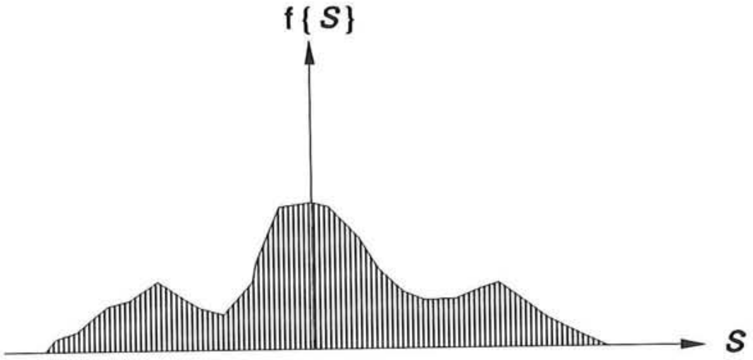

Figure 2-3: Example of probability density function

Substitution of equation (2.7) in (2.6) gives:

$$B_f \int_0^P \frac{\partial z_b}{\partial t}\,\mathrm{d}t + P\,\frac{\partial}{\partial x}\int_{-\infty}^{+\infty} S\,\mathrm{f}\{S\}\mathrm{d}S = 0 \tag{2.8}$$

A profile is a dynamic equilibrium profile, if for a time P, which is long enough, the condition holds:

$$\int_0^P \frac{\partial z_b}{\partial t}\,\mathrm{d}t = z_b(x,P) - z_b(x,0) = 0 \tag{2.9}$$

hence

$$\frac{\partial}{\partial x}\int_{-\infty}^{+\infty} S\,\mathrm{f}\{S\}\mathrm{d}S = 0 \tag{2.10}$$

If a profile fulfils this condition the profile is regarded as a dynamic equilibrium profile. The condition is fulfilled when the averaged (net) sediment transport through every cross-section is equal.
From equation (2.9) it can be seen that the dynamic equilibrium profile is a periodic phenomenon.

2.4 Sediment transport probability density function

The probability density function $f\{S\}$ in equation (2.10) is not known beforehand. Therefore the condition for a dynamic equilibrium profile cannot be applied.
In order to approximate the probability density function $f\{S\}$ two assumptions are made:

1. The river discharge Q_0 can be regarded as quasi-steady ($\frac{\partial Q_0}{\partial x} = 0$).
2. The (tidal) motion at the river mouth can then be represented by a repetitive function ($f(t) = f(t+n \cdot T)$) with a period T.

The probability density function can thus be approximated by:

$$f\{S\} = \left(\int_0^T S \, dt\right) f\{Q_0\}$$

herein: $f\{Q_0\}$ = probability density function of the river discharge.

The net sediment transport over one tidal period is defined as $\int_0^T S \, dt$

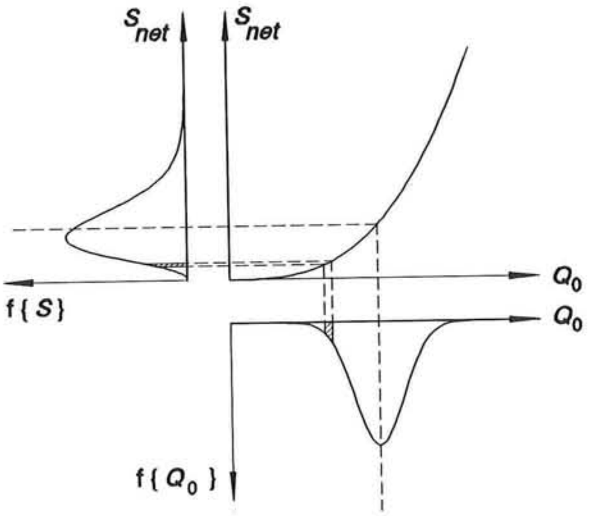

Figure 2-4: Example of net sediment transport probability density function

The condition for a dynamic equilibrium profile now reads:

$$\frac{\partial}{\partial x}\left[\int_0^{\infty}\left\{\left(\int_0^T S \, dt\right) f\{Q_0\}\right\} dQ_0\right] = 0 \tag{2.11}$$

Two extremes can be distinguished viz.:

1. The river discharge Q_0 is constant, $f\{Q_0 = \text{const}\} = 1$
   equation (2.11) then reduces to:

$$\frac{\partial}{\partial x}\left[\int_0^T S \, \mathrm{d}t\right] = 0 \qquad (2.12)$$

2. No tidal influence is present, $T=0$ (non-tidal rivers).
   equation (2.11) then reduces to:

$$\frac{\partial}{\partial x}\left[\int_0^\infty \{\, S(Q_0)\ f\{Q_0\}\,\}\ \mathrm{d}Q_0\right] = 0 \qquad (2.13)$$

2.5 Conclusions

From the previous Sections it can be concluded that a profile is in dynamic equilibrium if the following equations are satisfied:

$$B\frac{\partial h}{\partial t} + \frac{\partial Q}{\partial x} = 0 \qquad (2.14)$$

$$\frac{\partial Q}{\partial t} + \frac{\partial Qu}{\partial x} + gaB_f\frac{\partial h}{\partial x} + g\frac{Q|Q|}{C^2a^2B_f} = 0 \qquad (2.15)$$

$$\frac{\partial}{\partial x}\left[\int_0^\infty \left\{ (\int_0^T S \ \mathrm{d}t\,) f\{Q_0\} \right\} \ \mathrm{d}Q_0\right] = 0 \qquad (2.16)$$

$$S = B_f f(u,\ C,\ a,\ D_{50},\ ....) \qquad (2.17)$$

In the equations (2.14) ... (2.17) one assumption is made. In the continuity- and momentum equation for water and mass-balance equation for sediment, it is assumed that the profile does not differ too much from the dynamic equilibrium profile. It is expected that the error, as a result of the variable actual profile, is negligible.
Applying these assumptions and sufficient boundary conditions, to a tidal or non-tidal system, a dynamic equilibrium profile can be derived.

3 A simple single-channel model

3.1 General

Wang (1992) analysed a dynamic equilibrium profile for a simple single-channel model. This model contains a short basin compared to the length of the tidal wave. This model is presented partly in this Chapter.
First, in Section 3.2, a simple model is considered which contains only one tidal component at the boundary, viz. the M_2 component. It will be shown that there is no net sediment transport over a tidal period, thus any bathymetry is a dynamic equilibrium profile.
Later, in Section 3.3, the simple model will be extended to obtain a net sediment transport in order to define a more realistic dynamic equilibrium profile. This is achieved by taking five factors into account: the down-slope effect, phase-lag between discharge and water depth, tidal distortion, relaxation in time and incipient motion.
Finally, in Section 3.4, the morphological development of a single-channel basin is considered.
For the sake of simplicity only a small tidal basin is considered.

3.2 Simple single-channel model

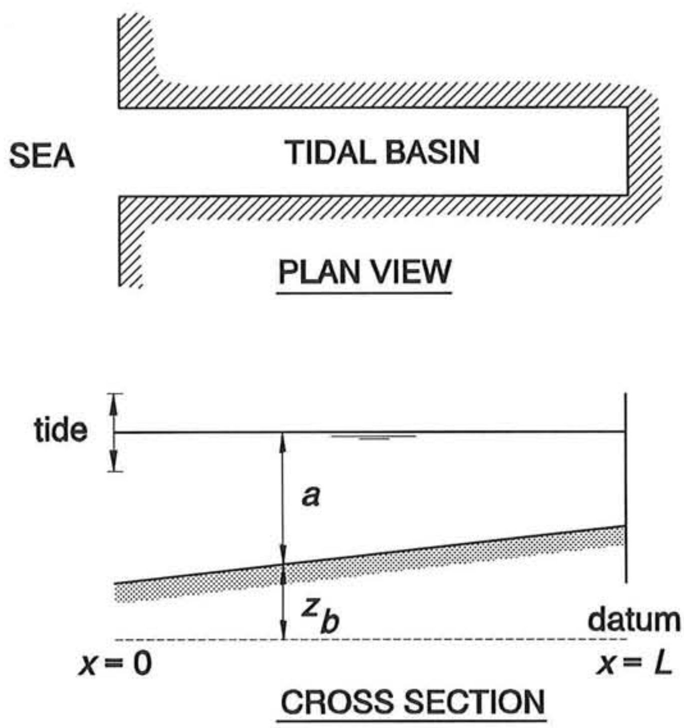

Figure 3-1: Definition sketch

The tidal basin has a constant width, so the system of equations (2.1) ... (2.4) can be rewritten to:

$$\frac{\partial a}{\partial t} + \frac{\partial u a}{\partial x} = 0 \qquad (3.1)$$

$$\frac{\partial u}{\partial t} + u\frac{\partial u}{\partial x} + g\frac{\partial a}{\partial x} + g\frac{\partial z_b}{\partial x} + g\frac{u|u|}{C^2 a} = 0 \qquad (3.2)$$

$$\frac{\partial z_b}{\partial t} + \frac{\partial s}{\partial x} = 0 \qquad (3.3)$$

$$s = \mathrm{f}(u,\ C,\ a,\ D_{50},\ ....) \qquad (3.4)$$

The system of equations (3.1) ... (3.4) is still too complex to handle analytically if a tidal river problem is studied.

To simplify the problem further, the following four assumptions are made:

1. The length of the tidal basin is less than 1/20 of the length of the tidal wave, so the 'storage basin consideration' can be applied.
2. The sediment transport rate depends only on the local flow velocity and the transport equations for steady-state sand transport can be applied.
   Well-known formulae are given by Meyer-Peter Müller (1948), Engelund Hansen (1967), Einstein Brown (1950) and Van Rijn (1984).
   These equations are simplified to: $s = mu^n$
   If $n=5$ and the proper value for m is applied, the Engelund Hansen formula results.
3. Only one single rectangular channel is considered.
4. No tidal flats are taken into account.

Due to assumption 1. the water level in the whole region may be approximated as horizontal. The level in this case is a time dependent sine function as a result of the applied boundary conditions:

for $x=0$: $z_s = H \sin(\omega t)$

At the end of the basin a closed boundary is applied:

for $x=L$: $q(t) = 0$

herein:

z_s	= water level measured from the average water level	[m]
H	= tidal amplitude	[m]
ω	= frequency of the tide	[rad s^{-1}]
q	= discharge	[$m^3 s^{-1} m^{-1}$]

The water depth as function of time and space then reads:

$$a(x,t) = a_0(x) + H\sin(\omega t) \tag{3.5}$$

where $a_0(x)$ is the mean water-depth.

The water discharge as a function of time and space then follows from the continuity equation:

$$q(x,t) = \frac{\partial z_s}{\partial t}(L-x) \quad \text{or}$$

$$q(x,t) = \omega(L-x)H\cos(\omega t) \tag{3.6}$$

So the flow velocity is:

$$u(x,t) = \frac{q(x,t)}{a(x,t)} = \frac{\omega(L-x)H\cos(\omega t)}{a_0(x) + H\sin(\omega t)} \tag{3.7}$$

The instantaneous sediment transport rate follows from the power law:

$$s = mu^n$$

$$s(x,t) = m\left(\frac{\omega(L-x)H\cos(\omega t)}{a_0(x) + H\sin(\omega t)}\right)^n \tag{3.8}$$

The functions $u' = \dfrac{u}{\omega(L-x)}$ and $s' = \dfrac{s}{m(\omega(L-x))^n}$ are normalised by dividing them by respectively $u'(x,0)$ and $s'(x,0)$.

The functions are shown in following figures.

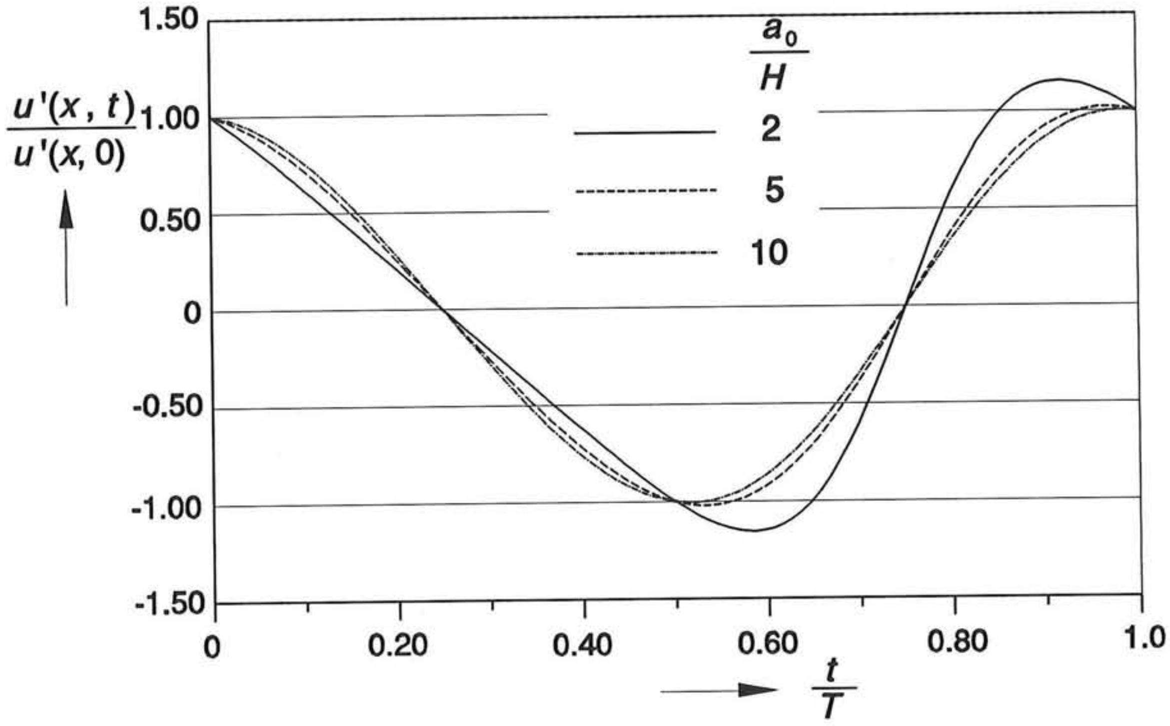

Figure 3-2: Flow velocity

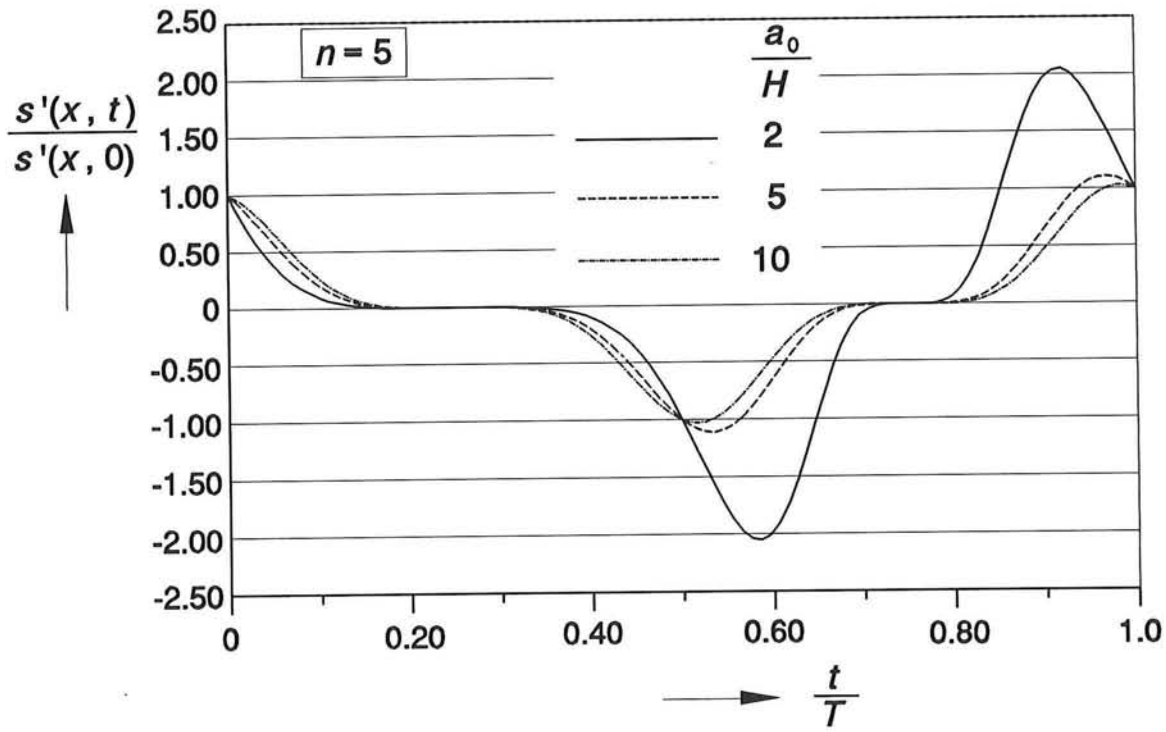

Figure 3-3: Sediment transport

It can be proved by integrating equation (3.8) that the net sediment transport over a tidal period is zero:

$$s_{net}(x) = \int_0^T s(x)\,\mathrm{d}t = 0 \tag{3.9}$$

Equation (3.9) is zero, independent of x and of the factor a_0/H

The condition for a dynamic equilibrium profile reads:

$$\frac{\partial}{\partial x}\left[\int_0^T S\ \mathrm{d}t\right] = 0 \tag{3.10}$$

As a result of $S_{net}(x) = \int_0^T s(x)\,\mathrm{d}t = 0$ the condition for a dynamic equilibrium profile is always satisfied for any bathymetry $z_b(x)$. This is physically not very realistic.

Conclusions:
With the model described above the condition for a dynamic equilibrium profile is always satisfied for any bathymetry $z_b(x)$, as a result of the absence of a net sediment transport.
Apparently too many assumptions are made in the model described above.

3.3 Extension of the simple single-channel model

3.3.1 General

In the simple single-channel model no realistic dynamic equilibrium profile is found. As a result of a number of neglected factors there is no net sediment transport over a tidal period and this is apparently a prerequisite for a realistic geometry. In this Section several factors are added to the previous model to obtain a net sediment transport.
Six factors are studied.

1. down-slope effect
2. phase-lag between discharge and water depth
3. higher frequency tidal components (tidal distortion)
4. relaxation effect of suspended transport
5. sediment transport which depends on water depth
6. incipient motion sediment

3.3.2 Down-slope effect

In general, sediment moves easier downhill than uphill. This effect is called the down-slope effect.
In a transport formula which depends only on the local flow conditions, the down-slope effect of the bed can be taken into account by adding the term $\pm\beta\frac{\partial z}{\partial x}$ to the formula for transport. The sign of $\beta\frac{\partial z}{\partial x}$ is different at flood and ebb tide.

during flood:
$$s = mu^n(1-\beta\frac{\partial z}{\partial x}) \qquad (3.11a)$$

during ebb:
$$s = mu^n(1+\beta\frac{\partial z}{\partial x}) \qquad (3.11b)$$

In the equation β is a constant coefficient. The down-slope coefficient β influences the magnitude of the transport rate. Van Lieshout (1993) reports that according to Struiksma (1988), the β-coefficient has a theoretical value of $0.05\frac{C^2}{g}$.
The extra term acts as a diffusion term. This can easily be seen by substitution of $s = mu^n(1-\beta\frac{\partial z}{\partial x})$ in the mass-balance equation for sediment.
The down-slope then effects the net sediment transport, which can be seen when integrating the sediment transport over a tidal period:

$$s_{net}(x) = \int_0^T s(x)\mathrm{d}t =$$

$$= \int_{ebb} s(x)\mathrm{d}t + \int_{flood} s(x)\mathrm{d}t =$$

$$= \int_{ebb}(mu^n + mu^n\beta\frac{\partial z}{\partial x})\mathrm{d}t + \int_{flood}(mu^n - mu^n\beta\frac{\partial z}{\partial x})\mathrm{d}t =$$

$$= \int_{ebb} +mu^n\beta\frac{\partial z}{\partial x}\mathrm{d}t + \int_{flood} -mu^n\beta\frac{\partial z}{\partial x}\mathrm{d}t =$$

$$= +s_{ebb}\beta\frac{\partial z}{\partial x} - s_{flood}\beta\frac{\partial z}{\partial x} =$$

$$s_{net}(x) = +2\beta\frac{\partial z}{\partial x}s_{ebb} \qquad (3.12)$$

where s_{ebb} is the total ebb-transport when the down-slope effect is not taken into account.
The net transport is directed downhill, which leads to a horizontal bed profile $\frac{\partial z}{\partial x} = 0$ when the condition for a dynamic equilibrium profile is applied:

$$\frac{\partial}{\partial x}\left[\int_0^T s(x)\,\mathrm{d}t\right] = 0 \qquad (3.13)$$

with as boundary condition:for $x = L$ $s_{net} = 0$

equation (3.13) is then only satisfied when

$$\frac{\partial z}{\partial x} = 0 \Rightarrow z = \text{constant}$$

<u>Conclusions:</u>
Extension of the simple model with the down-slope effect results in a horizontal dynamic equilibrium profile.
The level of the dynamic equilibrium profile is determined by the boundary condition at $x=0$: $z(0,t) = z_0$

The bed level $z_b(x)$ is constant in the whole region, which is still rather unrealistic.
The impacts on the results regarded, it can be concluded that the down-slope effect should be added to the model.

3.3.3 Phase-lag between discharge and water depth

Until now the water level in whole basin was assumed to be in phase (i.e. storage basin consideration).
As a result of the tidal propagation the tidal phase is not everywhere the same, but a function of x. Consequently there is also a phase-lag between the discharge $q(x,t)$ and the water depth $a(x,t)$, as $q(x,t)$ is a result of the variation of the water level in the region x to L, see Figure 3-4.

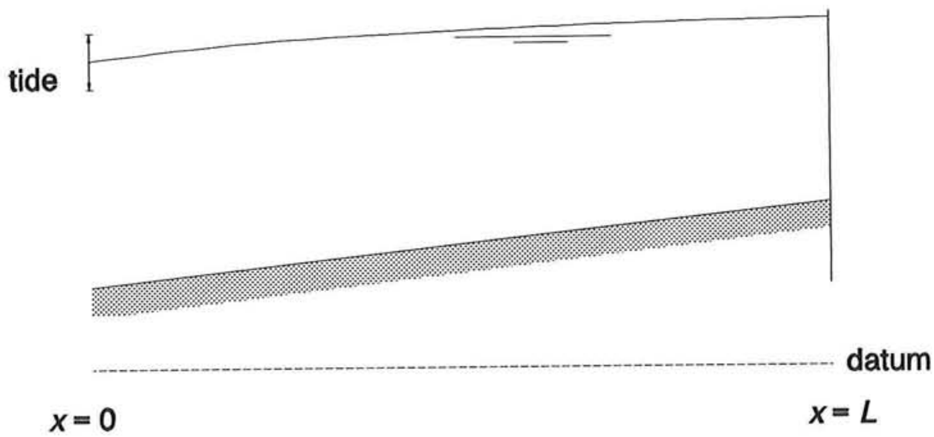

Figure 3-4: Variation of the water level

$$q(x,t) = \int_x^L \frac{\partial h}{\partial t}\,\mathrm{d}x \tag{3.14}$$

In case of the phase-lag the flow velocity at a certain location x can be described as:

$$u(x,t) = \frac{q(x,t)}{a(x,t)} = \frac{\omega\,(L-x)\,H\,\cos(\omega t-\theta)}{a_0(x) + H\,\sin(\omega t)} \tag{3.15}$$

where θ is the phase-lag between discharge and water depth.

Figures 3-5 and 3-6 show respectively the resulting flow velocity and the sediment transport.

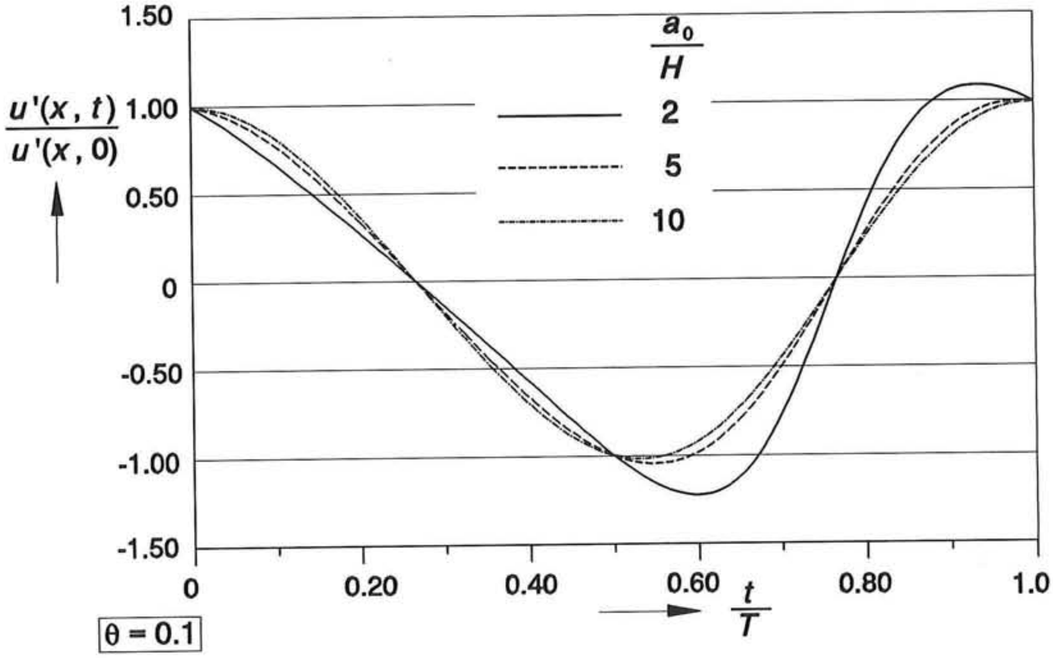

Figure 3-5: Flow velocity

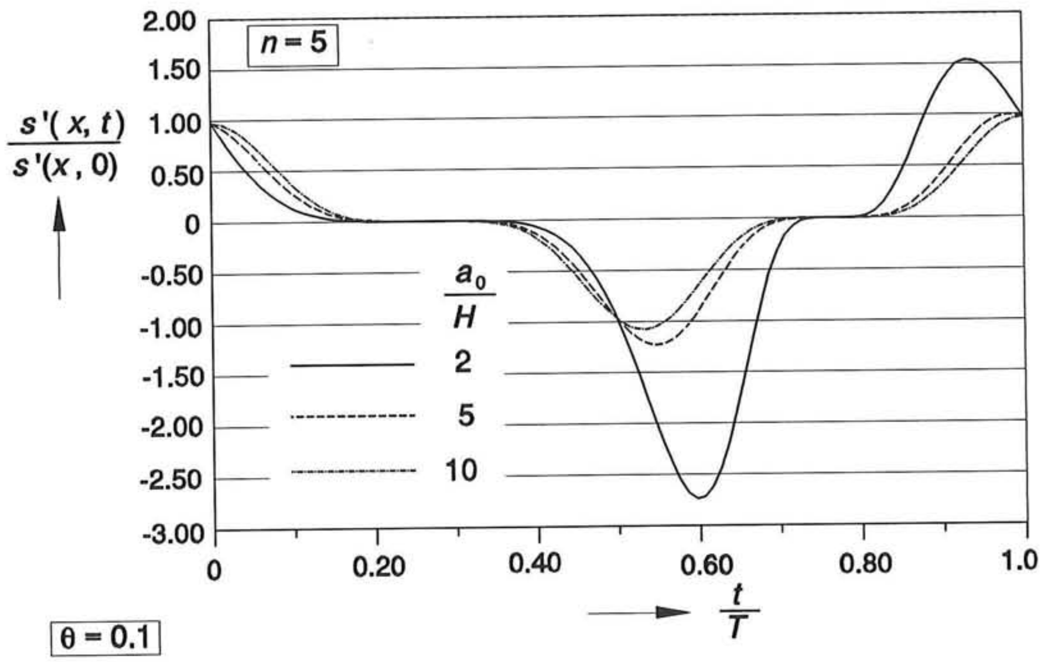

Figure 3-6: Sediment transport

Figure 3-6 shows that the net sediment transport over a tidal period is directed outward for $\theta=0.1$.
If the down-slope effect is also taken into account, the model will then result in a single equilibrium bathymetry $z_b(x)$.
The bed level is then inclined such that it is deeper landinwards. This is again far from realistic.

Conclusions:
The effects of the phase-lag on the geometry regarded, it can be concluded that the phase-lag has to be added to the model.

3.3.4 Higher frequency tidal components (tidal distortion)

So far, the boundary condition consisted out of one harmonic component, viz. the M_2 component.

for $x=0$: $$z_s = H\sin(\omega t)$$

However, the boundary condition can contain higher frequency components, M_4, M_6 and so on. Higher frequency components are generated both externally (boundary condition) and internally (a result of non-linear terms in the momentum equation).
As a result of the higher frequency components there is a tidal distortion. Due to the distortion, the net sediment transport over a tidal period is not beforehand zero.

boundary condition of the model:
To the existing boundary condition of the model, one harmonic component is added. In many estuaries the M_2 component is the dominating tidal component. Along the Dutch coast the most important higher frequency tidal component of the M_2 component is the M_4 component, having an amplitude of about 10% of that of the M_2 component (Wang, 1992).
A boundary condition of the model which contains the M_2 and M_4 components causes an asymmetry in the tide, thus a net sediment transport.
Wang (1992) determined the net sediment transport as a result of the M_2 and M_4 boundary condition given by:

$$z_s = a\cdot\cos(\frac{2\pi}{T}t) + b\cdot\cos(\frac{4\pi}{T}t - \theta) \tag{3.16}$$

herein:

z_s =	water level	[m]
a =	amplitude of the M_2 component	[m]
b =	amplitude of the M_4 component	[m]
θ =	phase-lag of M_4 component	[rad]
T =	tidal period	[s]

Again, the sediment transport is calculated with the power law, with $n=5$ (Engelund Hansen).

$$s = m\,u^5$$

Over a tidal period, this leads to a net sediment transport through a cross-section of:

$$s_{net} = -\frac{16\pi^5 m x^5}{T^4 a_0^5(x)} (5a^4 b + 30a^2 b^3) \sin\theta \tag{3.17}$$

herein:

x = distance between the cross section and the closed boundary [m]

$a_0(x)$ = mean water depth [m]

In order to see the effect of θ, Figure 3-7 illustrates the impact of θ for a specific case.

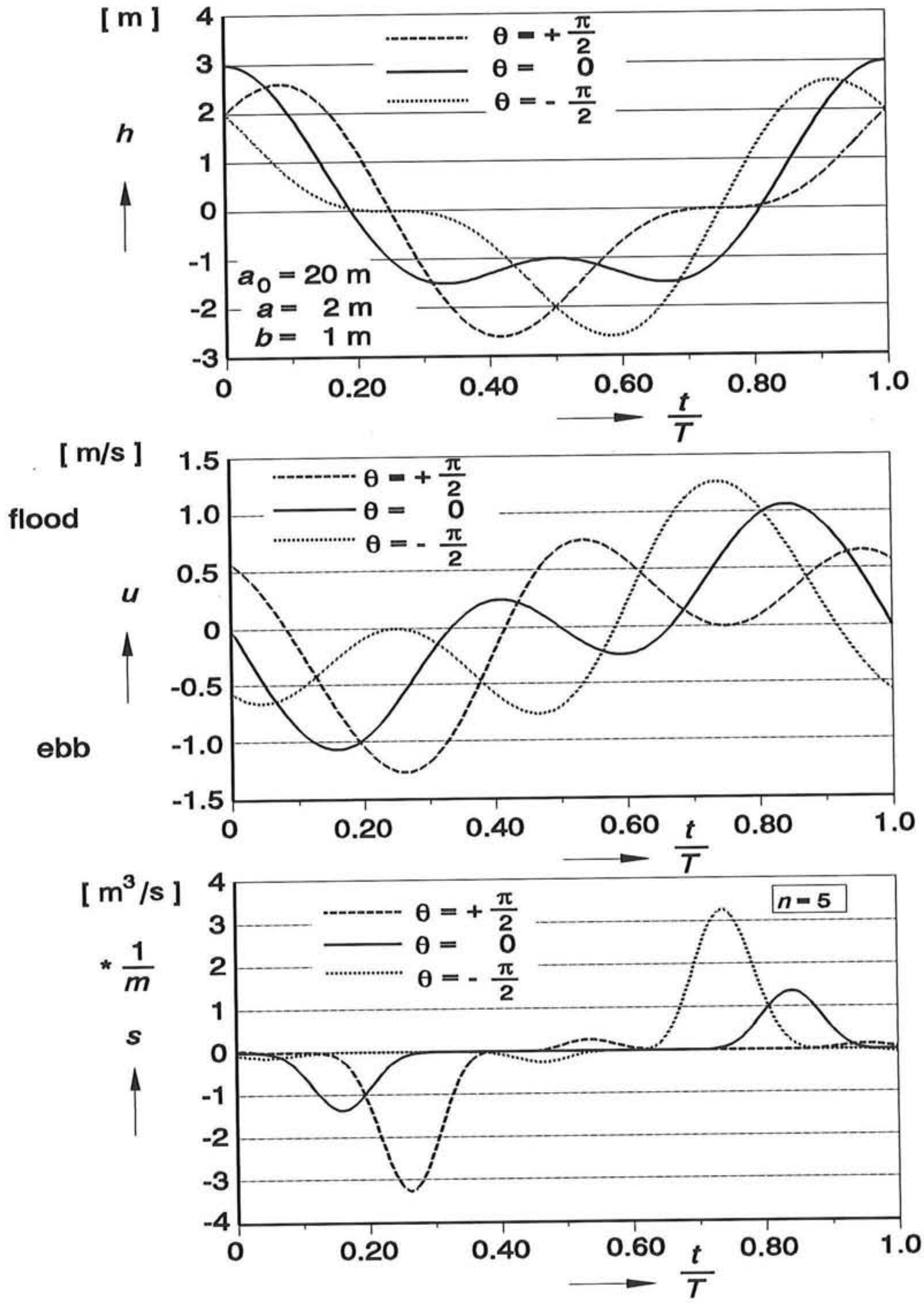

Figure 3-7: Effect of phase-lag θ on the sediment transport

The phase-lag θ of the M_4 component proves to be a very important parameter, as the phase-lag θ determines the magnitude and direction of the net sediment transport. The magnitude of the net sediment transport also depends strongly on the distance x and the amplitudes a and b.

<u>internally generated higher frequency components:</u>
So far the internally generated higher frequencies were neglected.
Even if the boundary condition contains only an M_2 tidal component, the M_2 component still can generate an asymmetry in the tide as a result of shallow water effects.
Shallow water effects are generated by both hydraulic friction and convection. Both terms are non-linear terms in the momentum equation for water and proportional with the square of the flow velocity.

Kalkwijk (1975) gives also additional non-linear tide generating phenomena:

- variable storage width as a result of tidal flats
- the tidal propagation velocity is not constant, as it depends on the water depth
- non-linear influences of currents with relative high velocities (high kinetic energy)

These non-linear phenomena can also generate higher frequency components.
This can be shown by rewriting the hydraulic friction term in Fourier series e.g.:

$$u(t) \sim \sin(\omega t)$$

$$R \sim \sin(\omega t)\ |\sin(\omega t)| = \frac{8}{3\pi}\sin(\omega t) + \frac{8}{15\pi}\sin(3\omega t) + ...$$

So, M_2 generates M_6 and higher components as a result of the hydraulic friction.

<u>Conclusions:</u>
As a result of higher frequency components the tide is asymmetric, so a net transport will occur.
Note: As a result of the short length of the model, compared to the tidal wave length, internally generated components are not able to develop well and are negligible compared to the higher frequency components in the boundary condition of the model.

3.3.5 Relaxation effect of suspended transport

It is assumed that the sediment transport only depends on the local flow velocity. This is reasonable for bed load transport.
If there is suspended transport, relaxation in time and space may cause a net sediment transport over a tidal period.
Figure 3-8 illustrates relaxation of suspended sediment transport in time. An accelerating flow transports less sediment compared to calculations based on the local flow velocity only. A decelerating flow transports more sediment compared to calculations based on the local flow velocity only.
Taking this effect into account requires a complete two-dimensional morphological computation using the 2-DV convection-diffusion equation, see e.g. De Vries (1994) or a depth-integrated model based on the 2-DV convection-diffusion equation (Galappatti, 1983).

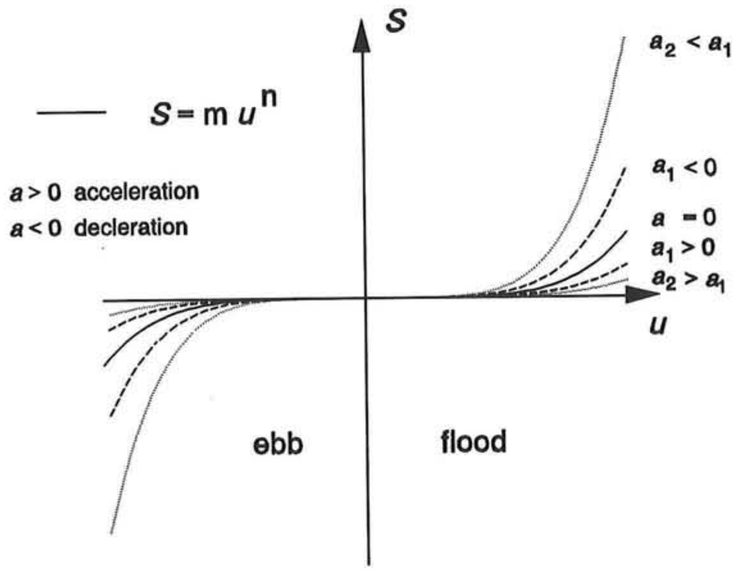

Figure 3-8: Relaxation in time

This exceeds the scope of this study. Therefore no relaxation is taken into account.

3.3.6 Sediment transport which depends on the water depth

The dependence of the sediment transport on the water depth is usually negligible. The sediment transport only depends on the flow velocity.

$$s = m\ u^n$$

3.3.7 Incipient motion

Sediment transport occurs when the flow velocity is higher than a critical value (Shields, 1936). The net sediment transport over a tidal period may be effected as a result of this critical value.

3.3.8 Conclusions

For a single-channel model, a number of small factors have to be taken into account to obtain a more or less realistic net sediment transport over a tidal period. The higher frequency components in the boundary condition are the most dominating factors.
The other studied factors result in a relatively small or zero net sediment transport.

3.4 Morphological behaviour

In this Section the morphological development of a single-channel basin is considered. In Section 3.3 it is shown that the boundary condition at the seaside plays an important role in the net sediment transport. In this Section it is assumed that there is a net sediment transport inward as a result of the boundary condition.

As a result of the net sediment transport, a sand wave propagates in the basin, till the quasi-dynamic equilibrium is reached, see Figure 3-9 (phase **e**). Van Lieshout (1993) demonstrates this with numerical computations.

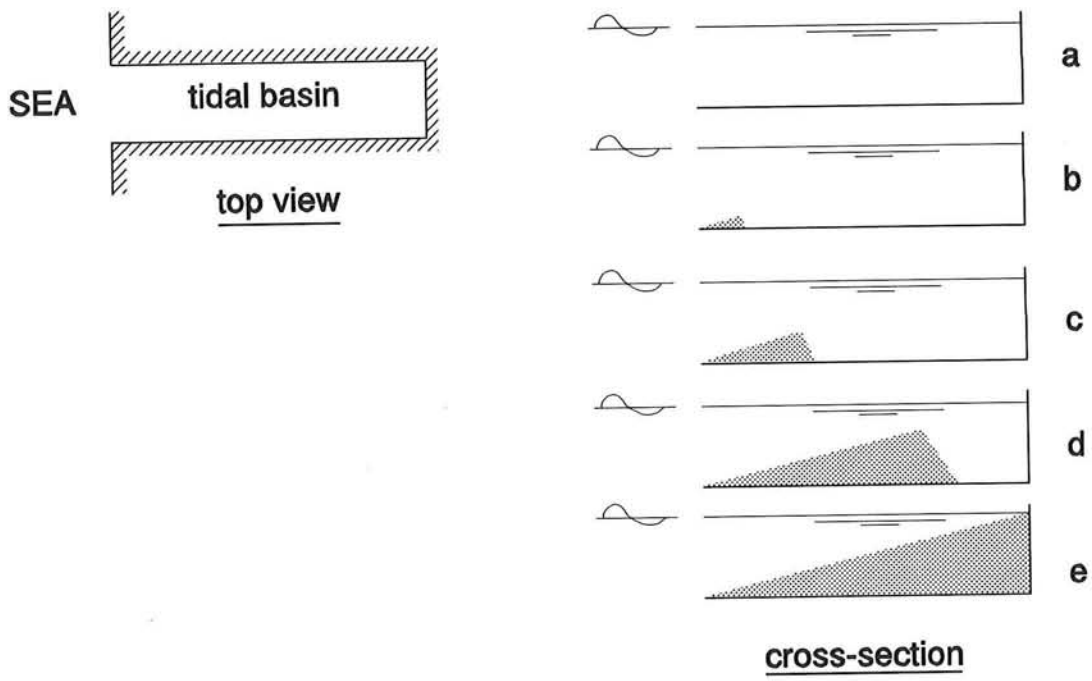

Figure 3-9: Quasi-dynamic equilibrium

Phase **e** in Figure 3-9 is called the quasi-dynamic equilibrium. In Section 4.2 the shape of quasi-dynamic equilibrium profile is calculated.
In this situation the net sediment transport is equal for every cross-section, thus there is no gradient in net transport. However, the net sediment transport is not zero, so it is not possible to define a dynamic equilibrium profile, as a result of the boundary condition:

for $\quad x = L: \qquad s_{net} = 0$

As a result of the inward directed net sediment transport the basin is filled.
Figure 3-10 illustrates this in a schematic way (not based on calculations). Finally the basin will be filled and the coastline is not interrupted anymore.

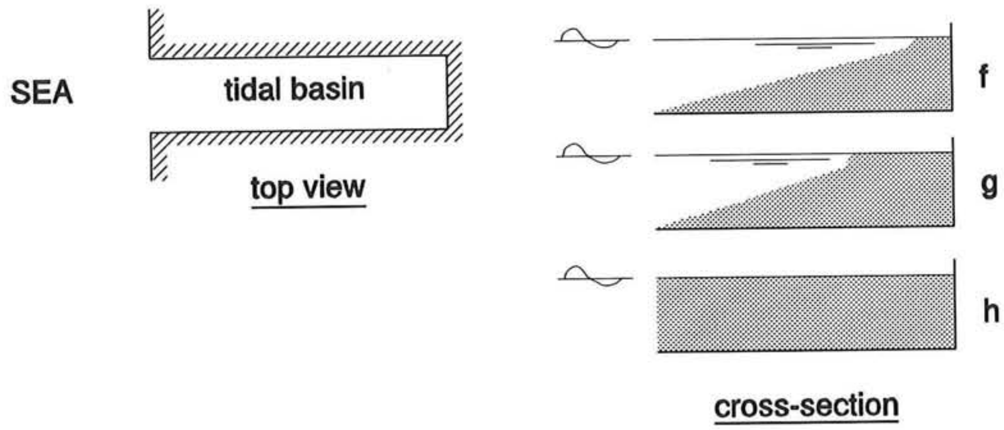

Figure 3-10: Equilibrium

In phases **a** ... **e** there is much more sediment transported inward than outward over a tidal period. In phases **f** ... **h** there is only a small difference between the inward and outward transported sediment, viz. the net sediment transport is small.
So phases **a** ... **e** will develop faster than phases **f** ... **h**.

3.5 Conclusions

The use of a simple single-channel model will result in unrealistic results.
In a simple single-channel model, a quasi-dynamic equilibrium profile can exist as there is no gradient in net sediment transport.
However, the net sediment transport is not zero. As a result of the closed boundary condition, only a trivial dynamic equilibrium profile can be defined, viz. a filled basin.

4 A simple two-channel model

4.1 General

A simple single-channel model has only a trivial dynamic equilibrium profile, viz. a filled basin, as a result of the boundary condition:

for $x = L$ $\qquad\qquad S = 0$

In this Chapter a two-channel model is considered, as in estuaries often systems of ebb and flood channels exist.

An ebb channel is thereby defined as the channel where the volume of water that passes through the channel during the ebb period is bigger than during the flood period. A flood channel, in contrast, is defined as the channel where the volume of water that passes through the channel during the flood period is bigger than during the ebb period. As a result of this phenomenon, there is a net transport in ebb direction for an ebb channel and a net transport in flood direction for the flood channel.

Over a tidal period, horizontal circulation occurs as a result of this net transport.

4.2 Simple two-channel model

The simple two-channel model, analysed by Wang (1992), consists of two channels, an ebb channel and a flood channel. It is assumed that the two channels have the same geometry. The width of the channels is kept constant. This is illustrated in Figure 4-1.

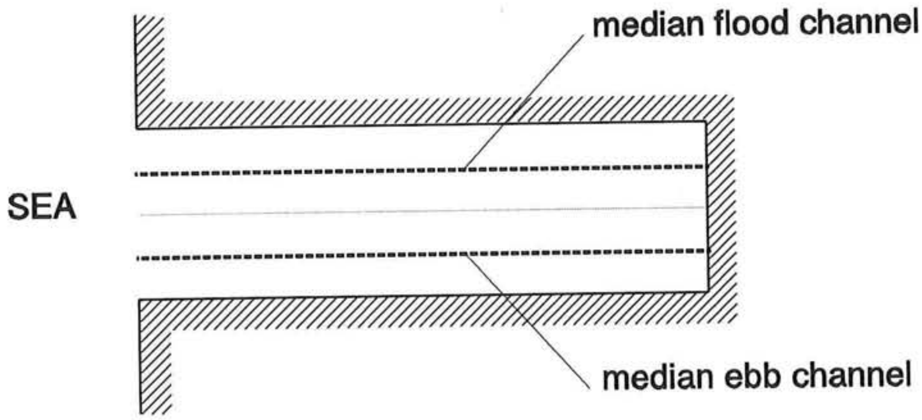

Figure 4-1: Two-channel model

The same assumptions as in the simple single-channel model are applied (i.e. the tidal storage consideration).

At the boundary only the M_2 component is present.

The water depths in the two channels are:

$$a_{flood}(x,t) = a_{flood_0}(x) + H\sin(\omega t) \tag{4.1a}$$

$$a_{ebb}(x,t) = a_{ebb_0}(x) + H\sin(\omega t) \tag{4.1b}$$

herein

$a_{flood}(x,t)$	= water depth in the flood channel	[m]
$a_{flood_0}(x)$	= mean water depth in the flood channel	[m]
$a_{ebb}(x,t)$	= water depth in the ebb channel	[m]
$a_{ebb_0}(x)$	= mean water depth in the ebb channel	[m]

The averaged specific discharge is still

$$q(x,t) = \omega x \, H \cos(\omega t) \tag{4.2}$$

but the discharge during ebb and flood through the ebb channel (q_e) is different from that through the flood channel (q_f).
The following distribution is assumed:

during ebb:

$$q_f = (1-\alpha)q \tag{4.3a}$$

$$q_e = (1+\alpha)q \tag{4.3b}$$

and during flood:

$$q_f = (1+\alpha)q \tag{4.4a}$$

$$q_e = (1-\alpha)q \tag{4.4b}$$

herein is α assumed to be constant.

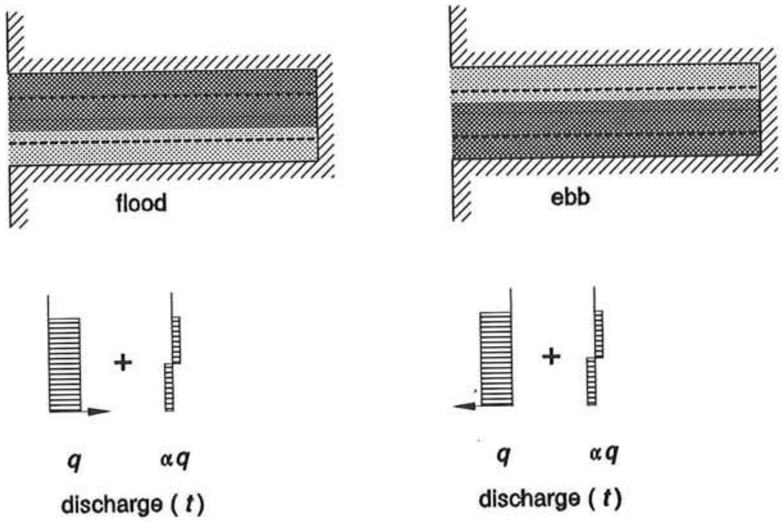

Figure 4-2: Contribution of the channels to the discharge

The basin is mainly filled by the flood channel, as can be seen in Figure 4-2. The basin is mainly emptied by the ebb channel.
The discharge can be split up in a symmetric part (q) and an asymmetric part (αq), see Figure 4-2.

The flow velocity and the sediment transport are not any longer symmetric in the ebb and in the flood channel (Figures 4-3 ... 4-6).

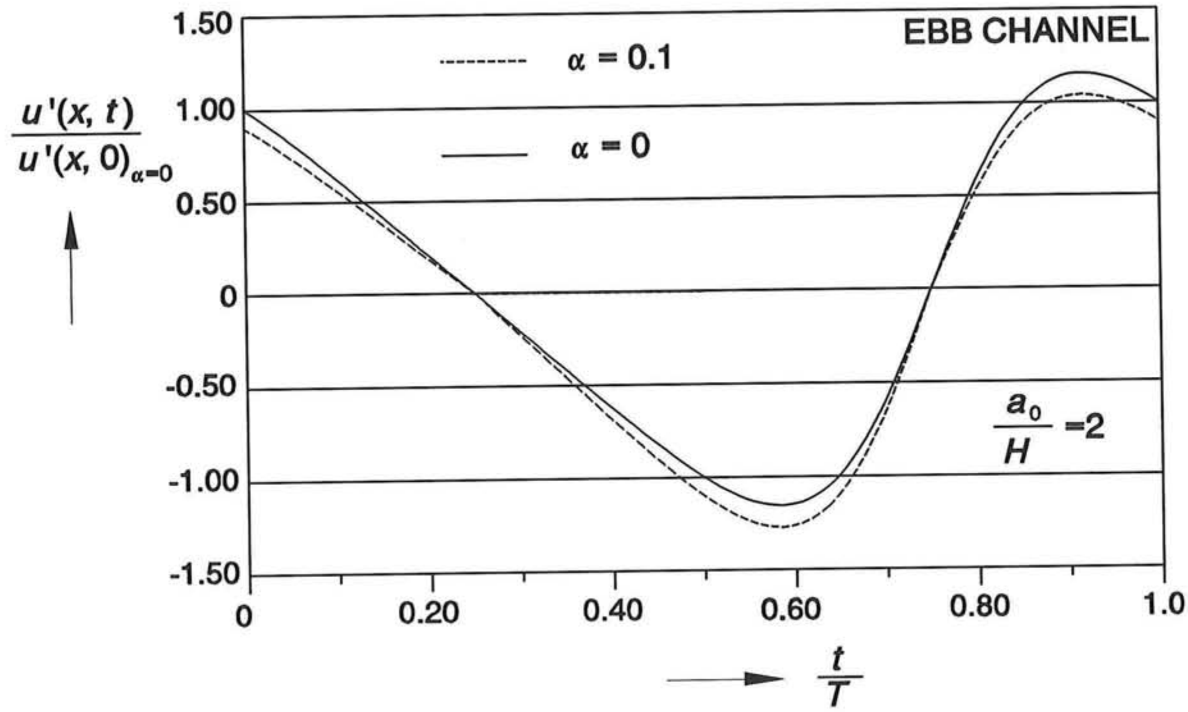

Figure 4-3: Flow velocity, ebb channel

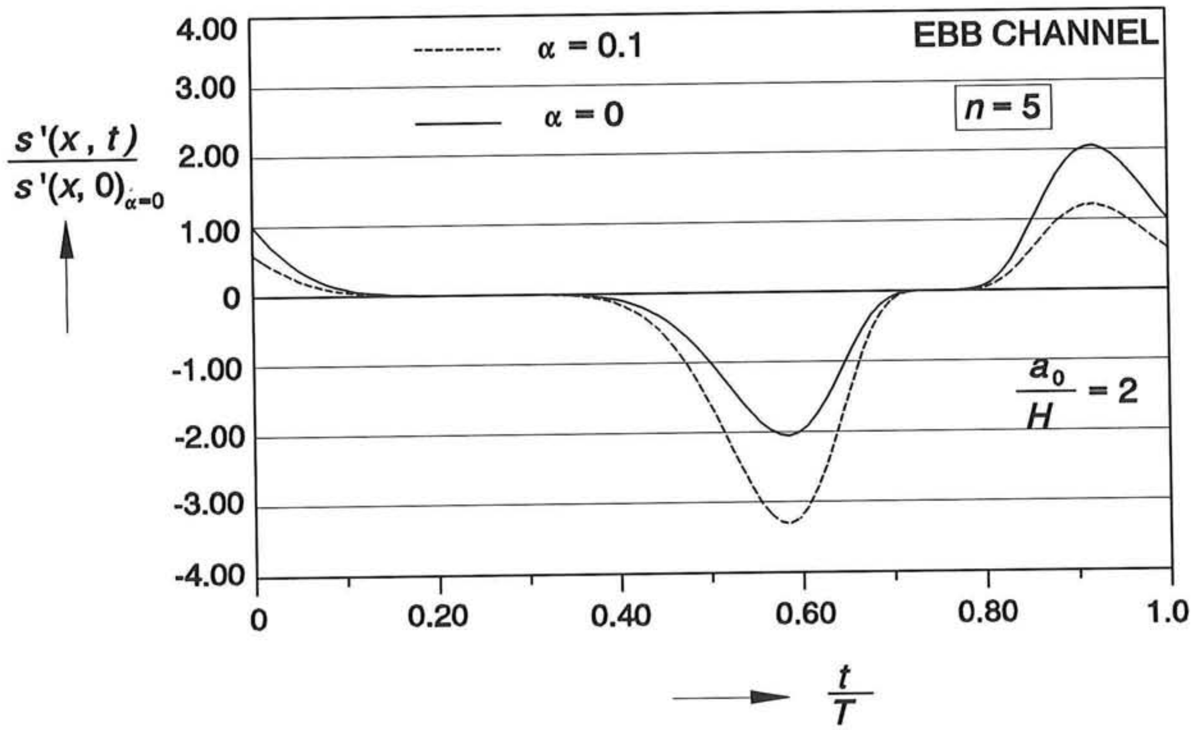

Figure 4-4: Sediment transport, ebb channel

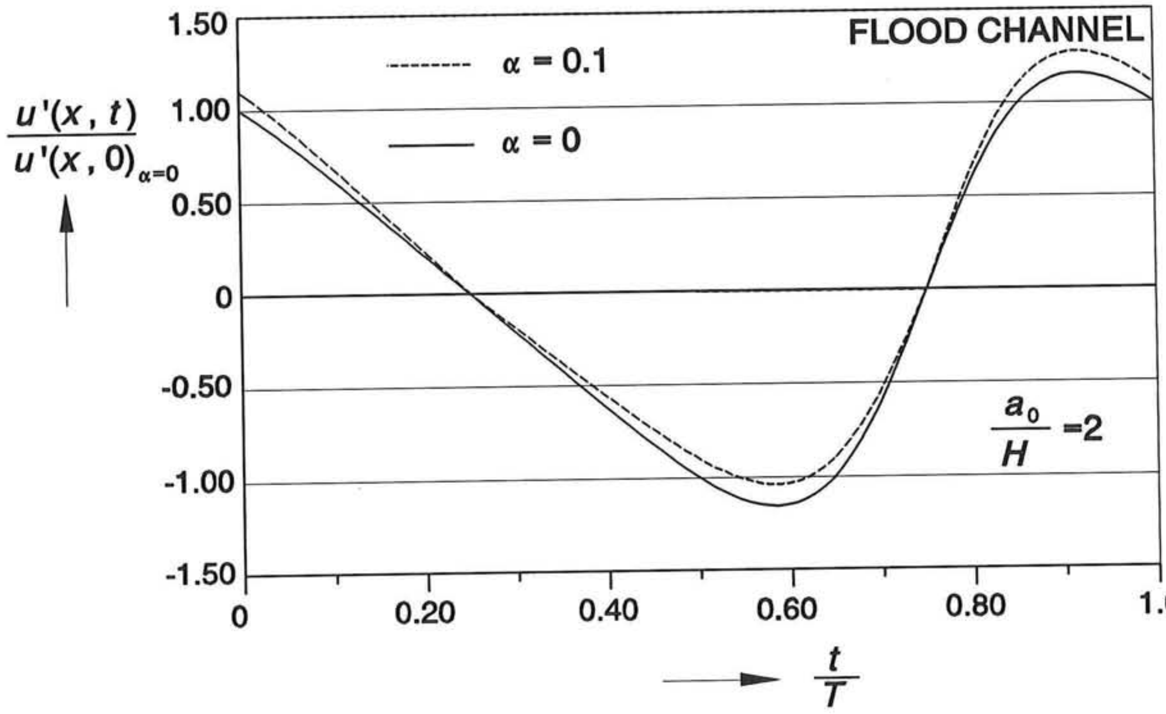

Figure 4-5: Flow velocity, flood channel

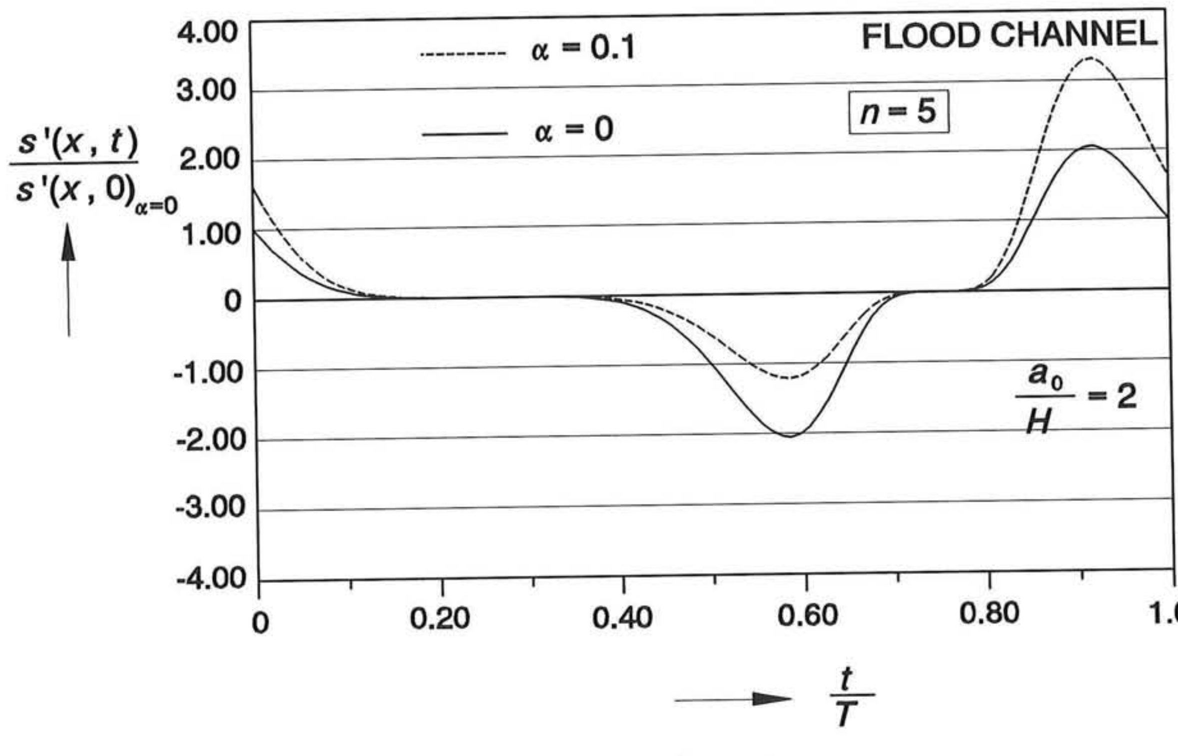

Figure 4-6: Sediment transport, flood channel

In this simple two-channel model, the net transport over a tidal period through the ebb channel is:

$$s_e = \int_0^T s \, dt = [(1+\alpha)^n - (1-\alpha)^n] s_{ebb} \tag{4.5a}$$

The net transport over a tidal period through the flood channel is:

$$s_f = \int_0^T s \, dt = [(1-\alpha)^n - (1+\alpha)^n] s_{ebb} \tag{4.5b}$$

In these two equations s_{ebb} is the same as in the case of the single-channel model.

The dynamic equilibrium conditions for the ebb and flood channel are respectively:

$$\frac{\partial s_e}{\partial x} = 0 \tag{4.6a}$$

and

$$\frac{\partial s_f}{\partial x} = 0 \tag{4.6b}$$

For both channels the condition is satisfied for $\alpha \neq 0$ if and only if:

$$\frac{\partial s_{ebb}}{\partial x} = 0 \tag{4.7}$$

$$s_{ebb} = F(t) = \text{constant} \tag{4.8}$$

where s_{ebb} is the total ebb-transport defined as $s_{ebb} = \int_{ebb} m u^n \, d\,t$.

This equation can be solved analytically.
For $n=3$ (power in the transport formula) the solution is:

$$s_{ebb} = -m\,\omega^2\,x^3 \left[\frac{2\frac{a_0}{H}}{\left(\frac{a_0}{H}\right)^2 - 1} - \ln\left(\frac{\frac{a_0}{H} + 1}{\frac{a_0}{H} - 1} \right) \right] = \text{constant} \tag{4.9}$$

and for $n=5$:

$$s_{ebb} = -m\,\omega^4\,x^5 \left[\frac{-\frac{10}{3}\frac{a_0}{H} + 2\left(\frac{a_0}{H}\right)^3}{\left(\left(\frac{a_0}{H}\right)^2 - 1\right)^2} + \ln\left(\frac{\frac{a_0}{H} + 1}{\frac{a_0}{H} - 1} \right) \right] = \text{constant} \tag{4.10}$$

In general :

$$s_{ebb} = m\,\omega^{n-1}\,x^n\,F\left(\frac{a_0}{H}\right) = \text{constant} \tag{4.11}$$

For the distance x equation (4.11) can be rewritten into:

$$x = \left(\frac{s_{ebb}}{m\,\omega^{n-1}} \right)^{\frac{1}{n}} \cdot G\left(\frac{a_0}{H}\right) = L \cdot G\left(\frac{a_0}{H}\right) \tag{4.12}$$

where $L = \left(\dfrac{s_{ebb}}{m\ \omega^{n-1}} \right)^{\frac{1}{n}}$ is a characteristic length scale and $G\left(\frac{a_0}{H}\right) = \left(F\left(\frac{a_0}{H}\right) \right)^{-\frac{1}{n}}$.

This characteristic length scale can be estimated by:

$$s_{ebb} \approx \frac{1}{2}\, m\, u^n\, T$$

$$\omega = \frac{2\pi}{T}$$

hence

$$L \approx \frac{1}{2} \left(\frac{1}{2\pi} \right)^{\frac{n-1}{n}} u\, T \tag{4.13}$$

where u is a characteristic velocity scale during the tidal period.

Figure 4-7 shows the results of equations (4.9) and (4.10).
The water depth a_0 is normalised with the tidal amplitude H and the horizontal coordinate x is normalised with L.

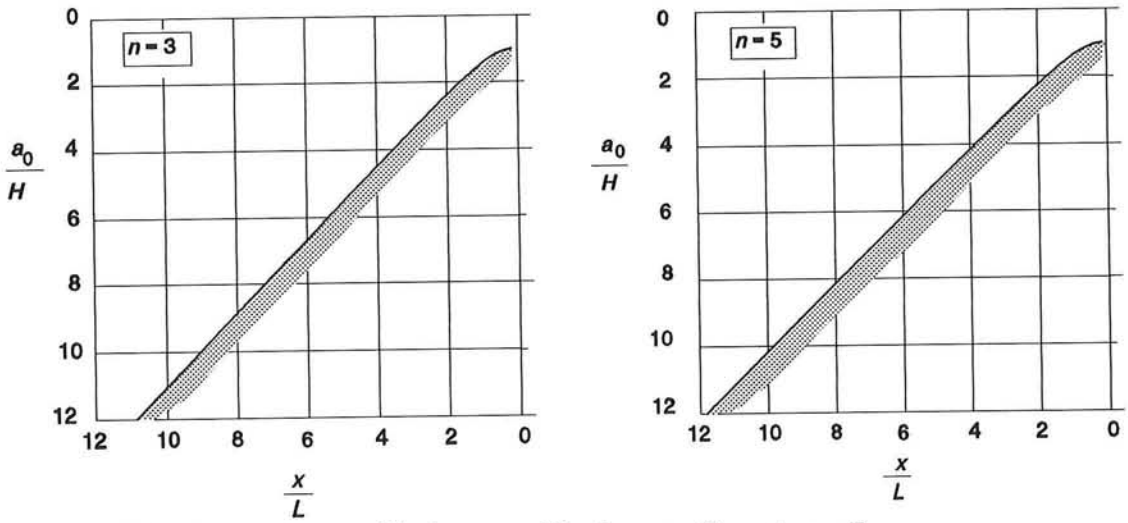

■ Figure 4-7: Dynamic equilibrium profile for $n = 3$ and $n = 5$

In this simple model, the shape of the ebb and flood channels are the same, this follows from the assumption that α is constant and because the condition for a dynamic equilibrium profile is satisfied by only one equation, namely $\dfrac{\partial s_{ebb}}{\partial x} = 0$.

Figure 4-7 shows that the power n in the transport formula has little influence on the shape of the channel. For both values of n a nearly linear relation between water depth and the horizontal coordinate is found. This agrees well with the empirical relation that the cross-section area should be proportional to the tidal volume (Allersma, 1994).

4.3 Conclusions

With the simple two-channel model, a well-defined dynamic equilibrium profile exists. In the simple single-channel model, only a quasi dynamic equilibrium profile exists as a result of the closed boundary condition which superimposed the condition $s = 0$ on the basic condition for dynamic equilibrium ($\frac{\partial s}{\partial x}$ = constant).

In the simple two-channel model the closed boundary becomes an internal boundary:

$$\sum_{i=1}^{2} S_i = 0$$

herein:

$S_1 = S_{net_{flood}}$

$S_2 = S_{net_{ebb}}$

So there is a dynamic equilibrium if: $S_{net_{flood}} = S_{net_{ebb}}$

As a result of this, a horizontal circulation occurs, see Figure 4-8.

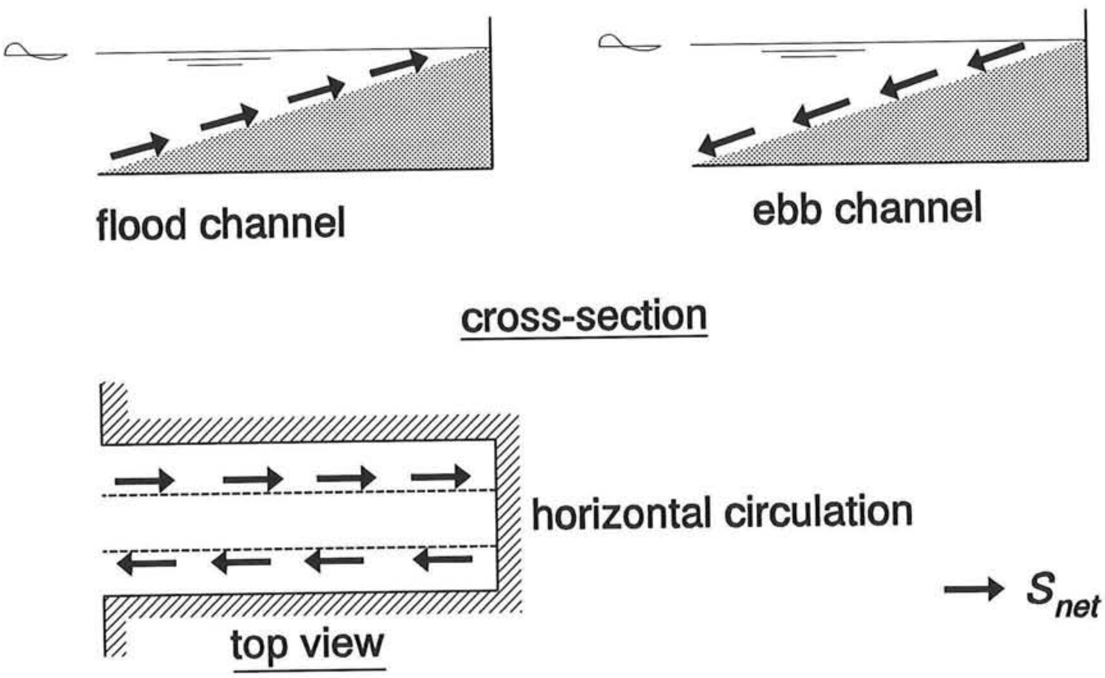

Figure 4-8: Horizontal circulation

5 Reference case

5.1 General

In this Chapter first a description is given of the ebb and flood channel systems of the Western Scheldt. Secondly an ebb and flood channel system is chosen as a reference case. Geometrical, hydraulic and morphological characteristics about the chosen ebb and flood channel system are gathered in order to get proper dimensions for the numerical model, see Chapter 6.

5.2 Western Scheldt

Figure 5-1 shows the bathymetry of the Western Scheldt, Annex 1a shows Figure 5-1 in colour.

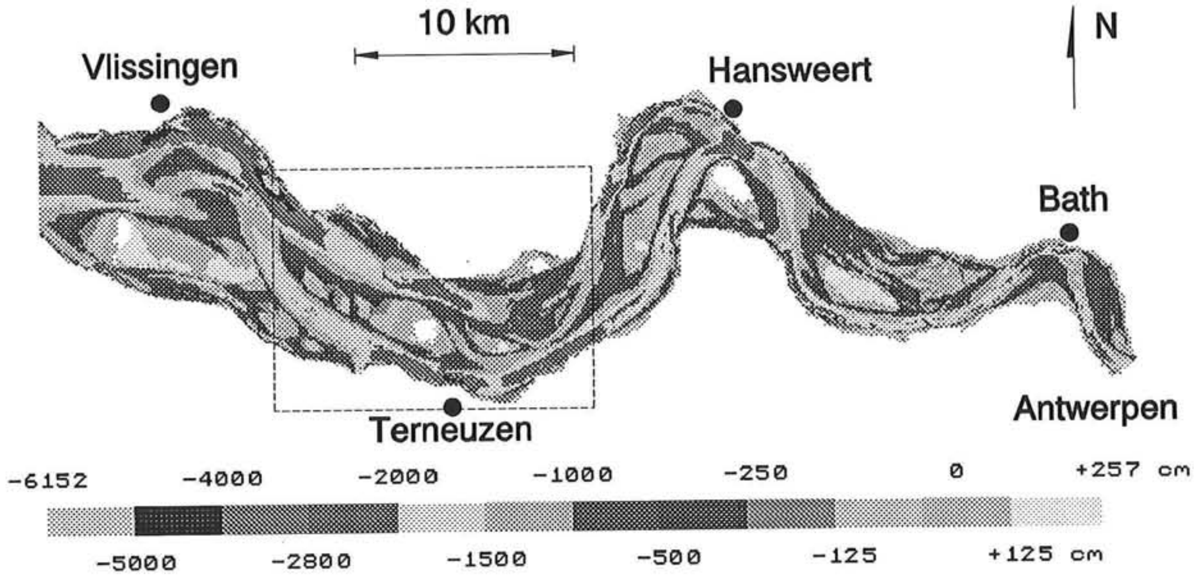

■ Figure 5-1: Bathymetry of the Western Scheldt (1992)

It can be seen that systems of ebb and flood channels are connected from Vlissingen to Antwerp. In the systems, the ebb and flood channels become shorter landinwards and the ebb channels form more or less a through channel from the North Sea to Antwerp. The system 'Pas van Terneuzen - Everingen', see Fig. 5-2, is chosen as reference case because the available discharge and sediment-transport measurements which were carried out by Ministry of Public Works and Transport (RWS) in September 1993, for the design of a planned bridge and tunnelcomplex.

5.3 Aerial view of the 'Pas van Terneuzen - Everingen'

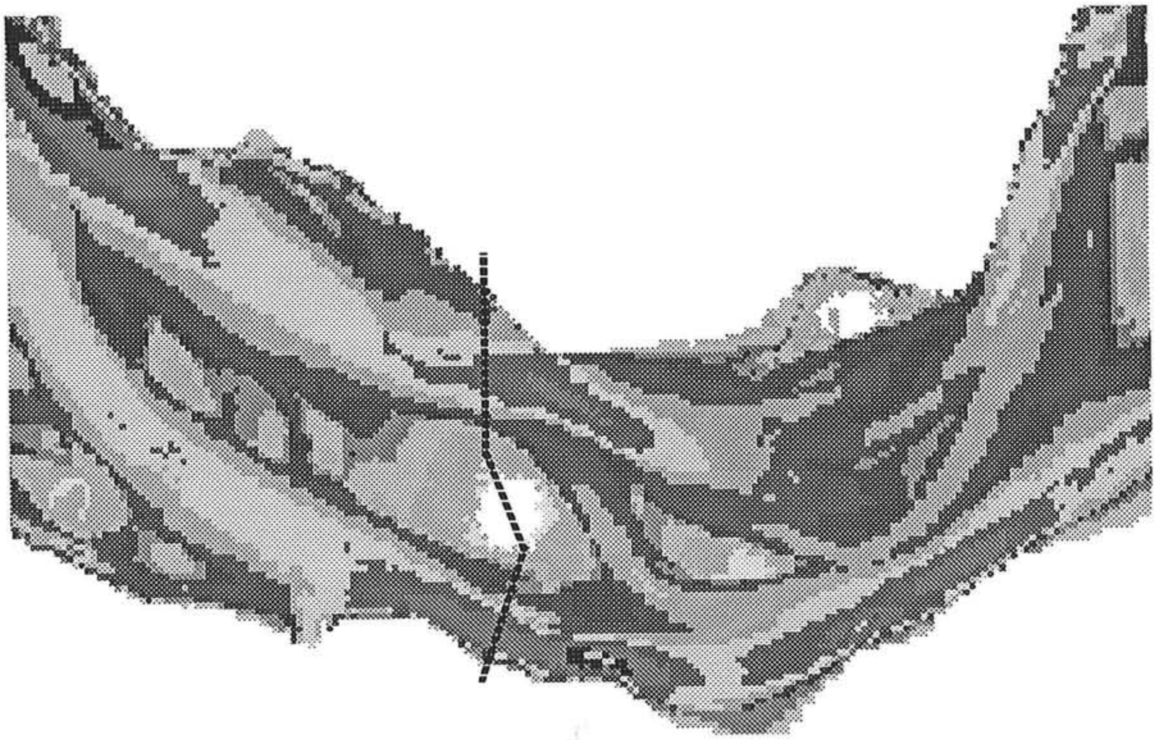

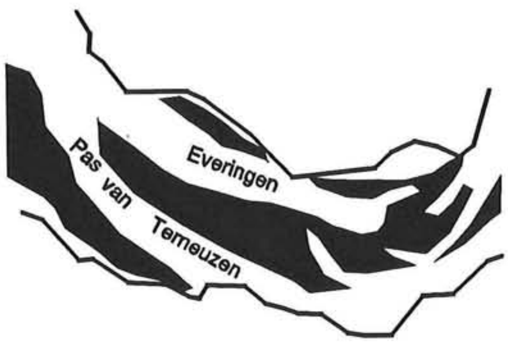

■ Figure 5-2: 'Pas van Terneuzen - Everingen':
above: bathymetry
below: sketch (different scale)

In the chosen system, the 'Pas van Terneuzen' is the ebb channel and the 'Everingen' the flood channel. The 'Pas van Terneuzen' and 'Everingen' are separated by shallows (tidal flats) and there are some small gullies which connect the two channels at several places.

The channels are different in length:
The 'Everingen' is about :14 km
The 'Pas van Terneuzen' is about :18 km

According to literature (e.g. Van Veen, 1950), in general, flood channels begin deep and narrow at the seaside and end shallow and wide at the landside, in contrast to ebb channels. These end shallow and wide at the seaside and end deep and narrow at the landside. This is, however, hard to see in Figure 5-2.
Both the ebb and flood channels are situated in a bend. The western part of the bend has a radius of 9 km and the eastern part of 7 km (Allersma, 1992).

5.4 Available data

5.4.1 Cross-section

Figure 5-2 shows the location of the cross-section of the ebb and flood channel which is represented in Figure 5-3. Annex 1 gives more detailed information about the location.
The profile of the cross-section was measured in detail by RWS in September 1993.

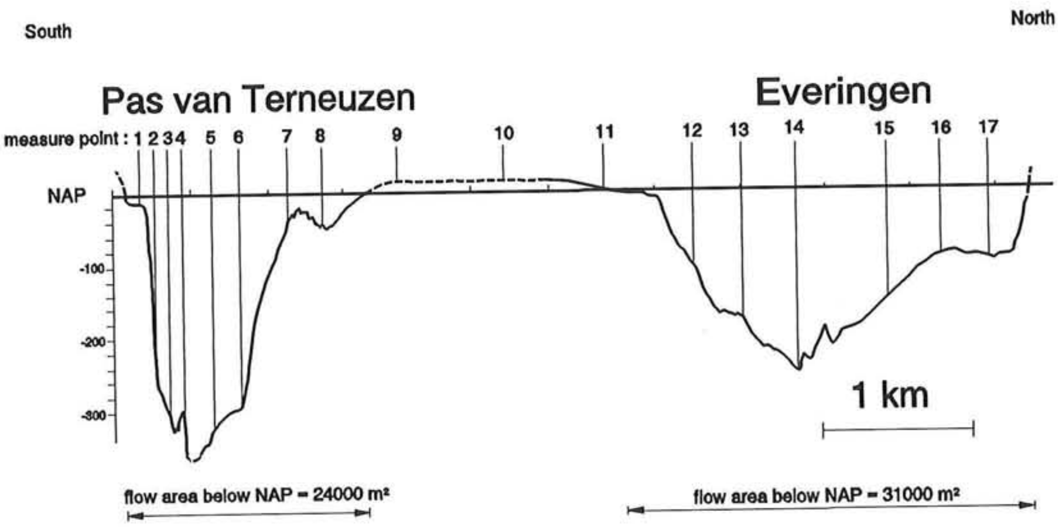

Figure 5-3: Cross-section

5.4.2 Hydraulic data

water levels
From two water-level gauges, Vlissingen and Terneuzen, the data of the tidal components are available.
The most important semi-diurnal components are respectively M_2, S_2, N_2. The most important quarter-diurnal components are respectively M_4, MS_4.
Annex 2 gives detailed information of the 32 main tidal components for Vlissingen and Terneuzen.

discharge
The tidal prism and the flood volume of the Western Scheldt is represented in Figure 5-4.

The discharge of the River Scheldt varies from 50 m^3/s in the summer period to 180 m^3/s in the winter period (Allersma, 1992).
During the measurements in September 1993 the local discharge was measured in the ebb and flood channels, 'Pas van Terneuzen - Everingen' (Figure 5-5).

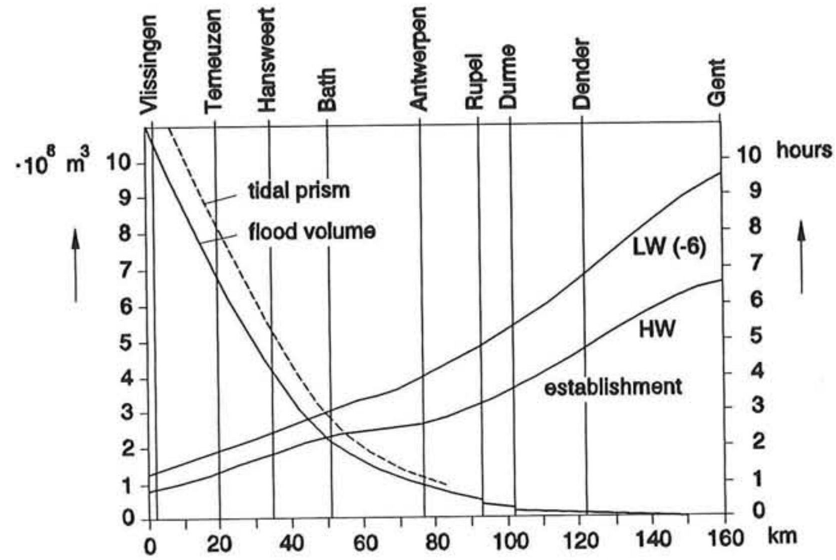

Figure 5-4: Tidal prism (after Allersma, 1992)

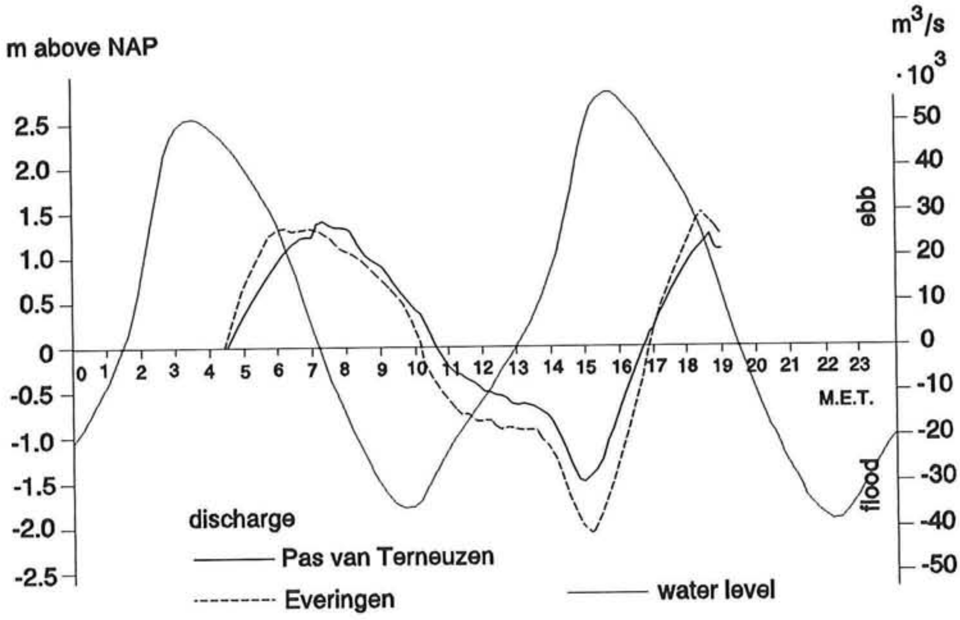

Figure 5-5: Measured discharges, September 1993 (RWS)

The measured volume of water that passed the cross-section of a channel during the ebb and flood period is shown in Table 5.1.

channel \ period	ebb [10^6 m³]	flood [10^6 m³]	ebb - flood [10^6 m³]
Pas van Terneuzen	369	311	58
Everingen	366	477	-111
total	735	788	-53

Table 5.1: Measured volume of water that passed the cross-section of a channel

According to Table 5.1 the 'Pas van Terneuzen' is ebb dominated and 'Everingen' flood dominated. The order of magnitude of the volumes of Table 5.1 is in agreement with Figure 5-4.
The volume of water that passes through each channel during each ebb and each flood period is about 3.5 10^9 m³.
The last column of Table 5-1 shows the difference between the total volume of water that passes the channels during flood and during ebb. The net volumes are not real. Considering the whole system, it is not possible that there is a net flow in flood direction as the system is virtually closed with only a small tributary river inflow. The difference is due to errors in the measurements.

The errors in the measurements are estimated according to ISO (1974), see Annex 3.
In the estimate it is assumed that the total error in a measurement is normally distributed and that all measurements are complete. The relative standard deviation is then about 5% per measurement (Annex 3).
This leads to a relative standard deviation for the ebb and flood volume of:

$$\frac{1}{\sqrt{37}} \cdot 5\% = 0.8\%$$

where 37 is the number of measurements performed during the ebb and the flood period.
This result is an upper limit for the accuracy for the given number of measuring points.
The result is in contrast with Table 5.1 where an error of about 5% occurs.
The discrepancy between the estimated error and observed error can reasonably well be explained by the fact that the measurements are not complete, as is assumed in Annex 3.

As a result of the error it is impossible to determine the net volume of water that passes a channel over a tidal period.

5.4.3 Morphological data

sediment transport

The sediment transport was measured in several points viz. mp.2, mp.4, mp.6, mp.7, mp.12, mp.16 (mp. = measuring point). For the location of these points see Figure 5-3 and Annex 1. For the points 6, 12 and 16 the measurements are complete.
According to the data there is a significant sediment concentration all over the vertical. This illustrates that there is suspended load next to bedload.
To illustrate this Figure 5-6 gives an example of the measured sediment concentration profiles at measuring point 6.

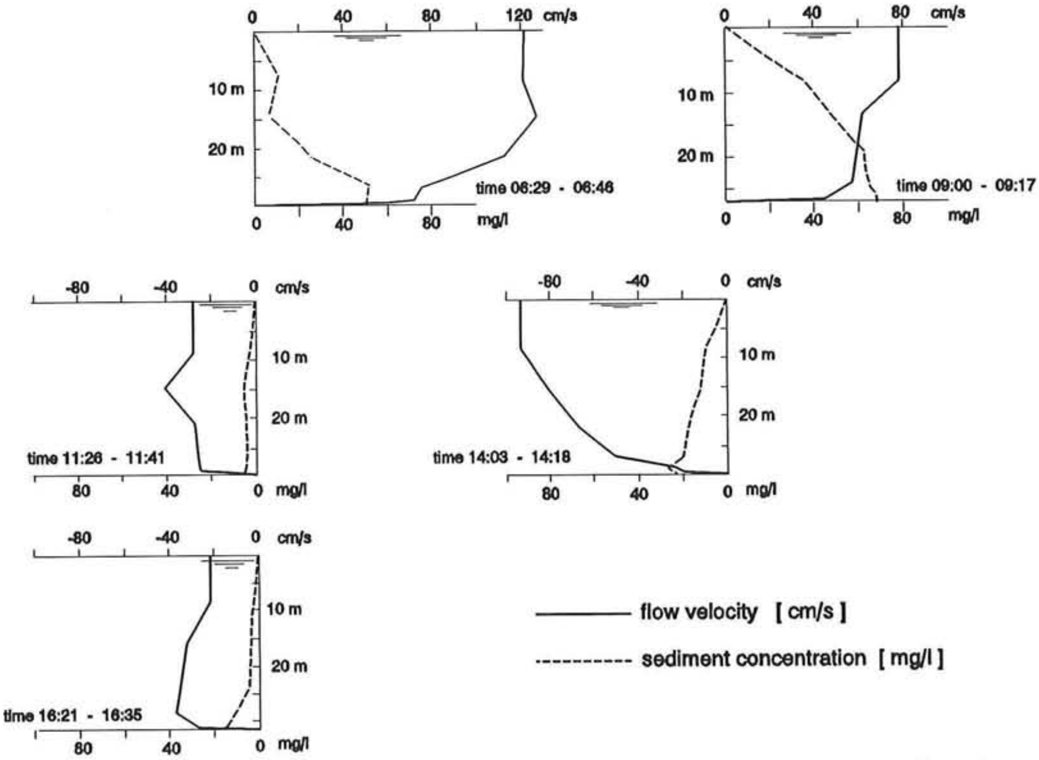

Figure 5-6: Examples of some sediment concentration profiles (mp. 6)

Figure 5-7 shows the measured sediment transport.
The measurements, during the ebb and flood periods, in the ebb and flood channels are used to get an impression of the sediment transport.
Measuring point 6 is used to estimated the sediment transport for the whole ebb channel. Measuring points 12 and 16 are used to estimated the sediment transport for the whole flood channel. The total sediment transport is defined as: $|S_{ebb}| + |S_{flood}|$

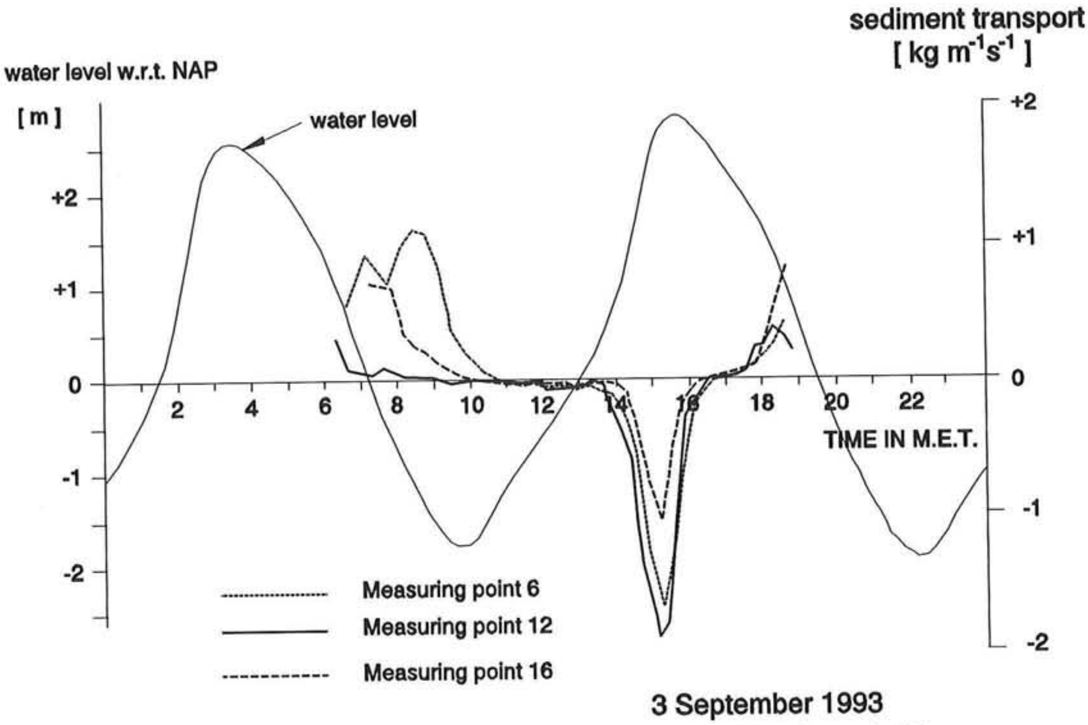

Figure 5-7: Measured sediment transport mp. 6, 12 and 16

measuring point	sediment transport ebb period [ton m^{-1}]	sediment transport flood period [ton m^{-1}]	total sediment transport [ton m^{-1}]
6	10.7	7.4	18.1
12	1.8	8.8	10.6
16	5.0	2.6	7.6

Table 5-2: Sediment transport at measuring point 6, 12 and 16.

Table 5-2 contains the integrated sediment transport perpendicular to the cross-section over the ebb and flood period from Figure 5-7.

<u>ebb channel 'Pas van Terneuzen':</u>

The estimated amount of sediment that passes the cross-section of the ebb channel over a tidal period is determined by simplifying the cross-section of the 'Pas van Terneuzen' to a rectangular profile, see Figure 5-8.

mp.	depth at measuring point [m]	estimated averaged depth profile [m]	estimated averaged width profile [m]	estimated sediment transport ebb period [ton]	estimated sediment transport flood period [ton]
6	29	29	1000	$10.7 \cdot 10^3$	$7.4 \cdot 10^3$

Table 5-3: Estimated sediment transport, ebb channel

If the porosity is 40% then this is equal to about $7 \cdot 10^3$ m^3 sediment (bulk) during the ebb period and $5 \cdot 10^3$ m^3 sediment during the flood period.

flood channel 'Everdingen':
In a similar way the amount of sediment that passes the cross-section of the flood channel over a tidal period is estimated by simplifying the cross-section of the 'Everingen' to a rectangular profile, see Figure 5-8.

mp.	depth at measuring point [m]	estimated averaged depth profile [m]	estimated contribution to averaged width profile [m]	estimated sediment transport ebb period [ton]	estimated sediment transport flood period [ton]
12	10	16	750	$2.2 \cdot 10^3$	$10.6 \cdot 10^3$
16	9	16	750	$6.7 \cdot 10^3$	$3.5 \cdot 10^3$
			total	$8.9 \cdot 10^3$	$14.1 \cdot 10^3$

Table 5-4: Estimated sediment transport, flood channel

If the porosity is 40% then the estimated amount of sediment that passes the cross-section of the flood channel is equal to about $6 \cdot 10^3$ m^3 sediment (bulk) each ebb period and $9 \cdot 10^3$ m^3 each flood period.

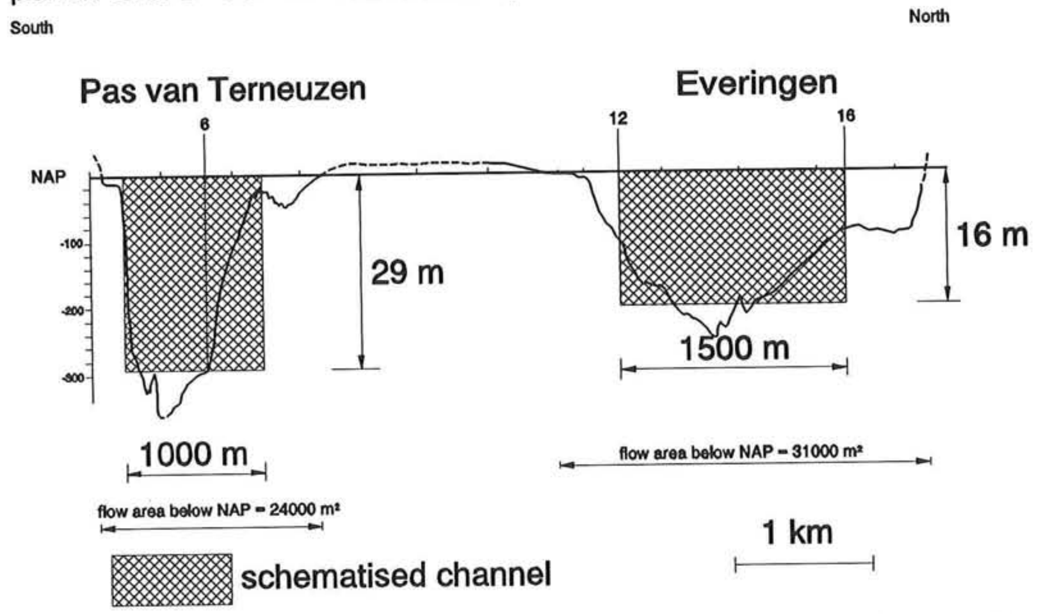

Figure 5-8: Schematisation of the cross-sections to rectangular profiles

The error in the sediment transport measurements is estimated in the same way as for the discharge of water, see Annex 3. The error in the sediment concentration measurement is also taken into account.
The relative standard deviation is then about 5% (Annex 3).
This leads to a relative standard deviation in the sediment transport during ebb

and flood of:

$$\frac{1}{\sqrt{37}} \cdot 5\% = 0.8\%$$

Again the estimated error is too optimistic.

diameter sand

The diameter of the sand in the cross-section can be characterised with D_{90}, D_{50}, D_{10}. Table 5-6 shows the diameters in the measuring points 6, 12 and 16. The diameter of the sand is required for the sedimenttransport formula.

measuring point	D_{90} [μm]	D_{50} [μm]	D_{10} [μm]
6	430	320	230
12	450	294	198
16	282	206	158

Table 5-6: Sand diameters

5.5 Summary

Systems of ebb and flood channels consist in the Western Scheldt estuary. The ebb channel forms more or less a through channel from Vlissingen to Antwerp. The ebb and flood channels becomes shorter landinwards.
In general the flood channels are shorter than the ebb channels.

In the Western Scheldt the ebb and flood channel 'Pas van Terneuzen - Everingen' is taken as a reference case. The following data is available:

1. The most important tidal components are M_2, S_2, N_2, M_4 and MS_4. These components are known for Vlissingen and Terneuzen.
2. The discharge and sediment transport are determined in order of magnitude by measurements.
3. The discharge of water is about $3.5 \cdot 10^9$ m³ each ebb and flood period for each channel.
4. For the 'Pas van Terneuzen - Everingen', the discharge of the River Scheldt is negligible compared to the discharge due to the tidal motion.
5. The estimated amount of sediment that passes the cross-section of a channel during the ebb and flood period is about $6 \cdot 10^3$ m^3 for the ebb and flood channel each.
6. Sand diameter D_{50} is about 200 to 300 μm.
7. There is suspended in addition to bed load.

6 Schematic representation of reference case

6.1 General schematisation

In Chapter 5 a general description is given of the reference case 'Pas van Terneuzen - Everingen'.
In this Chapter it is tried to model this system. First attention is given to the geometry of an ebb and flood channel system and the boundary conditions to be applied to a model of such a system.
Later on the reference case is schematised into a simple 1D-network model.
The dimensions of the 1D-network model are of the same order as in the reference case.

6.2 Geometry of an ebb and flood channel system

6.2.1 General

The geometry of the main ebb and flood channels have to be chosen in such a way that the relevant physical processes are taken into account. As stated in Chapter 4, circulation is important for an ebb and flood channel system.
Next to the main channels there are small gullies in the system which connect the two channels at several places, see Figure 5-2. In the schematisation these gullies are neglected. It is assumed that these gullies are only important when two- and three-dimensional phenomena are taken into account.

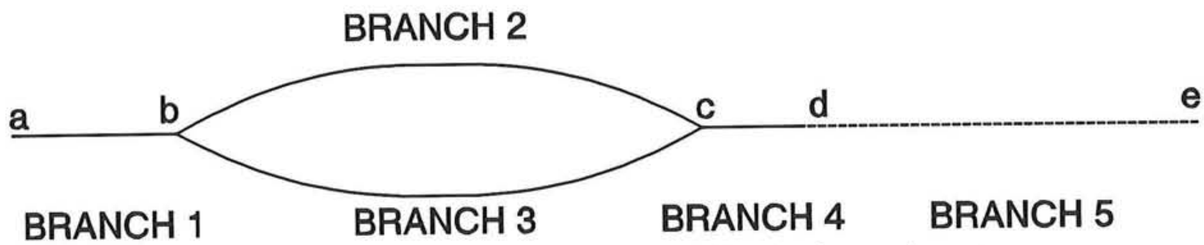

Figure 6-1: Configuration of an ebb and flood channel system

The model of the ebb and flood channel system consists of five channels:two channels, branch 2 and 3 are respectively the 'Everingen' and the 'Pas van Terneuzen'. Branch 1 represents the connections to the sea and branch 4 connects the system to another system (branch 5).
For a one dimensional approach each channel is characterized by four parameters, viz.:

1. length of the channel, L
2. width of the channel, $B(x)$
3. Chézy coefficient of the channel, $C(t)$
4. water depth of the channel, $a(x)$

The bed level of the channel is determined by the averaged water level and the water depth. As the morphodynamical development of the system is considered, the water depth is taken as the dependent variable.
So the three remaining parameters viz. the length, width and Chézy coefficient of the channels have to be chosen properly to create an ebb and flood channel system.

6.2.2 Parameters

Width of the channels:
For an ebb and flood channel system it is important that the width of the channels alter. When the width and depth of the ebb channel is constant and the same as the width of the flood channel, the channels are identical and no circulation will occur due to the width or depth of the channels.
However, if the width of a channel alter along the channel, circulation of water occurs as a result of the convective term in the momentum equation. This is shown in Annex 4 for a steady flow situation.
The change in width will also effect the water depth. It is likely to expect that a large width corresponds with a small water depth. This is in agreement with observations (Van Veen, 1950).

Chézy coefficient which depends on flow direction:
For an ebb and flood channel system it is also important that the Chézy value alters as circulation occurs when the Chézy coefficient depends on the flow direction.
The Chézy coefficient is chosen for the flood channel such that:

$$C_{flood} > C_{ebb}$$

and for the ebb channel such that:

$$C_{ebb} > C_{flood}$$

It follows that the ebb and flood flow will be unequal when the width of the channels is constant and there is no river discharge:
For the flood channel it yields:

$$\int_{flood} Q(t)\ \mathrm{d}t \ > \ \int_{ebb} Q(t)\ \mathrm{d}t$$

For the ebb channel it yields:

$$\int_{ebb} Q(t)\ \mathrm{d}t \ > \ \int_{flood} Q(t)\ \mathrm{d}t$$

When the two channels are considered as a whole and under the assumption the river discharge is zero, it follows:

$$\int_{ebb} Q(t)\ \mathrm{d}t \ = \ \int_{flood} Q(t)\ \mathrm{d}t$$

This is not the only effect. As a result of the Chézy coefficient which depends on flow direction, not only the discharges through the channels change but also the M_4 component is effected.
Fokkink (1995) demonstrates that the M_2 component remains the same when the following condition is fulfilled:

$$\frac{1}{C^2} = \frac{1}{2}\frac{1}{C_{ebb}^2} + \frac{1}{2}\frac{1}{C_{flood}^2} \tag{6.1}$$

In Annex 5 it is shown that as a result of the Chézy coefficient, which depends on the flow direction, the M_4 component is influenced.
As the combination of the M_2 and M_4 components determines the magnitude and direction of the net sediment transport, a Chézy coefficient which depends on the flow direction should be added to any estuarien model.

Length of the channels:
In general, the length of the ebb channel is larger than the length of the flood channel. As a result of different lengths of the ebb and flood channels, the discharges through the channels differ for identical cross-sections due to differences in resistance. The resistance depends on the Chézy coefficient, water depth and also the length of the channel.
As a result of the tidal propagation, there will be a phase difference between the channels.

6.3 Boundary conditions

6.3.1 General

Besides a proper geometry boundary conditions also have to be chosen.
The are two types of boundary conditions:

1. boundary conditions at the borders of the model (points **a** and **e**)
2. internal boundary conditions (points **b** and **c**)

Type 1. and 2. contain hydraulic and morphological boundary conditions. Type 1. conditions are necessary to drive the model.
Type 2. conditions are necessary to close the system of equations at the points where the channels bifurcate and where the channels congregate.

6.3.2 Boundary conditions at the borders of the model

seaside of the model (point a)

Hydraulic boundary condition:

At the seaside the water level is induced by two harmonic components viz. a semi-diurnal and a quarter-diurnal component.
This is a schematisation of reality as many harmonic components are present. A numerical calculation should be carried out at least over the period of the longest period of component present at the boundary. This is practically impossible to handle.
However, not all components are that important for the morphological development. Important components are the semi-diurnal and quarter-diurnal components. In Chapter 5 it is stated that the M_2, S_2 and N_2 are the dominating semi-diurnal components and M_4 and MS_4 are the dominating quarter-diurnal components.

The amplitudes and phases of these components are composed as shown in Figure 6-2.

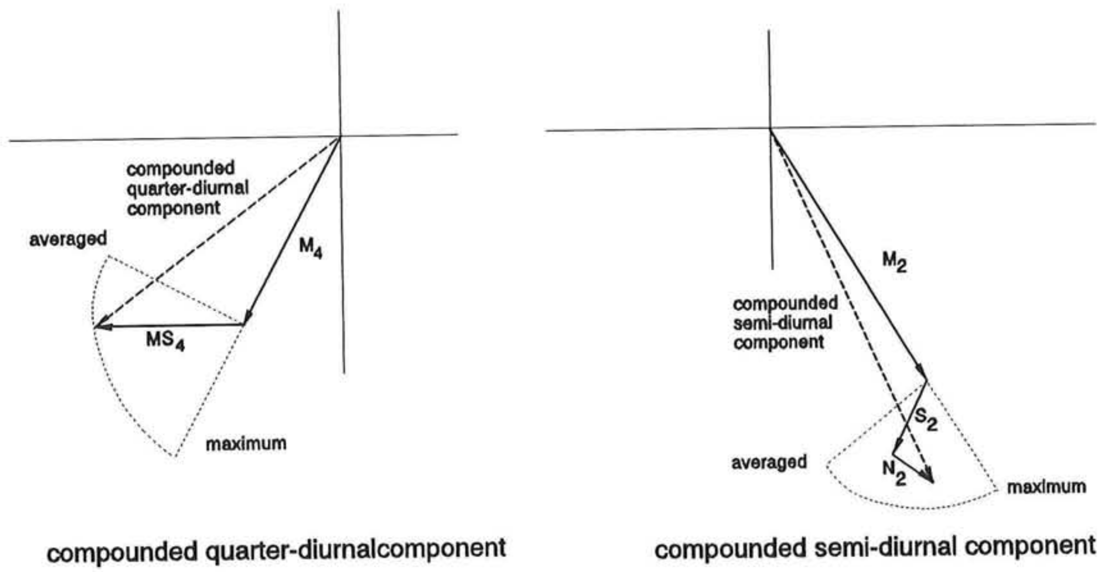

Figure 6-2:Compounded semi-diurnal and quarter-diurnal components

The amplitude and phase of the compounded semi-diurnal component are constructed by adding the M_2, S_2 and N_2 components to each other, their phase differences taking into account. The frequencies of the semi-diurnal components are taken the same as the M_2 component.
The compounded quarter-diurnal component is constructed by adding the M_4 and MS_4 to each other. The frequency the MS_4 component is taken the same as the MS_4 component, see also Figure 6-2.

Morphological boundary condition:
The phase difference between the M_2 and M_4 components is such that net sediment transport over a tidal period is directed landinwards. This implies one incoming characteristic at the model boundary, so one boundary condition must be prescribed. At the seaside the bed level or the sediment transport has to be fixed as boundary condition.

*landside of the model (point **e**)*

Hydraulic boundary condition:
As there is no river discharge assumed ($Q_{river} = 0$), at the end of the model the discharge is prescribed ($Q = 0$).

Morphological boundary condition:
There is no incoming characteristic at the model boundary, so a boundary condition does not have to be prescribed.

6.3.3 Internal boundary conditions

Nodal point relation

The are two nodal points in the model. The nodal point **b** is a *bifurcation* during the flood period and turns into a *confluence* during the ebb period. The nodal point **c** is a confluence during the flood period and turns into a bifurcation during the ebb period.
At a nodal point, regardless whether it is a confluence or a bifurcation, the following two conditions have to be satisfied:

1. mass-balance of water: $$\sum_{i=1}^{m} Q_i = 0 \qquad (6.2)$$

2. mass-balance of sediment: $$\sum_{i=1}^{m} S_i = 0 \qquad (6.3)$$

herein

Q_i	=	discharge from branch *i* to the nodal point	[m³/s]
S_i	=	sediment transport from branch *i* to the nodal point	[m³/s]
m	=	number of branches connected to the nodal point	[-]

For a *confluence* the system of equations is closed.

For a *bifurcation*, however, two extra equation are needed. An equation which

describes that the waterlevel is the same for all branches at the nodal point. The other equation describes the distribution of sediment over the branches.
Wang (1993) derived a conditionally stable nodal point relation of a form equal to Equation (6.4).
The k-value in Equation (6.4a) ... (6.4c) determines whether or not the nodal point relation is stable, but it also determines the time scale of the morphological process and the equilibrium depths of the channels when the widths of the channels differ at the nodal point.
The nodal point relation is stable when the sediment distribution over the branches is such that both channels stay open. The nodal point relation is stable when $k > n/3$ (where n is the exponent in the power law for sediment transport).
In the Western Scheldt ebb and flood channels exist for a long time, so it is likely to expect that both channels stay open. A stable nodal point relation is thus required.

The nodal point **b** connects the branches 1, 2 and 3 and for this point the following equations are prescribed:

Branch 1:
$$\frac{s_2}{s_3} = \left(\frac{Q_2}{Q_3}\right)^k \cdot \left(\frac{B_2}{B_3}\right)^{1-k} \tag{6.4a}$$

Branch 2:
$$\frac{s_1}{s_3} = \left(\frac{Q_1}{Q_3}\right)^k \cdot \left(\frac{B_1}{B_3}\right)^{1-k} \tag{6.4b}$$

Branch 3:
$$\frac{s_1}{s_2} = \left(\frac{Q_1}{Q_2}\right)^k \cdot \left(\frac{B_1}{B_2}\right)^{1-k} \tag{6.4c}$$

Nodal point **c** can be treated in a similar way.

6.4 Sediment transport

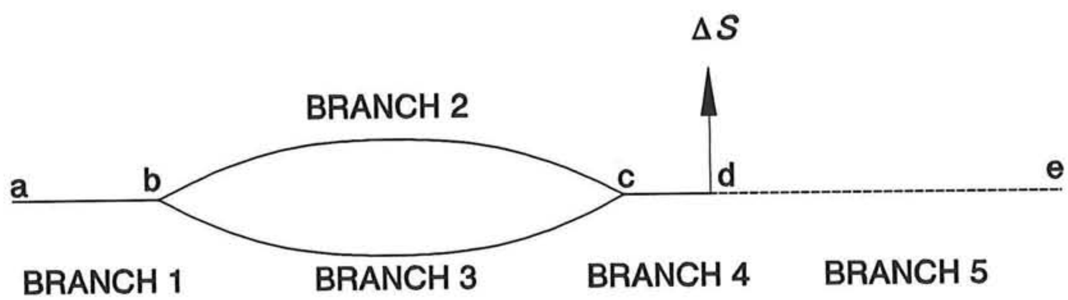

Figure 6-3: Withdraw of sediment

The tidal prism of the ebb and flood channel system is small compared to the

tidal prism of the estuary. In order to control the flow velocities in the ebb and flood channel system, a basin is added to the model to simulate the tidal prism of the estuary (branch 5). As a result of the prescribed boundary condition (point **a**) the net sediment transport is directed landinwards. This net transport will be withdrawn from the basin. In this way the closed boundary will not influence the dynamic equilibrium profile.
The sediment transport depends on the local hydraulic conditions only. The sediment transport is calculated with the Engelund-Hansen formula (so $n=5$). The total amount of sediment transport in the model is adjusted to the reference case by changing e.g. the diameter of the sand.

6.5 Schematisation of the reference case

6.5.1 General

In the previous Sections the important parameters and boundary conditions have been described. In this Section numerical values are assigned. Figure 6-4 gives the final result.
In Chapter 7 a number of parameters of this model are slightly changed in order to see the impacts on morphological behaviour.

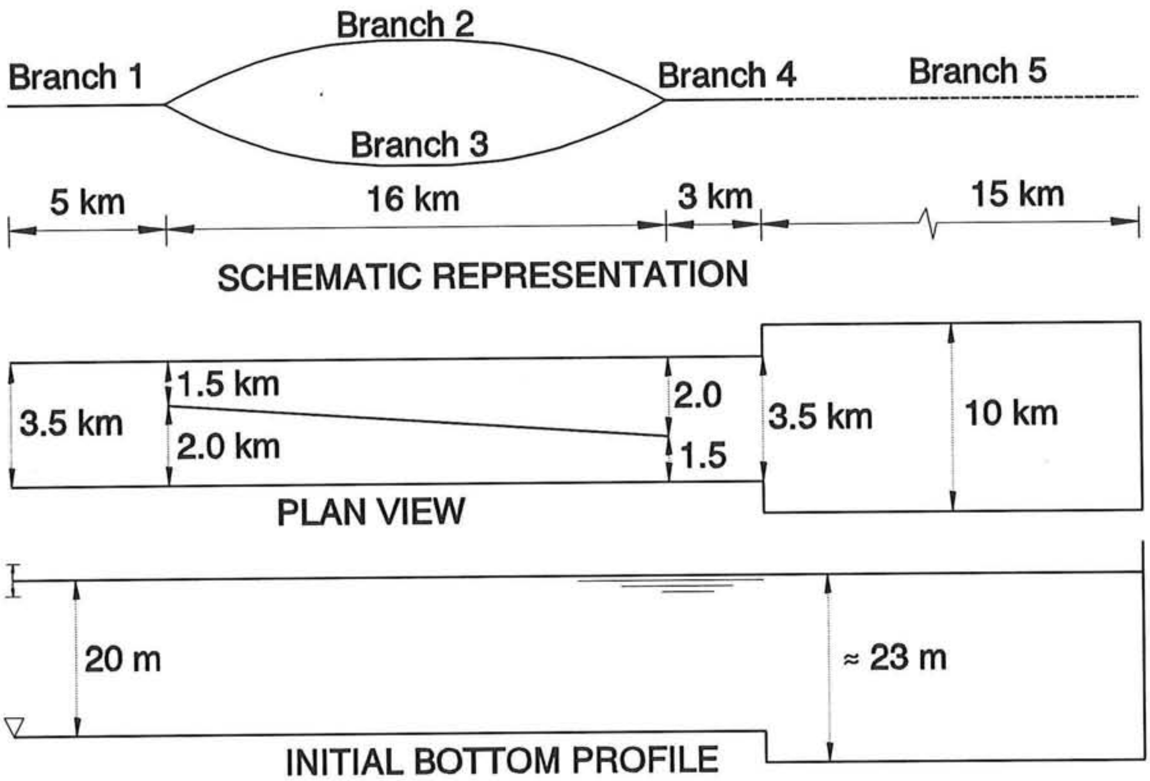

Figure 6-4: Schematic representation

6.5.2 Geometry of the channels

The flow width is taken equal to the storage width. The size of the basin (branch 5) is taken such that the tidal prism is roughly the same as in the reference case, see Figure 6-4.

Length of the channels
In Figure 6-4 the length of branches 2 and 3 is 16 km. In this way the ebb and flood channels are symmetrical.

Width of the channels

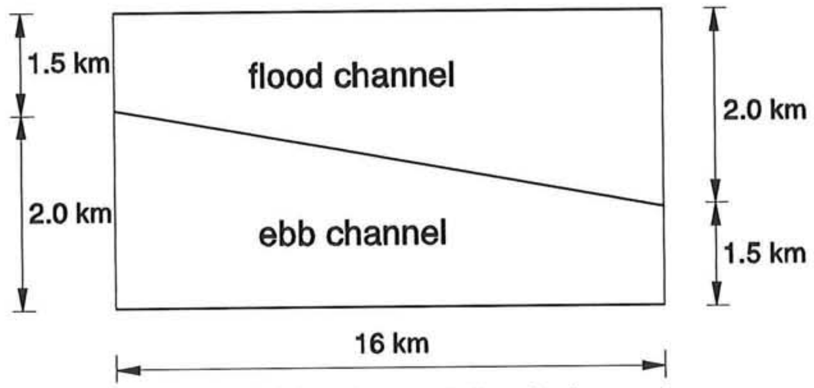

Figure 6-5: Change in width, ebb and flood channels

The banks are fixed. There is a gradient in width, see Figure 6-5. The change in width is taken linear for simplicities sake only.

Chézy coefficient
At first the Chézy coefficient is taken constant (not dependent of the flow velocity) and the same for both channels, viz. 50 $m^{1/2}/s$.

initial bed level
The bed level in the channels will be calculated with SOBEK. The initial value of the depth is 20 m.

6.5.3 Boundary conditions

Hydraulic characteristics
At the seaside a water level is induced by two harmonic components viz. a semi-diurnal and a quarter-diurnal component.

$$h(t) = 2.00 \cdot \cos(\omega \cdot t - \tfrac{\pi}{2}) + 0.20 \cdot \cos(2 \cdot \omega \cdot t - \tfrac{\pi}{2})$$

$$\text{herein: } \omega = \frac{1}{44700} \quad [s^{-1}]$$

The amplitudes of the semi- and quarter diurnal component are chosen between the averaged and maximum value possible and the phases are chosen such that the net sediment transport is directed landinwards.
At the landside end of the model (point **e**) the discharge is zero.

Morphological characteristics
At the seaside the bed level is fixed at NAP - 20 m.

Nodal point relation
For k the value of 2.5 is chosen as some experimental data (Roosjen and Zwanenburg, 1995) show that k may be in this order.

7 SOBEK computations

7.1 General

The model SOBEK has been used to compute the morphological development. Annex 6 describes, in brief, the way SOBEK treats an estuarine morphological computation.
In general a numerical model has the disadvantage that it is not immediately clear in what way the various parameters influence the results. For this purpose a parameter study has to be performed, in which each parameter is varied independently. In order to investigate the influences of the various parameters on the morphological development of the ebb and flood channels, the model as described in Chapter 6 will be taken as scenario 1, and various parameters will be varied. In this Chapter six scenarios are worked out.
First the numerical parameters for the model SOBEK are presented. Subsequently the results of the scenarios are shown and discussed.
Note: For the computations the computerprogram SOBEK (development version 1.00) is used. As the program is still in development the integrated sediment transport as is shown in graphs for Annex 7 ... 12 shows sometimes a wrong value at the end of a branch. However, SOBEK uses the right value to compute the bed level.

7.2 Numerical parameters of SOBEK

spatial step

Figure 6-4 shows the geometry of the model.
For all scenarios the following spatial step sizes are used:

Branch	spatial step (Δx)	number of cells
1	1 km	5
2	1 km	16
3	1 km	16
4	1 km	3
5	15 km	1

To make sure the spacial step size does not influence the solution, the spatial step size has been checked by verifying a same computation with the half spatial step size.

hydraulic module

boundary conditions:
branch 1 at $x=0$ m:

$$h(t) = 2.00 \cdot \cos(\omega \cdot t - \frac{\pi}{2}) + 0.20 \cdot \cos(2 \cdot \omega \cdot t - \frac{\pi}{2})$$

$$\text{herein: } \omega = \frac{1}{44700} \quad [s^{-1}]$$

branch 5 at $x=15$ km: $Q(t) = 0$

numerical parameters of the hydraulic module:

Δt	= 300 s (Courant number ≈ 4)
T_p	= 44700 s
adaptation time	= 2 tides

To make sure the time step does not influence the solution, the time step has been checked by verifying a same computation with the half time step.

The storage width of the channels is chosen equal to the flow width of the channels.

transport and bed-level module

boundary conditions:
branch 1 at $x=0$ m: z_b = NAP - 20 m
The morphological development of branch 5 is not taken into account as this branch is only added to simulate the tidal prism.
In branch 5 at $x=0$ m sediment is withdrawn to make sure the branch will not fill up with sediment (ΔS = 2.125 m^3/s).

numerical parameters of the bed-level module:

Δt_{morph}	= 100 tides = 100 · 44700 s
	≈ 52 days (Courant number ≈ 0.5)

All computations start at the January 1st 1990 (1990-01-01).

numerical parameters of the transport module:
For the sediment transport the Engelund Hansen formula is used, so $n=5$.

The nodal point relation reads: $\dfrac{S_1}{S_2} = \left(\dfrac{Q_1}{Q_2}\right)^k \cdot \left(\dfrac{B_1}{B_2}\right)^{1-k}$

In this relation $k=2.5$ is chosen.
The diameter of the sand: D_{50} = 200 μm in the computation.

7.3 Scenarios

Six scenarios are worked out. The parameters used for the different scenarios are shown in table 7-1.

scenario			1	2	3	4	5	6
flood channel (branch 2)								
width	begin	[km]	1.5	1.75	1.75	1.75	1.5	1.5
	end	[km]	2.0	1.75	1.75	1.75	2.0	2.0
Chézy coefficient	flood	[$m^{½}/s$]	50	50	57.15	50	57.15	57.15
	ebb	[$m^{½}/s$]	50	50	45	50	45	45
length of channel		[km]	16	16	16	14	16	16
ebb channel (branch 3)								
width	begin	[km]	2.0	1.75	1.75	1.75	2.0	2.0
	end	[km]	1.5	1.75	1.75	1.75	1.5	1.5
Chézy coefficient	flood	[$m^{½}/s$]	50	50	45	50	45	45
	ebb	[$m^{½}/s$]	50	50	57.15	50	57.15	57.15
length of channel		[km]	16	16	16	18	16	16
Branch 1 $x=0$ km								
M_2 component	amplitude	[m]	2.0	2.0	2.0	2.0	2.0	2.0
	phase $\alpha 1$	[°]	+90	+90	+90	+90	+90	+90
M_4 component	amplitude	[m]	0.2	0.2	0.2	0.2	0.2	0.2
	phase $\alpha 2$	[°]	+90	+90	+90	+90	+90	+137.5

Table 7-1: Parameters of the different scenarios

In scenario 1 the effect of the change in width of the ebb and flood channels is considered. Scenario 2 considers the ebb and flood channels with a constant width. In scenario 3 the Chézy coefficient depends on the flow direction. In Scenario 4 the length of the ebb channel is larger than the flood channel. Scenario 5 considers the change in width of the ebb and flood channels and a Chézy coefficient which depends on the flow direction. In scenario 6 the boundary condition at the seaside is changed.

As the discharge of the River Scheldt is very small, compared to the discharge due to the tidal motion at the 'Pas van Terneuzen - Everingen', this parameter is not varied, so for all scenarios $Q_{river}=0$.

7.4 Scenario 1: Change in width of the channels

7.4.1 General

In this scenario the width of the ebb and flood channels is taken as is shown in Figure 6-5, see also Table 7-1.
In this section the numerical results are presented and discussed.
Initial bed level NAP - 20 m for all branches, see Annex 7.

7.4.2 Results

<u>Bed level</u>

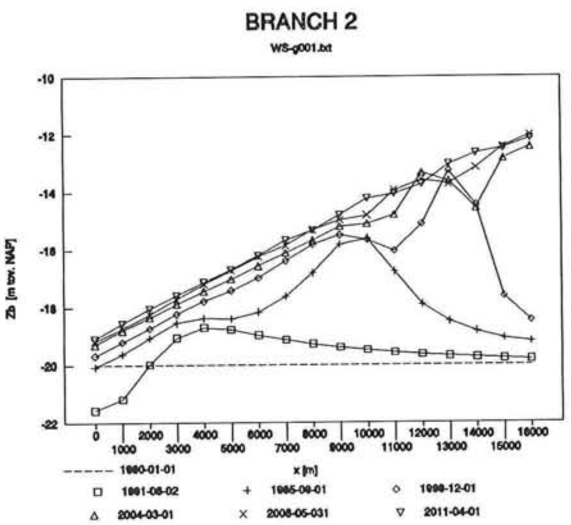

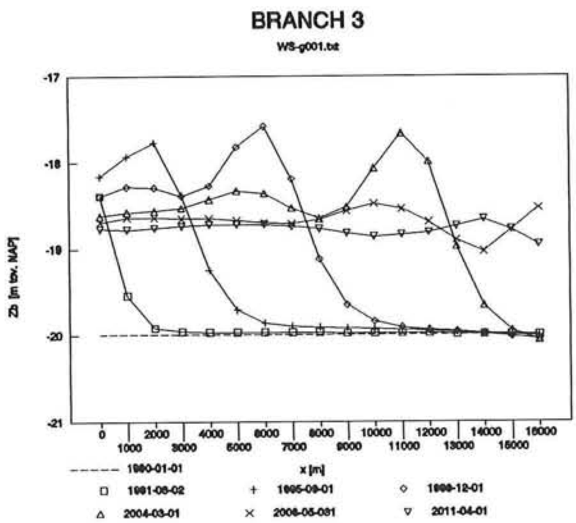

Figure 7-1:Bed levels branch 2 and 3

Annex 7 shows the development of the bottom profile as a function of time.
In brief a description is given.

branch 1:	Within 5 years a linear inclining profile develops.		
	bed level	begin	end
	NAP	-20 m	-18.9 m
		(boundary condition)	
	bottom slope: $2.2 \cdot 10^{-4}$		

branch 2: A shock-wave propagates through the branch and finally (after ≈ 25 years) a nearly linear inclining profile is formed.

bed level	begin	end
NAP	-19.1 m	-12.2 m

bottom slope: $4.3 \cdot 10^{-4}$

branch 3: First a shock-wave propagates through the branch and finally (after ≈ 20 years) a nearly horizontal profile is formed.

bed level	begin	end
NAP	-18.8 m	-19.0 m

bottom slope: $0.1 \cdot 10^{-4}$

branch 4: A nearly horizontal profile at NAP ≈ -15 m develops.

bed level	begin	end
NAP	-15.2 m	-14.3 m

bottom slope: $3.0 \cdot 10^{-4}$

From branch 3 it is determined that the propagation velocity of a disturbance at the bed is ≈ 1 km/year. This agrees well with an analytical estimation:

$c_{bed} = n \dfrac{S_i}{a} =$ 1.4 km/year.

Discharges

Table I of Annex 7 shows a net transport of water over a tidal period landinwards, see branches 1 and 4. This is odd as the tidal basin is closed. However, as a result of the withdrawal of sediment, also water is withdrawn from the system. The net transport of water is about 150 m^3/s, this is equal to an averaged velocity of 0.002 m/s and can thus be neglected.

Branch 2 is flood dominated, the net volume of water decreases in time from 7 to 3 % of the flood volume of the flood channel. Branch 3 is ebb dominated, the net volume of water decreases from 5 to 1 % of the flood volume of the ebb channel.

The flood channel is flood dominated and the ebb channel is ebb dominated as a result of the change in width of the ebb and flood channels, see Annex 4.

In branch 2 a linear inclining bed profile develops, as a result of this, the convective term in the momentum equation decreases and thus the net transport of water decreases, see Annex 4.

Annex 7 shows also a graph of the discharges as a function of time at different places for the end of the calculation (2011-04-01). The discharges of the ebb channel (branch 3) is larger than that of the flood channel.

The discharges at branch 1 are larger than the discharges at branch 4 as a result of storage in branch 2 and 3.

Water levels and tidal components

Annex 7 shows also a graph of the water levels as a function of time at different places for the end of the calculation (2011-04-01). There is a significant distortion further landinwards.

An harmonic analysis is used to determine the M_2, M_4 and M_6 components present in the tidal curve. The results are presented in Annex 7, Table II. The amplitudes of the M_2 and M_4 components in branch 4 are resp. 11% and 100% larger than for branch 1.

Table III, Annex 7, shows the phase difference between the M_4 and M_2 components and between the M_6 and M_2 components. As a result of the bed profiles that develop in time the phase differences change in time as is shown in the following table:

time\branch	branch 1 x = 4 km	branch 2 x = 8 km	branch 3 x = 8 km	branch 4 x = 2 km
1991-06-02	0	0	0	0
1995-09-01	-0.4	-1.1	-0.9	-0.9
1999-12-01	-0.9	-4.4	-5.1	-5.3
2004-03-01	-1.0	-5.2	-6.5	-7.3
2008-05-31	-0.9	-5.9	-7.0	-9.3
2011-04-01	-0.9	-5.9	-7.0	-6.0

Table 7-2: Change of phase difference between M_2 and M_4 in time [°]

In time the phase difference between the M_2 and M_4 components decreases. As a result of this the sediment transport also changes.

Annex 7 shows for the different points the water levels as a function of the tidal period at different times.

Sediment transport

Annex 7 shows the sediment transport as a function of the tidal period.

As a result of the bed profiles that develop in the branches, the flow velocities change and thus the sediment transport changes in time. Table IV shows the volumes of sediment transported during the ebb and flood period.

Integrated sediment transport

In Annex 7 also the integrated sediment transport at all places in the branches are shown for given times.
There is a net sediment transport landinwards for all the branches.
At the end of the calculation 45% of the net sediment transport passes branch 2 and 55% passes branch 3.
For the points: branch 1 $x=0$ m, branch 2 $x=8$ km, branch 3 $x=8$ km, branch 4 $x=2$ km the development of the integrated sediment transport as a function of time is shown.
At the end of the calculation there is still a gradient in the integrated sediment transport, so the dynamic equilibrium profile is still not reached.

7.4.3 Conclusions

Due to the prescribed change of width for the ebb and flood channels, a linear inclining bed profile develops for branch 2 and a nearly horizontal bed profile develops for branch 3.
This is explained in the following. As a result of a decreasing tidal volume further landinwards a nearly linear inclining bed profile develops (see also scenario 2). Due to the change in width also a linear inclining bed profile develops from a small width to a large width. These two effects intensify each other for branch 2. However, for branch 3 these effects weaken each other and a nearly horizontal bed profile develops.

7.5 Scenario 2: Constant width of the channels

7.5.1 General

In order to get rid of the shock-wave the following initial bed level conditions, in [m] with respect to NAP, are applied (see also annex 8):

	begin	end
branch 1	-20	-18.9
branch 2	-18.9	-15
branch 3	-18.9	-15
branch 4	-15	-15
branch 5	-17	-17

The width of the ebb and flood channels is taken 1.75 km, see also Table 7-1.
In this section the numerical results are presented and discussed.

7.5.2 Results

<u>Bed level</u>

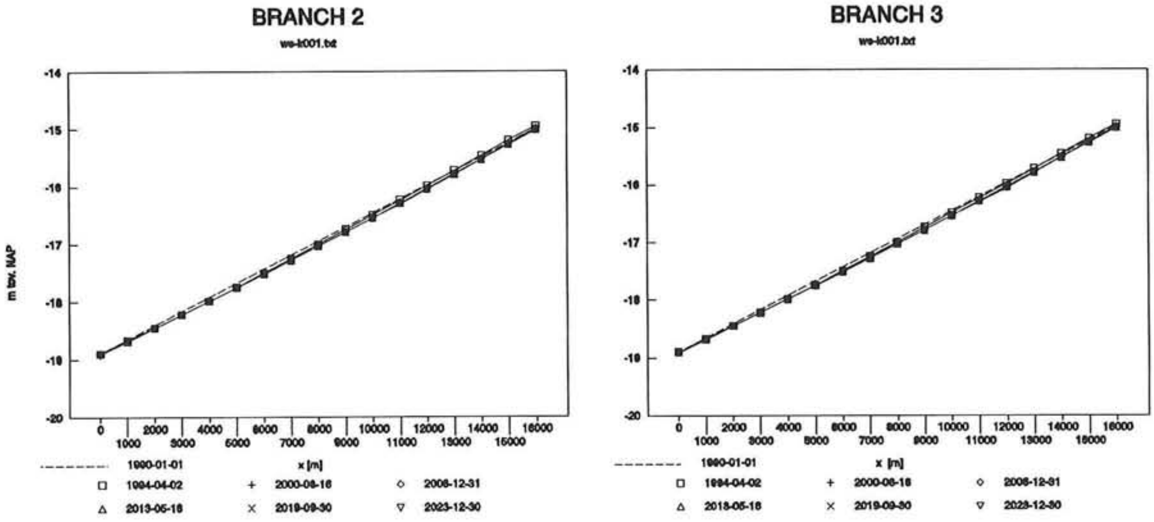

Figure 7-2:Bed levels branch 2 and 3

Annex 8 shows the development of the bottom profile as a function of time.

branch 1: The initial condition is chosen properly so there is no change in the bed level.

bed level	begin	end
NAP	-20 m	-18.9 m
	(boundary condition)	

bottom slope: $2.2 \cdot 10^{-4}$

branch 2 and 3: Both channels develop identical, as was expected as the channels are symmetric. The initial conditions are chosen properly, so there is less change in the bed levels. The bed levels do not develop exactly linear, more convex.

bed level	begin	end
NAP	-18.9 m	-15.0 m

bottom slope: $2.4 \cdot 10^{-4}$

branch 4: A linear inclining profile develops.

bed level	begin	end
NAP	-15 m	-14.2 m

bottom slope: $2.7 \cdot 10^{-4}$

Discharges

Annex 8 shows a graph of the discharges at branch 1 $x=4$ km, branch 2 $x=8$ km, branch 3 $x=8$ km, branch 4 $x=2$ km. The discharges are the same for branch 2 and 3. Table I of Annex 8 shows the volumes of water which pass a channel during the ebb and flood period at the end of the calculation (2023-12-30). The volumes are the same for the ebb and flood channels.

Water levels and tidal components

Annex 8 shows the water levels as a function of the tidal period at 4 places.
There is a strong tidal distortion as a result of the bed profiles of branches 2 and 3. As a result of the linear inclining profile the convective term in the momentum equation becomes important and a lot M_4 is generated.
The harmonic analysis confirms this, see Table II of Annex 8.

Sediment transport

Annex 8 shows the sediment transport as a function of the tidal period. Table IV shows the volumes of sediment transported during the ebb and flood period.

Integrated sediment transport

In Annex 8 also the integrated sediment transport at all places in the branches are shown for given times. Again branch 2 and 3 are identical.
There is a net sediment transport landinwards for all branches. During the computation 50% of this net transport passes branch 2 and 50% passes branch 3.
For the points: branch 1 $x=0$ m, branch 2 $x=8$ km, branch 3 $x=8$ km, branch 4 $x=2$ km the development of integrated sediment transport as a function of time is shown.
At the end of the calculation there is almost no gradient in the integrated sediment transport, so the dynamic equilibrium profile is almost reached.

7.5.3 Conclusions

For ebb and flood channels with a constant width a nearly linear inclining bed profile develops, as a result of the decrease of the tidal volume further landinwards.

7.6 Scenario 3:Chézy coefficient depends on flow direction

7.6.1 General

Annex 9 shows the initial bed level conditions that are applied.
In this scenario the width of the channels is taken constant. The values taken for the Chézy coefficient are shown in Table 7-1.
In this section the numerical results are presented and discussed.

7.6.2 Results

<u>Bed level</u>

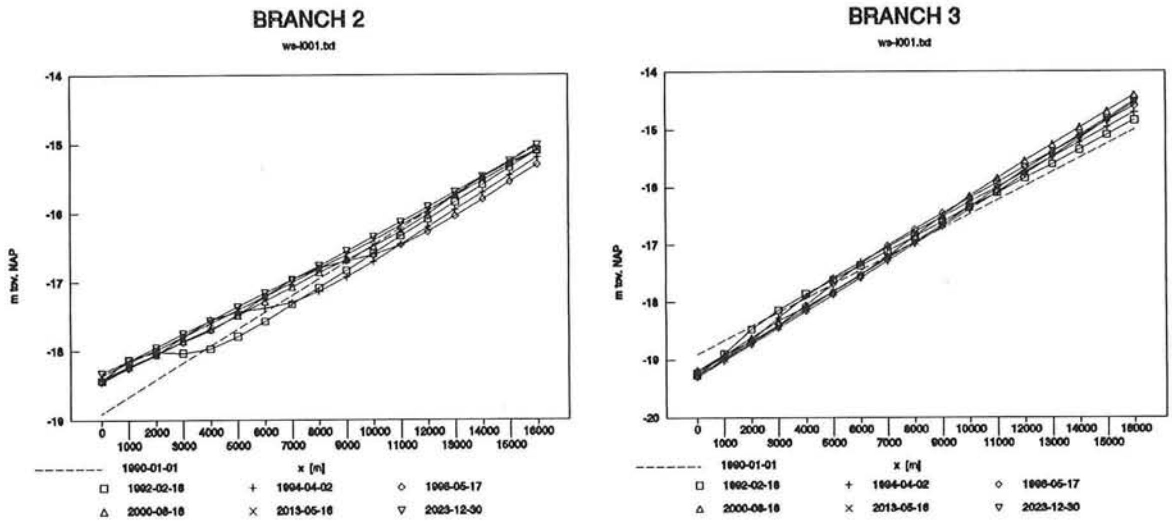

Figure 7-3:Bed levels branch 2 and 3
Annex 9 shows the bed profile at certain times.

branch 1: The initial condition is chosen properly so there is no change in the bed level.

bed level	begin	end
NAP	-20 m	-18.9 m
	(boundary condition)	

bottom slope: $2.2 \cdot 10^{-4}$

branch 2: end of computation:

bed level	begin	end
NAP	-18.3 m	-15.0 m

bottom slope: $2.06 \cdot 10^{-4}$

A shock-wave propagates through the channel.

branch 3:	end of computation:		
	bed level	begin	end
	NAP	-19.3 m	-14.5 m
	bottom slope: $3.0 \cdot 10^{-4}$		
	An expansion-wave propagates through the channel.		
branch 4:	end of computation:		
	A linear inclining profile develops.		
	bed level	begin	end
	NAP	-15.0 m	-14.2 m
	bottom slope: $2.7 \cdot 10^{-4}$		

Discharges

As a result of the properly chosen initial bed levels, the discharges are almost the same for all times.
Branch 2 is flood dominated, the net volume is 25% of flood volume. Branch 3 is ebb dominated, the net volume is 30% of flood volume, see Table I of Annex 9.

Water levels and tidal components

Annex 9 shows the water levels at different places as a function of the tidal period. Table II of this annex shows the tidal components.

Sediment transport

Annex 9 shows the sediment transport as a function of the tidal period. Table IV shows the volumes of sediment transported during the ebb and flood period.

Integrated sediment transport

Annex 9 also shows the integrated sediment transport at all places in the branches for a number of times.
There is a net sediment transport landinwards for all the branches.
At the end of the computation 65% of this net transport passes branch 2 and 35% passes branch 3.
For the points: branch 1 $x=0$ m, branch 2 $x=8$ km, branch 3 $x=8$ km, branch 4 $x=2$ km the development of integrated sediment transport as a function of time is shown.
At the end of the calculation there is still a small gradient in the integrated sediment transport, so the dynamic equilibrium profile is not reached completely.

7.6.3 Conclusions

Due to the Chézy coefficient which depends on the flow direction, the bed slope of the flood channel becomes flatter and the bed slope of the ebb channel becomes steeper.

7.7 Scenario 4: Different lengths of the channels

7.7.1 General

The length of the flood channel is taken 14 km, the length of the ebb channel is taken 18 km.
Annex 10 shows the initial bed level conditions that are applied.
In this section the numerical results are presented and discussed.

7.7.2 Results

Bed level

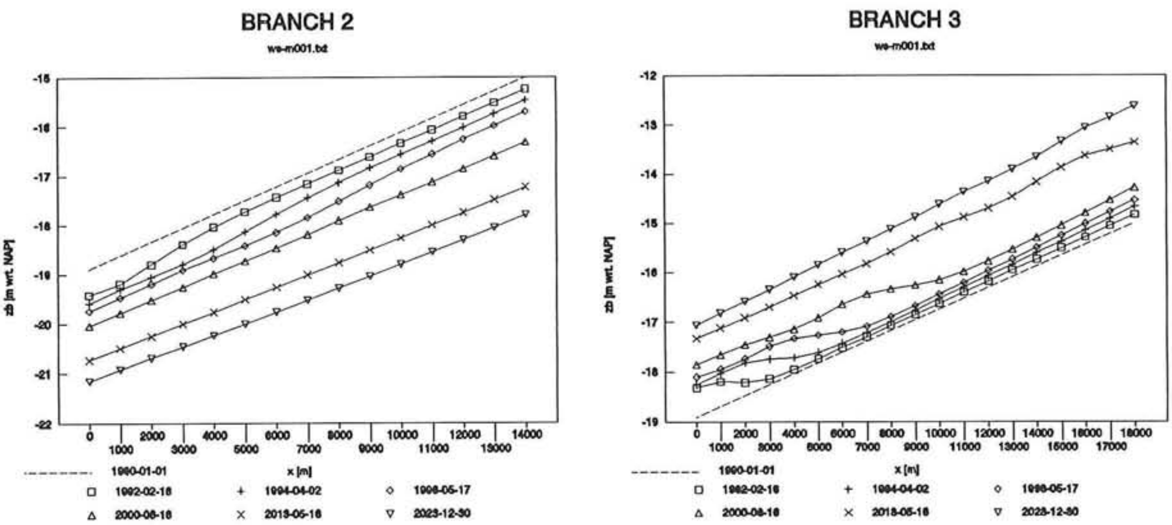

Figure 7-4:Bed levels branch 2 and 3

Annex 10 shows the bed profile of the branches at certain times.

branch 1: The initial condition is chosen properly so there is no change in the bed level.

bed level	begin	end
NAP	-20 m	-18.9 m
	(boundary condition)	

bottom slope: $2.2 \cdot 10^{-4}$

branch 2:	end of computation:		
	bed level	begin	end
	NAP	-21.2 m	-17.8 m
	bottom slope: $2.39 \cdot 10^{-4}$		
branch 3:	end of computation:		
	bed level	begin	end
	NAP	-17.1 m	-12.6 m
	bottom slope: $2.47 \cdot 10^{-4}$		
branch 4:	end of computation:		
	A linear inclining profile develops.		
	bed level	begin	end
	NAP	-15.0 m	-14.2 m
	bottom slope: $2.7 \cdot 10^{-4}$		

Discharges

Annex 10 shows the discharges at the end of the computation. The discharges in branch 2 are significantly larger than branch 3.
Table I of Annex 10 shows the volumes of water that passes a channel over the ebb and flood period. As a result of the morphological development, the discharges increase for branch 2 and decrease for branch 3.
Branch 2 is ebb dominated and branch 3 is flood dominated, see Table II.

Water levels and tidal components

For the points: branch 1 $x=0$ m, branch 2 $x=8$ km, branch 3 $x=8$ km, branch 4 $x=2$ km, Annex 10 shows the water levels as a function of the tidal period. Table II of this annex shows the tidal components.

Sediment transport

Annex 9 shows the sediment transport as a function of the tidal period. Table IV shows the volumes of sediment transported during the ebb and flood period.

Integrated sediment transport

Annex 10 also shows the integrated sediment transport at all places in the branches for a number of times.
There is a net sediment transport landinwards for all branches.
At the end of the computation 75% of this net transport passes branch 2 and 25% passes branch 3.
For the points: branch 1 $x=0$ m, branch 2 $x=8$ km, branch 3 $x=8$ km, branch 4 $x=2$ km the development of integrated sediment transport as a

function of time is shown.
At the end of the calculation there is still a gradient in the integrated sediment transport for branch 2 and 3, so the dynamic equilibrium profile is not reached.

7.7.3 Conclusions

As a result of the small length of the flood channel compared to the ebb channel, the flood channel transports most of the water and most of the integrated sediment transport. The ebb channel becomes shallow.

7.8 Scenario 5: Change of width and a Chézy coefficient which depends on the flow direction

7.8.1 General

This scenario is a combination of scenario 1 and 3.
Annex 11 shows the initial bed level conditions that are applied.
In this section the numerical results are presented and discussed.

7.8.2 Results

<u>Bed level</u>

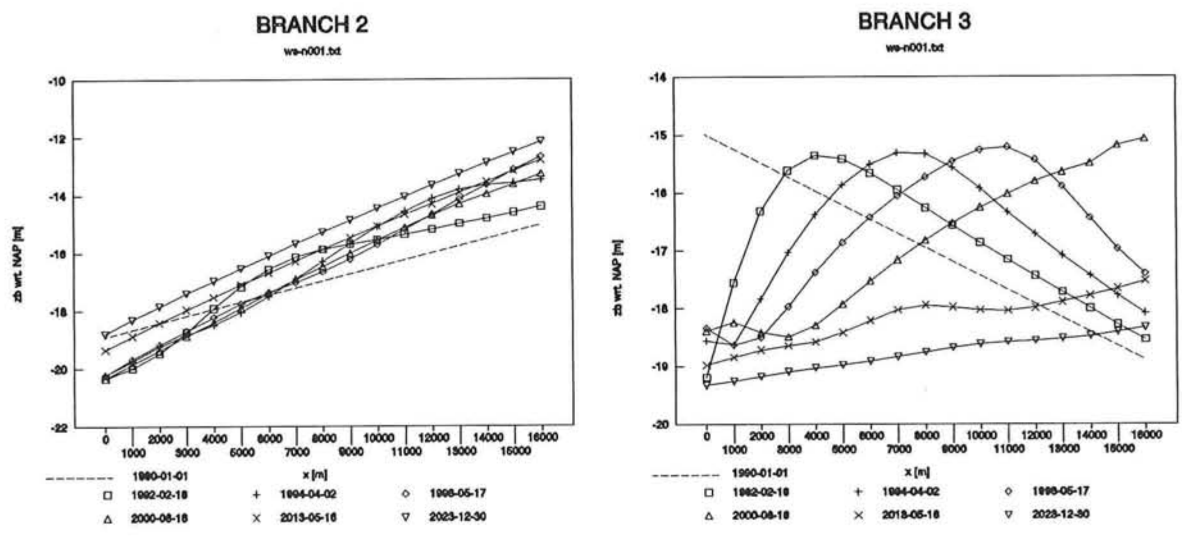

Figure 7-5:Bed levels branch 2 and 3
Annex 11 shows the bed profile at certain times.

branch 1:	The initial condition is chosen properly so there is no change in the bed level.		
	bed level	begin	end
	NAP	-20 m	-18.9 m
		(boundary condition)	
	bottom slope: $2.2 \cdot 10^{-4}$		
branch 2:	end of computation:		
	bed level	begin	end
	NAP	-18.8 m	-12.4 m
	bottom slope: $4.0 \cdot 10^{-4}$		
branch 3:	end of computation:		
	bed level	begin	end
	NAP	-19.3 m	-18.3 m
	bottom slope: $0.63 \cdot 10^{-4}$		
branch 4:	end of computation:		
	A linear inclining profile develops.		
	bed level	begin	end
	NAP	-15.0 m	-14.1 m
	bottom slope: $3.0 \cdot 10^{-4}$		

The initial value of the bed level of branch 3 has been chosen far from the equilibrium bed level. However, the bed level is quick adapted.

Discharges

Annex 11 shows the discharges at the end of the computation. Branch 2 is flood dominated and branch 3 is ebb dominated.
At the end of the computation branch 2 and branch 3 transport the same volume of water during the flood period. However, during the ebb period most of the water is transported by branch 3 (ebb channel), see Table I of Annex 11. This phenomenon is due to the size of the cross-sections and the Chézy coefficient which depends on the flow direction.

Water levels and tidal components

For the points: branch 1 $x=0$ m, branch 2 $x=8$ km, branch 3 $x=8$ km, branch 4 $x=2$ km, Annex 11 shows the water levels as a function of the tidal period. Table II of this annex shows the tidal components.

Sediment transport

Annex 11 shows the sediment transport as a function of the tidal period. Table IV shows the volumes of sediment transported during the ebb and flood period.

Integrated sediment transport

Annex 11 also shows the integrated sediment transport at all places in the branches for a number of times.
There is a net sediment transport landinwards for all branches.
At the end of the computation 60% of this net transport passes branch 2 and 40% passes branch 3.
Annex 11 also shows the development of the integrated sediment transport as a function of time.
At the end of the calculation there is still a small gradient in the integrated sediment transport for branch 2 and 3, so the dynamic equilibrium profile is not reached.

7.8.3 Conclusions

Due to the Chézy coefficient which depends on the flow direction and the change in width of the channels, the cross-section of branch 3 becomes bigger than branch 2. As a result of this, branch 2 and 3 transport the same volume of water during the flood period. During the ebb period branch 3 transports most of the water.

7.9 Scenario 6: Phase difference M_2 and M_4 component at the boundary

7.9.1 General

Annex 12 shows the initial bed level conditions that are applied.
In this scenario the effect of the phase difference between the M_2 and M_4 component at the boundary is studied. A comparison is made with scenario 5.
In this section the numerical results are presented and discussed.

7.9.2 Results

Bed level

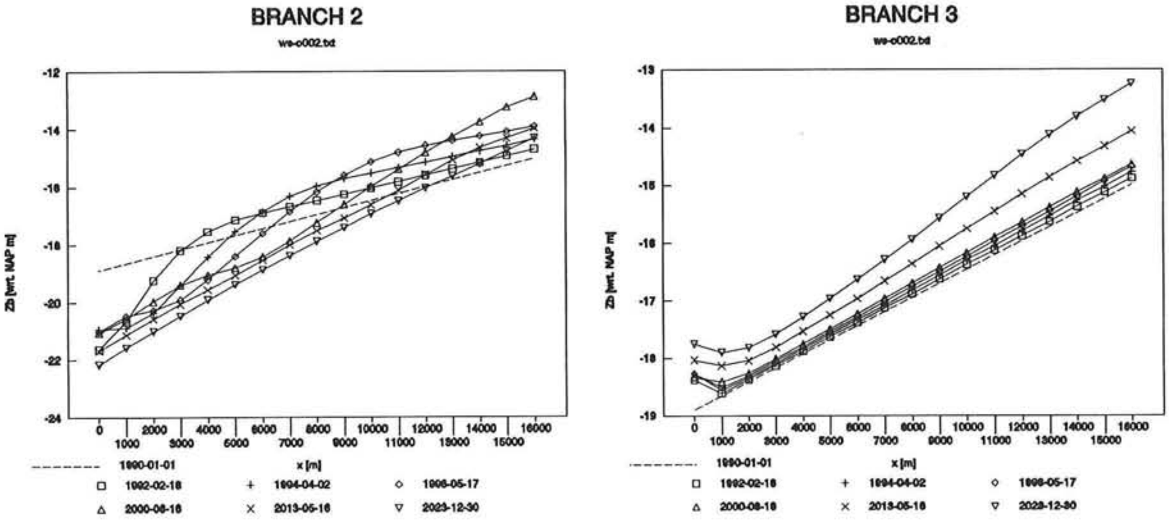

Figure 7-6:Bed levels branch 2 and 3

Annex 12 shows the bed profile at certain times.

branch 1: The initial condition is chosen properly so there is no change in the bed level.

bed level	begin	end
NAP	-20 m	-19.0 m
	(boundary condition)	

bottom slope: $2.0 \cdot 10^{-4}$

branch 2: end of computation:

bed level	begin	end
NAP	-22.2 m	-14.3 m

bottom slope: $4.9 \cdot 10^{-4}$

branch 3: end of computation:

bed level	x=1 km	end
NAP	-17.8 m	-13.2 m

bottom slope: $2.8 \cdot 10^{-4}$

The bed profile is curved at the beginning of this branch.

branch 4: end of computation:

A linear inclining profile develops.

bed level	begin	end
NAP	-15.5 m	-14.6 m

bottom slope: $3.2 \cdot 10^{-4}$

Discharges

Annex 12 shows the discharges at the end of the computation. Branch 2 is flood dominated and branch 3 is ebb dominated.
The volumes of water that passes the branches are shown see Table I of Annex 12.

Water levels and tidal components

For the points: branch 1 $x=0$ m, branch 2 $x=8$ km, branch 3 $x=8$ km, branch 4 $x=2$ km, Annex 12 shows the water levels as a function of the tidal period. Table II of this annex shows the tidal components.
Table II of this annex shows that the amplitude of the M_4 component at branch 4 $x=2$ km is 15 % smaller than in scenario 5. However, the M_6 component is about 15 % bigger than in scenario 5 for that point.

Sediment transport

Annex 9 shows the sediment transport as a function of the tidal period. Table IV shows the volumes of sediment transported during the ebb and flood period.

Integrated sediment transport

Annex 12 also shows the integrated sediment transport at all places in the branches for a number of times.
There is a net sediment transport landinwards for all branches.
At the end of the computation 115% of this net transport passes branch 2 and 15% returns via branch 3 to point **b**. So there is a circulation of net sediment transport.
Annex 12 also shows the development of the integrated sediment transport as a function of time.
At the end of the calculation there is still a gradient in the integrated sediment transport for all branches, so the dynamic equilibrium profile is not reached.

7.9.3 Conclusions

The net sediment transport that enters the system via branch 1 is distributed over branch 2 and 3. The distribution can be split up in a symmetric part and an asymmetric part. When the symmetric part is smaller (a small net transport) than the asymmetric part, circulation of net sediment occurs.
As a result of this the bed profile of the ebb channel is completely different than for scenario 5, where no circulation of net sediment occurred.

8 Conclusions and recommendations

8.1 Conclusions

dynamic equilibrium profile:

- As the bed profile is continuously in motion, a static equilibrium profile can not be defined. However, a bed profile is a dynamic equilibrium profile when the net sediment transport is equal for every cross-section.

short basin single-channel model:

- In the single-channel model only a net sediment transport occurs when a number of small factors are taken into account. The most important factor is the seaside boundary condition which contains at least the M_2 and M_4 component.
- The single-channel model will only lead to a trivial solution, viz. a filled basin a result of the closed boundary condition at the end of the basin. However, a quasi-dynamic equilibrium can be defined.

short basin two-channel model:

- The two channel model leads to a well defined dynamic equilibrium profile. The closed boundary condition does not influence the equilibrium as a result of horizontal circulation.
- The two channel model leads to a well defined dynamic equilibrium profile without taking into account a number of small factors. At the seaside boundary only the M_2 component is required.

available data of the reference case 'Pas van Terneuzen - Everingen':

- The net volume of water over a tidal period can not be determined as a result of the errors in the measurements.
- The net sediment transport is even more difficult to determine.
- To schematise a specific ebb and flood channel is difficult as the geometry is very complex.

computational results:

- The change of width of the ebb and flood channel is an important parameter for the morphological development of the channel system. For a flood channel with a increasing width from seaside to landside a linear inclining bed profile develops. For an ebb channel with a decreasing width from seaside to landside a nearly horizontal bed profile develops.
- As a result of the Chézy coefficient, which depends on the flow direction, the bed slope of the flood channel becomes smaller and the bed slope of the ebb channel becomes larger. The volumes of water that pass through

the ebb and flood channels change significantly.

When the difference between the Chézy coefficients during ebb and flood is large compared to the convective term in the momentum equation the M_2 component at the seaside boundary generates M_4.

- The phase difference between the M_2 and M_4 components at the seaside boundary is an important parameter as this determines the magnitude and direction of the net sediment transport. This net sediment transport can be split up in a symmetric and an asymmetric part over the ebb and flood channels. When the asymmetric part is larger than the symmetric part circulation of net sediment occurs.
- The length of the channels is another important parameter. The longest channel becomes shallow.

8.2 Recommendations for further research

To refine the model take into account:

- storage width as a function of the water level
- the effect of the river discharge on the morphological behaviour of an ebb and flood channel system with a relatively small tidal volume.
- the effect of channels that interconnect the ebb and flood channels.
- the effect of relaxation in time and space of the sediment transport. So the sediment transport does no longer depends on the local flow velocity only.

To compute an estuary problem

- connect two or more ebb and flood channel systems to each other, as is shown in Figure 8-1.

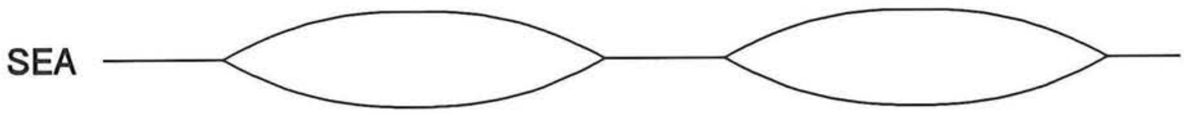

Figure 8-1: Coupled ebb and flood channel system

For further study:

- take into account 2-dimensional effects like bends and Coriolis
- how to interpret the numerical results for practice.

References

Allersma, E. (1992)
'Study arrangement eastern part Western Scheldt, analysis of the physical system' (in Dutch), DELFT HYDRAULICS, Report Z368

Allersma, E. (1994)
'Gullies in estuaries' (in Dutch), DELFT HYDRAULICS, Report H1828, H1970

Dekker, P. den & J.M. Van Voorthuizen (1994)
'Research on the morpholgical behaviour of bifurcations in rivers'
Delft University of Technology, Faculty of Civil Engineering, MSC-thesis

Engelund, F. & E. Hansen (1967)
'A monograph on sediment transport in alluvial streams', Teknisk Forlag, Copenhagen

Fokkink, R.J. & Z.B. Wang (1993)
'Study on fundamental aspects of 1D-network morphodynamic model', DELFT HYDRAULICS, Report Z654

Fokkink, R.J. (1995)
'SOBEK simulations of estuarine morphology in simple network systems', DELFT HYDRAULICS, Report Z855 (draft)

Galappatti, R (1983)
'A depth integrated model for suspended transport', Delft University of Technology, Faculty of Civil Engineering, Report no. 83-7

I.S.O. (1974)
'Investigation of the total error in measurement of flow by velocity-area methods', International Organization for Standardization

Kalkwijk, J.P.Th. (1975)
'The analysis of tides' (in Dutch), Lecture notes b75, Delft University of Technology, Faculty of Civil Engineering

Lieshout, M.C. van (1993)
'Morphological computations under tidal conditions', Delft University of Technology, Faculty of Civil Engineering, MSc-thesis

Meyer-Peter, E. & R. Müller (1948)
'Formulas for bed-load transport', Proc. IAHR, Stockholm, Vol. 2 paper 2.

Roosjen. R & C. Zwanenburg (1995)
'Research on bifurcations in rivers', Delft University of Technology, Faculty of Civil Engineering, MSc-thesis

Rijn, van L.C. (1984)
'Sediment transport'
'part I: bed-load transport',J.Hydr.Engrg., ASCE, Vol 110
'part II: suspended-load transport', J.Hydr.Engrg., ASCE Vol 110
'part III: bedforms and alluvial roughness',
J.Hydr.Engrg., ASCE Vol 110.

RWS (1993)
'Discharge and sediment measurements in the Western Scheldt', Ministry of Transport, Public Works and Water Management (1993), Report ZLMD93.N.039

Shields, A. (1936)
'Application of similitude mechanics and the research on turbulence to bed form movement' (in German), Mitt. Preuss. Versuchsanstalt für Wasserbau und Schiffbau, Belin, 26.

SOBEK, (1994)
'Technical reference guide', DELFT HYDRAULICS & Ministry of Transport, Public Works and Water Management

Struiksma, N. (1988)
'RIVCOM, a summary of results of test-computations', DELFT HYDRAULICS, Report Q794

Veen, J. van (1950)
'Ebb- and flood-channel systems in the Netherlands tidal waters' (in Dutch with Englisch summary), Tijdschr. KNAG, 1950 2nd series part 67 pp.303-325

Velzen, E.H. van (1986)
'Morphological equilibrium in tidal rivers' (in Dutch, draft version)
Delft University of Technology, Faculty of Civil Engineering, MSc-thesis

Vries, M. de (1994)
'River Engineering', Lecture notes f10, Delft University of Technology, Faculty of Civil Engineering

Wang, Z.B. (1992)
'Fundamental Considerations on Morphodynamic Modelling in Tidal Regions' (Part I: Theoretical analysis and 1D test computations), DELFT HYDRAULICS, Report Z331

Annex 1a: Bathymetry

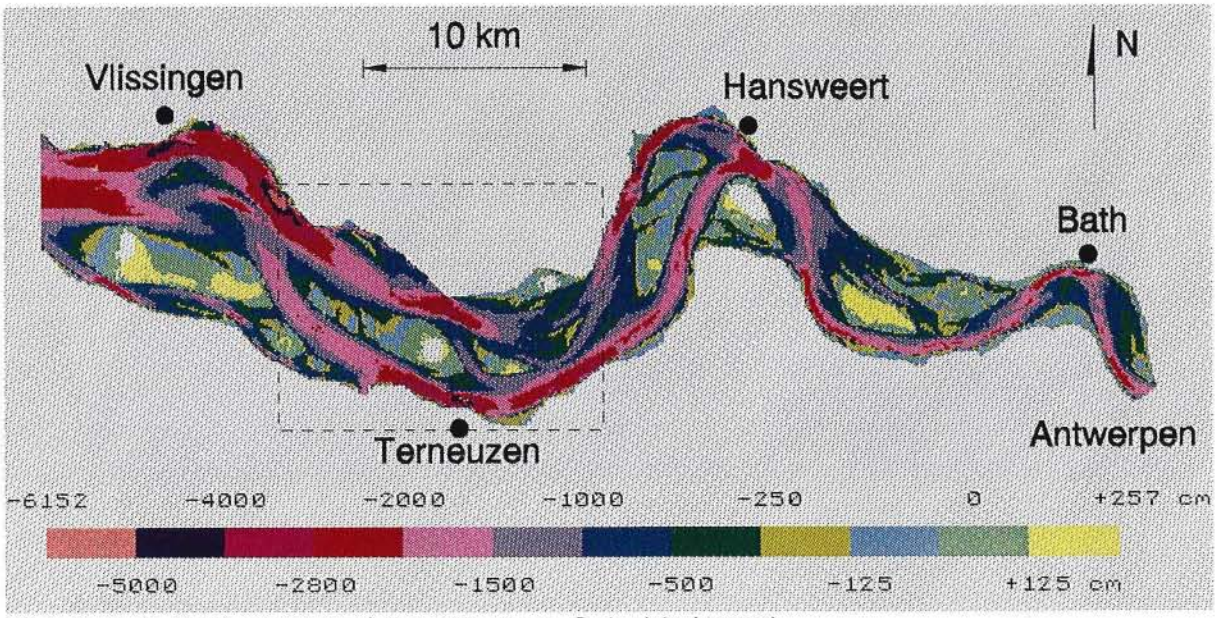

Figure 5-1: Bathymetry of the Western Scheldt (1992)

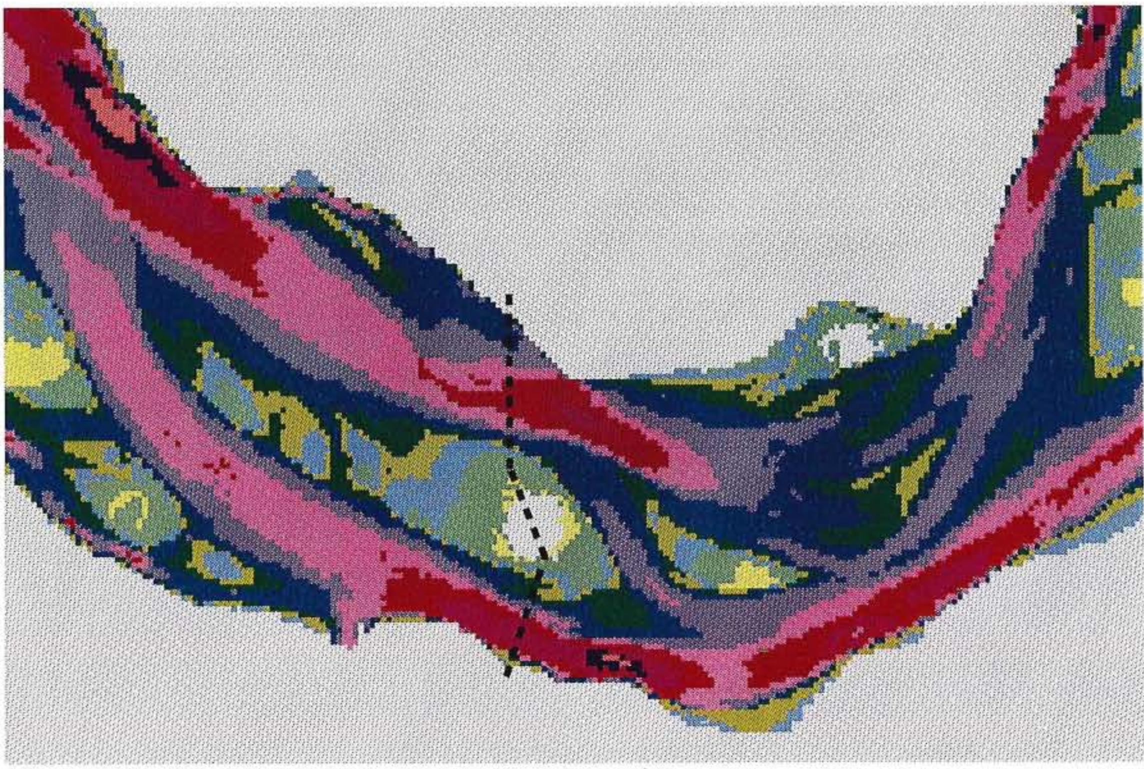
Figure 5-2: 'Pas van Terneuzen - Everingen'

Annex 1b: Location of the cross-section

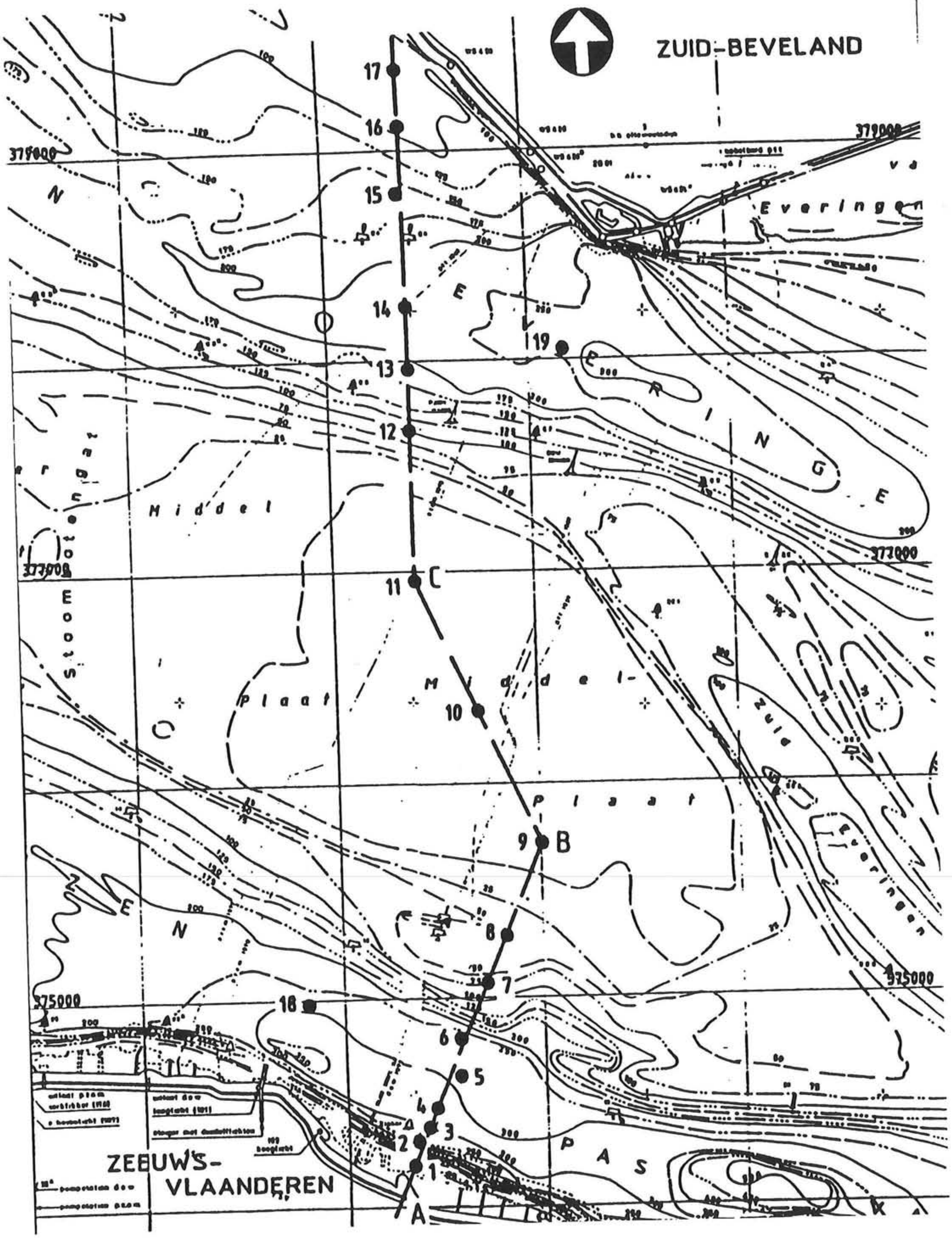

Annex 2: Main tidal components Vlissingen and Terneuzen

	Vlissingen		Terneuzen	
component	amplitude [cm]	phase [°]	amplitude [cm]	phase [°]
A_0 (wrt NAP)	-1		7	
SA	8	215	7	215
SM	4	47	5	49
Q_1	4	145	4	150
O_1	11	193	11	198
P_1	3	359	3	7
K_1	7	14	7	19
$3MS_2$	4	287	5	292
MNS_2	3	139	4	143
NLK_2	5	353	6	358
μ_2	13	163	15	167
N_2	29	34	31	44
NU_2	9	24	10	31
MPS_2	4	100	3	107
M_2	175	59	188	68
λ_2	6	75	7	83
$2MN_2$	14	257	15	265
S_2	48	116	51	116
K_2	14	115	15	126
$2SM_2$	5	346	5	355
$2MK_3$	3	163	4	181
MK_3	3	315	3	339
$3MS_4$	2	202	2	226
MN_4	5	97	4	111
M_4	13	118	12	133
MS_4	9	179	8	195
MK_4	3	180	2	196
$2MN_6$	5	83	5	126
M_6	8	106	9	150
$2MS_6$	9	157	9	200

(Source: Getijtafels voor Nederland 1993, Rijkswaterstaat dienst getijwateren)

Annex 3: Errors in discharge measurements

A3.1 General

In order to determine the volume of water that passes the cross-section of a channel during ebb and flood, every 10 minutes discharge measurements are carried out. In each measurement an error occurs. When the magnitude of this error is known the error in the ebb and flood volume can under certain circumstances be determined.

The cross-section is herefore divided in verticals. For each vertical the discharge per unit width is determined as the product of the mean velocity and depth in the vertical. In order to determine the mean velocity in the vertical, the velocity is measured in several point in the vertical (local points). The discharge of each vertical contributes to the total discharge of the cross-section.

Apart from the instrumental error, the error in the mean flow velocity in the cross-section can be divided into three independent types of errors:

Error type I	: exposure time of the local point velocity
Error type II	: number of points in the vertical
Error type III	: number of verticals in the cross-section

The report 'Investigation of the total error in measurement of flow by velocity-area methods (ISO, 1971)' provides information about the magnitude of these errors. In this investigation to the accuracy of the discharge measurements an examination of the accuracy of the instruments is not included.

The relative standard deviation of the total stochastic instrumental and sampling error (σ_1) can be approximated by:

$$\sigma_1^2 = \sigma_{S_d}^2 + \sigma_{S_h}^2 + \frac{1}{m}\left(\sigma_{\overline{V}_i}^2 + \sigma_{\overline{F}_i}^2 + \sigma_{S_{\overline{V}_i}}^2 + \sigma_{D_i}^2 + \sigma_{B_i}^2\right) \qquad \text{(A3.1)}$$

herein:

$\overline{v}_i$ = mean velocity in section i

m = number of verticals

σ_{S_d} = relative standard deviation due to the random sampling error of the depth profile (error type III)

σ_{S_h} = relative standard deviation due to the random sampling error of the horizontal velocity profile (error type III)

$\sigma_{\overline{V}_i}$ = relative standard deviation of the mean velocity due to the random instrumental error.

$\sigma_{\overline{F}_i}$ = relative standard deviation due to the random fluctuation error (error type I)

$\sigma_{S_{\overline{V}_i}}$ = relative standard deviation due to the random sampling error of the mean velocity in the vertical (error type II)

σ_{D_i} = relative standard deviation due to the random instrumental error determining depth of section *i*.

σ_{B_i} = relative standard deviation due to the random instrumental error determining width of section *i*.

A3.2 Discharge measurements in the Western Scheldt

data:
number of vertical in channel: 9
number of points in vertical : range 7 - 10
exposure time: 120 seconds
distance verticals: equidistant (approximately)

calculation, see equation (A3.1):

$\sqrt{\sigma_{\overline{F}_i}^2 + \sigma_{S_{\overline{V}_i}}^2}$ = 2.4 % (table I, ISO 1971) (error type II)

$\sqrt{\sigma_{S_d}^2 + \sigma_{S_h}^2}$ = 4.4 % (table II, ISO 1971) (error type III)

$\sigma_{\overline{V}_i} = \sigma_{D_i} = \sigma_{B_i} = 1$ % (estimated)

$$\sigma_1^2 = 4.4^2 + \tfrac{1}{9}(1^2 + 2.4^2 + 1^2 + 1^2) = 19.4 + 0.97 = 20.37$$

$$\sigma_1 = 4.5\ \%$$

It can be seen that the restricted number of vertical contributes much to the total error.
remark:

- it is assumed that all measurements are complete.
- in the 60 seconds measurements the flow is regarded as steady
- the accuracy of the instruments is not included

It can be concluded that σ_1 will be at least 4.5 % and probably larger in each measurement.

The error of the ebb and flood volume can be determined by:

$$\sigma_{volume} = \frac{1}{\sqrt{n}} \sigma_1$$

in the case n = 37.

$$\sigma_{volume} = \frac{1}{\sqrt{37}} 4.5 = 0.7\%$$

All values of errors are at one standard deviation.

A3.3 Sediment transport measurements (Western Scheldt)

The sediment transport is determined as:

$$S = \sum_{i=1}^{m} c_i \, B_i \, d_i \, U_i \qquad \text{(A3-2)}$$

herein:

m = number of sections

c_i = measured sediment concentration

B_i = width section

d_i = depth section

The relative standard deviation of the total stochastic instrumental and sampling error (σ_2) of the sediment transport is approximated by:

$$\sigma_2^2 = \sigma_{S_d}^2 + \sigma_{S_h}^2 + \frac{1}{m} (\sigma_{\overline{V}_i}^2 + \sigma_{\overline{F}_i}^2 + \sigma_{S_{\overline{V}_i}}^2 + \sigma_{D_i}^2 + \sigma_{B_i}^2 + \sigma_{c_i}^2) \qquad \text{(A3.3)}$$

where

σ_{c_i} = relative standard deviation due to the random instrumental error determining sediment concentration of section i.

σ_{c_i} = 3 % (estimated from calibration instrument)

$$\sigma_2^2 = 4.4^2 + \tfrac{1}{9}(1^2 + 2.4^2 + 1^2 + 1^2 + 3^2) = 19.4 + 1.97 = 21.37$$

$$\sigma_2 = 4.6 \ \%$$

The error of the sediment transport during flood and ebb can be determined by:

$$\sigma_{sediment transport} = \frac{1}{\sqrt{n}} \sigma_2$$

in the case $n = 37$.

$$\sigma_{sediment transport} = \frac{1}{\sqrt{37}} 4.6 = 0.8\%$$

Remark:
This result is too optimistic as equation (A3-2) is used to estimate the sediment transport.
The discharge of water close to the bed is small compared to the upper part of the vertical. An error in the flow velocity in the low part of the vertical does not effect the total discharge a lot.
However, most of the sediment transport takes place close to the bed. An error in the flow velocity in the low part of the vertical effects the total sediment transport a lot. In the previous consideration this effect is not taken in to account and will lead to much higher relative standard deviations.

Annex 4: Circulation due to change in width

A4.1 General

In an ebb and flood channel system the widths of the channels are not constant.
In general the width of the ebb channel decreases and the width of the flood channel increases from the seaside to the landside. In this annex it is shown that a gradually change in width effects the discharge.

A4.2 Basic equations

For a one-dimensional system the water motion is described mathematically by the following two equations:

continuity:
$$B\frac{\partial h}{\partial t} + \frac{\partial Q}{\partial x} = 0 \qquad \text{(A4-1)}$$

momentum:
$$\frac{\partial Q}{\partial t} + \frac{\partial}{\partial x}\left(\frac{Q^2}{A}\right) + gaB_f\frac{\partial h}{\partial x} + g\frac{Q|Q|}{C^2a^2B_f} = 0 \qquad \text{(A4-2)}$$

For steady flow and a horizontal bed the equations reduce to:

continuity:
$$\frac{\partial Q}{\partial x} = 0 \qquad \text{(A4-3)}$$

momentum:
$$\frac{\partial}{\partial x}\left(\frac{Q^2}{A}\right) + gaB_f\frac{\partial a}{\partial x} = -g\frac{Q|Q|}{C^2a^2B_f} \qquad \text{(A4-4)}$$

A4.3 Simple model

The width of the flood channel increases from the seaside to the landside, see Figure A4-1.

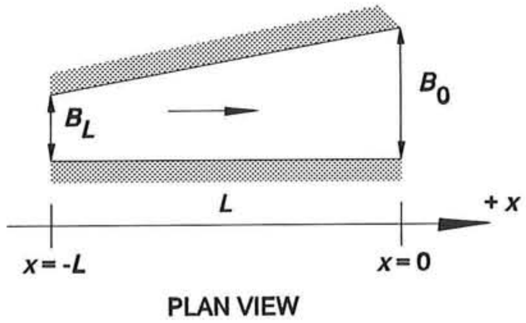

■ Figure A4-1: Flood channel

So the width is a function of x and can be written as:

$$B(x) = B_0 + \frac{B_0 - B_L}{L} \cdot x$$

The width of the ebb channel decreases from the seaside to the landside, see Figure A4-2.

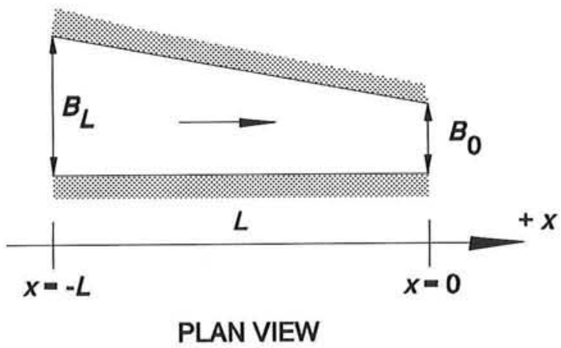

■ Figure A4-2: Ebb channel

Again the width is a function of x and can be written as:

$$B(x) = B_0 + \frac{B_0 - B_L}{L} \cdot x$$

Figure A4-3 illustrates the longitudinal section of the ebb and flood channels.
The question is how large must Δh be to obtain Q_0?

The cross-section is a function of x and reads:

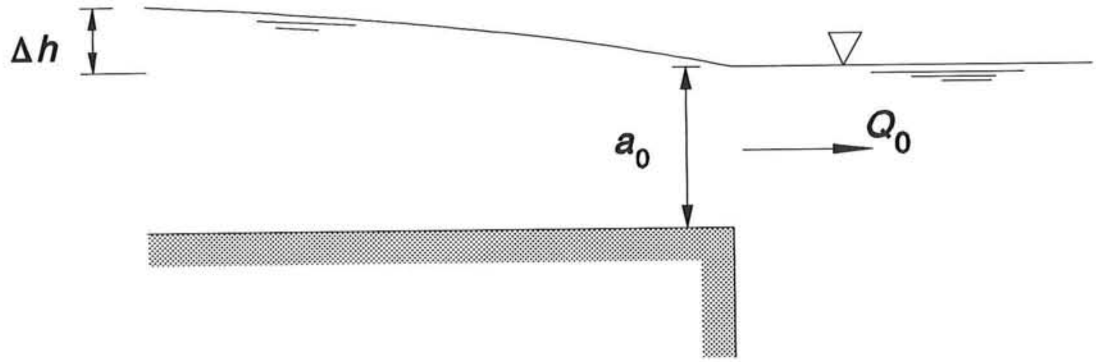

■ Figure A4-3: Longitudinal section of the channels

$$A(x) = B(x) \cdot a(x)$$

As the change in width is much bigger than the change in water depth it is assumed that $a(x) = \text{const} = a$.

So the cross-section becomes: $$A(x) = a \cdot \left(B_0 + \frac{B_0 - B_L}{L} \cdot x \right)$$

Substitution of the cross-section in the convective term of equation (A4-4) gives:

$$\frac{\partial}{\partial x}\left(\frac{Q^2}{A}\right) = Q^2 \cdot \frac{\partial}{\partial x}(\ A^{-1}\ ) =$$

$$= Q^2 \cdot \frac{-1}{a\left(B_0 + \frac{B_0 - B_L}{L} \cdot x\right)^2} \cdot \frac{B_0 - B_L}{L} \qquad \text{(A4-5)}$$

With this result and under the assumption that the forces at the borders are negligible, equation (A4-4) can be rewritten as:

$$\frac{\partial a}{\partial x} = \frac{-1}{gA}\frac{\partial}{\partial x}\left(\frac{Q^2}{A}\right) - \frac{Q|Q|}{C^2 a^3 B_f^2}$$

$$\frac{\partial a}{\partial x} = \frac{-1}{gA}\frac{-Q^2}{a\left(B_0 - \frac{B_0 - B_L}{L} \cdot x\right)^2} \cdot \left(\frac{B_0 - B_L}{L}\right) - \frac{Q|Q|}{C^2 a^3 B_f^2}$$

$$\frac{\partial a}{\partial x} = \frac{Q^2}{ga^2\left(B_0 - \frac{B_0 - B_L}{L} \cdot x\right)^3} \cdot \left(\frac{B_0 - B_L}{L}\right) - \frac{Q|Q|}{C^2 a^3 B_f^2} \qquad \text{(A4-6)}$$

So far we have rewritten the momentum equation (A4-4) with respect to the change in width.

If we assume that the discharge Q_0 = constant there must be a head difference Δh . The head difference follows from:

$$\Delta h = \int_0^{-L} \frac{\partial a}{\partial x}\, \mathrm{d}x \tag{A4-7}$$

For an increasing cross-section in x-direction:

$$B_0 > B_L \tag{A4-8}$$

so the second term in equation (A4-6) has a positive value.

$$\frac{\partial a}{\partial x} = \mathrm{CN} - R = W_{increase}$$

herein:

CN = convective term

R = resistance term

W = sum of convective and resistance term

where **CN** is positive.

For a decreasing cross-section in x-direction:

$$B_0 < B_L \tag{A4-9}$$

so the second term in equation (A-6) has a negative value.

$$\frac{\partial a}{\partial x} = \mathrm{CN} - R = W_{decrease}$$

where CN is negative.

herein:

$$\mathrm{CN} = \frac{Q^2}{g a^2 \left(B_0 - \dfrac{B_0 - B_L}{L} \cdot x\right)^3} \cdot \left(\frac{B_0 - B_L}{L}\right)$$

and

$$R = \frac{Q\,|Q|}{C^2 a^3 B_f^2}$$

As a result of the convective term:

$$|W_{decrease}| > |W_{increase}| \tag{A4-10}$$

The head difference is determined by equation (A4-7). As a result of equation (A4-10) the discharge of the flood channel will be larger than the discharge of the ebb channel for a given head difference.

A4.4 Conclusions

For a given Δh (head difference) $Q_1 > Q_2$ as a result of the geometry.

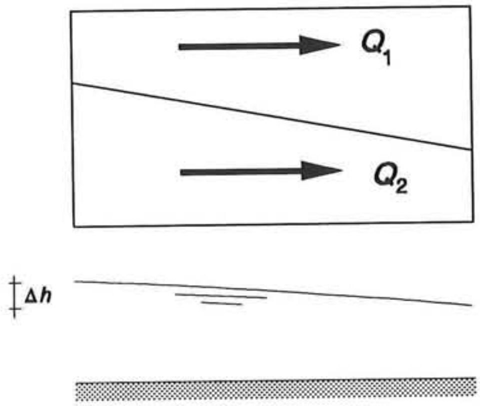

■ Figure A4-4: Definition sketch

This result is gathered under the following five assumptions:

1. $\frac{\partial z}{\partial x} = 0$ (horizontal bed) is considered.
2. $a(x) = a = \textbf{const}$, changes in water depth are expected to be small.
3. Forces at the borders as a result of the change in width are negligible.
4. The friction term is taken the same for the ebb and flood channel.
5. Only a steady flow situation is considered.

Order of magnitude estimation:

$$\frac{\partial a}{\partial x} = \frac{Q^2}{ga^2\left(B_0 - \frac{B_0 - B_L}{L}\cdot x\right)^3}\cdot\left(\frac{B_0 - B_L}{L}\right) - \frac{Q|Q|}{C^2a^3B_s^2}$$

$$\frac{Q^2}{ga^2\left(B_0 - \frac{B_0 - B_L}{L}\cdot x\right)^3}\cdot\left(\frac{B_0 - B_L}{L}\right) \sim \frac{Q|Q|}{C^2a^3B_s^2}$$

$$\frac{1}{g\left(B_0 - \frac{B_0 - B_L}{L}\cdot x\right)}\cdot\left(\frac{B_0 - B_L}{L}\right) \sim \frac{1}{C^2a}$$

$x = L$

$$\left|\frac{B_0 - B_L}{L}\right| \sim \left|\frac{gB_L}{C^2a}\right|$$

Annex 5: Chézy coefficient dependent on the flow direction effects M_4

A5.1 General

With a numerical computation Fokkink (1995) demonstrated that a Chézy coefficient which depends on the flow direction, effects the M_2, M_4 and other components.
In order to keep the M_2 component constant the following condition had to be fulfilled:

$$\frac{1}{C^2} = \frac{1}{2}\frac{1}{C_{ebb}^2} + \frac{1}{2}\frac{1}{C_{flood}^2} \tag{A5.1}$$

Under this condition the ebb and flood dependent Chézy coefficient only effects the M_4 component and higher components, while M_2 remains constant. This is proved by numerical computations. This seems to be a bit odd as the hydraulic friction term in the momentum equation normally generates mainly M_6 and higher components.

In this Annex it is stated that a Chézy coefficient, which depends on the flow direction, also effects the M_4 component.

A5.2 Basic equations

For a channel with a constant width and a fixed bed the water motion can be described by:

$$\frac{\partial a}{\partial t} + \frac{\partial u a}{\partial x} = 0 \tag{A5.2}$$

$$\frac{\partial u}{\partial t} + u\frac{\partial u}{\partial x} + g\frac{\partial a}{\partial x} + g\frac{\partial z_b}{\partial x} + \frac{g}{C^2}\frac{u|u|}{a} = 0 \tag{A5.3}$$

There are two sources of higher harmonics in (A5.2) and (A5.3). The first source is the boundary condition which contains the externally generated harmonic components. The second source are the non-linear terms in the momentum equation.
There are two non-linear terms in the momentum equation viz.:

1. hydraulic friction term $\quad \frac{g}{C^2}\frac{u|u|}{a}$

2. convective term $\quad u\frac{\partial u}{\partial x}$

A5.3 Generation of higher frequency components

A5.3.1 General

In this Section it is shown that a Chézy coefficient, independent of the flow direction, generates higher frequency components as a result of the hydraulic friction term and the convective term in the momentum equation.
By expanding a function in a Fourier series, it can be seen which higher frequency components are present in a function.

A5.3.2 Hydraulic friction term

For tidal problems the flow direction is a function of time. So the sign of the friction term is also a function of time.
If the Chézy coefficient is independent of the flow direction this coefficient can be regarded as constant.

As a result of the M_2 component at the boundary:

$$u(t) = \sin(\omega t)$$

The friction term is proportional to

$$u\,|u| \text{ or } u^2 \cdot \sigma$$

Where $\sigma = +1$ or -1

$$\sigma(t) = +1 \quad \text{for} \quad 0 \leq t < \frac{T}{2}$$

$$\sigma(t) = -1 \quad \text{for} \quad \frac{-T}{2} \leq t < 0$$

The block function $\sigma(t)$ with unit amplitude can be expanded in a Fourier series:

$$\sigma(t) = \frac{4}{\pi}\left(\sin\omega t + \frac{1}{3}\sin 3\omega t + \frac{1}{5}\sin 5\omega t + ... \right)$$

hence:

$$u^2(t)\,\sigma(t) =$$

$$= [\sin(\omega t)\sin(\omega t)]\cdot[\frac{4}{\pi}\sin(\omega t) + \frac{4}{3\pi}\sin(3\omega t)\ ] +$$

$$+ [\sin(\omega t)\sin(\omega t)]\cdot[\ \frac{4}{5\pi}\sin(5\omega t) + ...]$$

$$u^2(t)\,\sigma(t) = \frac{4}{\pi}\sin^3(\omega t) + \frac{4}{3\pi}\sin^2(\omega t)\sin(3\omega t) +$$

$$+ \frac{4}{5\pi}\sin^2(\omega t)\sin(5\omega t) + ...$$

can be written as:

$$u^2(t)\sigma(t) = \frac{8}{3\pi}\sin(\omega t) + \frac{8}{15\pi}\sin(3\omega t) + ... \qquad \text{(A5.4)}$$

It can be concluded that M_2 generates M_6 and so on, as a result of the hydraulic friction term in the momentum equation.

A5.3.3 Convective term

The convective term in the momentum equation reads:

$$u\frac{\partial u}{\partial x}$$

As a result of the M_2 component at the boundary:

$$u(x,t) = u_o \cdot \sin(\omega t - kx)$$

$$u\frac{\partial u}{\partial x} = u_0 \cdot \sin(\omega t - kx) \cdot -u_0 \cdot \cos(\omega t - kx) =$$

$$= \frac{-u_0}{2}\sin(2\omega t - 2kx) \qquad \text{(A5.5)}$$

It can be concluded that M_2 generates M_4, as a result of the convective term in the momentum equation.

A5.4 Chézy depends on the flow direction

So far it was assumed that the Chézy coefficient is constant during a tidal period. However, the Chézy coefficient can differ during ebb and flood as a result of the shape of the bed.

As
$$\frac{g}{C^2 a} u|u| = \frac{g}{C^2 a} u^2 \cdot \sigma$$

and
$$C = C_0 + \Delta C \cdot \sigma = C_0(1 + \sigma\frac{\Delta C}{C_0})$$

the coefficient in the friction term can be written as

$$\frac{g}{C^2} = \frac{g}{C_0^2\left(1 + \sigma\frac{\Delta C}{C_0}\right)^2} \approx \frac{g}{C_0^2}\left(1 - \sigma\frac{2\Delta C}{C_0}\right) \qquad \text{when} \qquad \Delta C \ll C_0$$

substitution of the coefficient in the friction term gives

$$\frac{g}{C^2 a} u^2 \sigma = \frac{g}{C_0^2 a}\left(1 - \sigma \frac{2\Delta C}{C_0}\right) u^2 \sigma$$

or

$$\frac{g}{C^2 a} u^2 \sigma = \frac{g}{C_0^2 a} u^2 \sigma - \frac{2g\Delta C}{C_0^3 a} u^2 \tag{A5.6}$$

As a result of the dependence of the Chézy coefficient on the flow direction an extra term appears, namely:

$$\frac{2g\Delta C}{C_0^3 a} u^2 \tag{A5.7}$$

as this term is proportional with u^2 it is evident that M_2 generates M_4 as a result of the extra term, like in the convective term.

A5.5 Contribution to the M_4 component

Both the convective term and the extra term, due to the dependence of the Chézy coefficient on the flow direction, generate an M_4 component as a result of the M_2 component at the boundary. The question is how large the contribution is.
The relative contribution to the generation of M_4 is therefore estimated for a rectangular channel.The terms should have the same order of magnitude.

$\frac{2g\Delta C}{C_0^3 a} u^2$ should be equal to $u\frac{\partial u}{\partial x}$

or

$$\frac{2g}{a}\frac{1}{C_0^2}\frac{\Delta C}{C_0} u = \frac{\partial u}{\partial x}$$

By substitution of

$\frac{2g}{a} \approx 1$ $[s^{-2}]$

$\frac{1}{C_0^2} \approx \frac{1}{50^2}$ $[S^2\ m^{-1}]$ and $u \approx 1$ $[ms^{-1}]$

and taking $\frac{\partial u}{\partial x}$ as $ku_0 = \frac{2\pi 1}{L} = \frac{2\pi}{\sqrt{ga}\,T} \approx \frac{2\pi}{500\ 10^3}$ $[rad s^{-1}]$,

it can be concluded that the contribution to the generation of M_4 by M_2, is dominated by the dependence of the Chézy coefficient on the flow direction if:

$$\frac{\Delta C}{C_0} > \frac{1}{32}$$

$$\Delta C > \frac{C_0}{32} \tag{A5.8}$$

In general C_0 is about 50 $m^{1/2}/s$, so if the Chézy coefficient differs more than 1.5 $m^{1/2}/s$ during ebb and flood, the Chézy coefficient will influence the M_4 component more than the convection term.

A5.6 Conclusions

If the Chézy coefficient depends on the flow direction and the Chézy coefficient differs at least 1.5 $m^{1/2}/s$ during ebb and flood, the M_4 component is influenced significantly for a rectangular profile with a horizontal bed.

The M_2 component is kept constant when:

$$\frac{1}{C^2} = \frac{1}{2}\frac{1}{C_{ebb}^2} + \frac{1}{2}\frac{1}{C_{flood}^2}$$

Annex 6: Numerical model SOBEK

SOBEK is a numerical model from Delft Hydraulics and the Directorate-General for Public Works and Water Management.
In this study SOBEK (version 1.00) is used to compute the estuarine morphology in a simple 1-D network.
The sediment transport is calculated as a function of the flow velocity (s = f(u)).
The bed level variation induced by gradients in sediment transport is described by the continuity equation for sediment. Together with the two flow equations (continuity and momentum) this forms a coupled set of equations which has to be solved numerically.
According to the 'technical reference guide' the continuity and momentum equation are discretised on the Preismann box scheme. The continuity equation for sediment is solved with an explicit numerical method of the Lax-Wendroff type.
The flow equations are solved using a fixed known cross-section, being the last computed cross-section. After this computation, the new cross-sections are computed by applying the continuity equation for sediment, using the latest computed flow field. So the equations are solved in a quasi-uncoupled way, this is allowed if the celerities of the flow and of the bed level perturbations are of different order of magnitude.
The water levels and discharges are computed at the nodes and velocities at the middle of the sections. The variations of the cross-sectional area ΔA within one bed level time step will be computed at the grid points of a branch. ΔA will be computed by evaluation of the sediment transport time integrals just in between the grid points and at the begin and end of the branch.

For a morphodynamic computation in an estuary, two time scales are important:
1. the time scale of the flow computation
2. the morphological time scale

Before the start of the computation, the user defines the period over which the flow computation is performed (T_p). During the period T_p the cross-sectional area is assumed constant. The time step of the flow computation should fit a whole number of times in T_p: $T_p = n \cdot \Delta t$, see Figure A6-1.

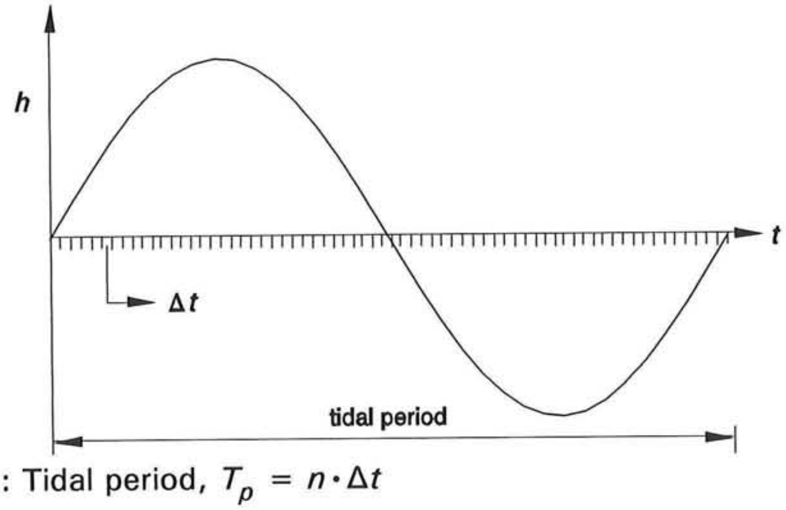

■ Figure A6-1: Tidal period, $T_p = n \cdot \Delta t$

The morphological time step consists of a whole number of tidal periods ($\Delta t_{morp} = m \cdot T_p$).
Figure A6-2 shows the flow diagram of the computation as described above.

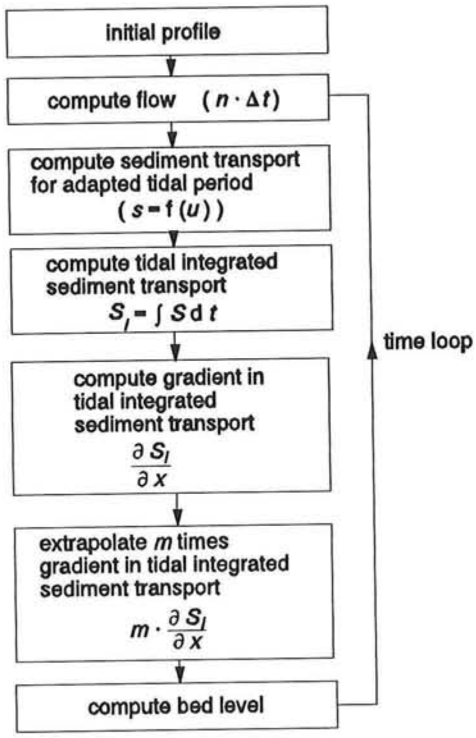

■ Figure A6-2: Flow diagram

In order to get rid of the initial conditions the flow field has to be fully adapted and become periodic, before the sediment transport is computed (as a function of the flow velocity), see Figure A6-3.

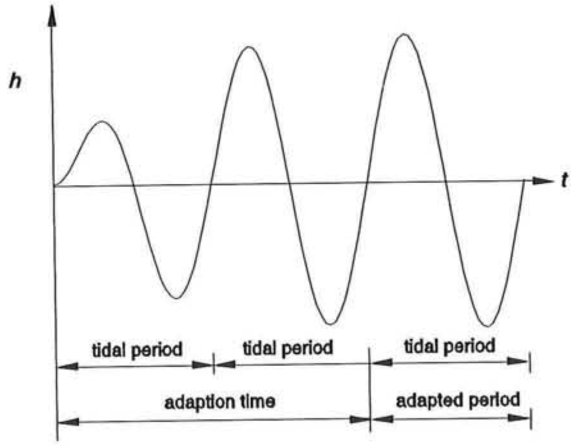

■ Figure A6-3: Adaption time

For more detailed information, see the Technical Reference Guide (March, 1994).

Annex 7: SOBEK computations: scenario 1

Annex 7: SOBEK computations: scenario 1

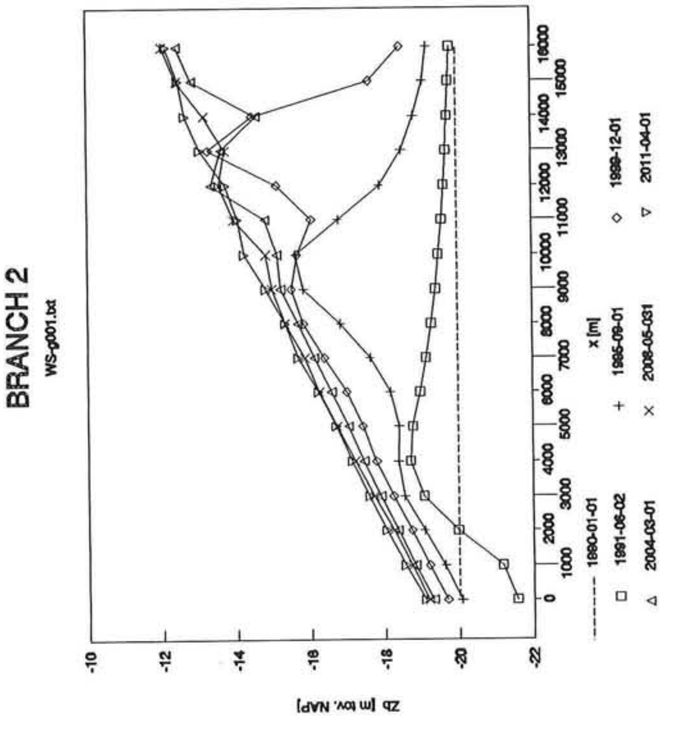

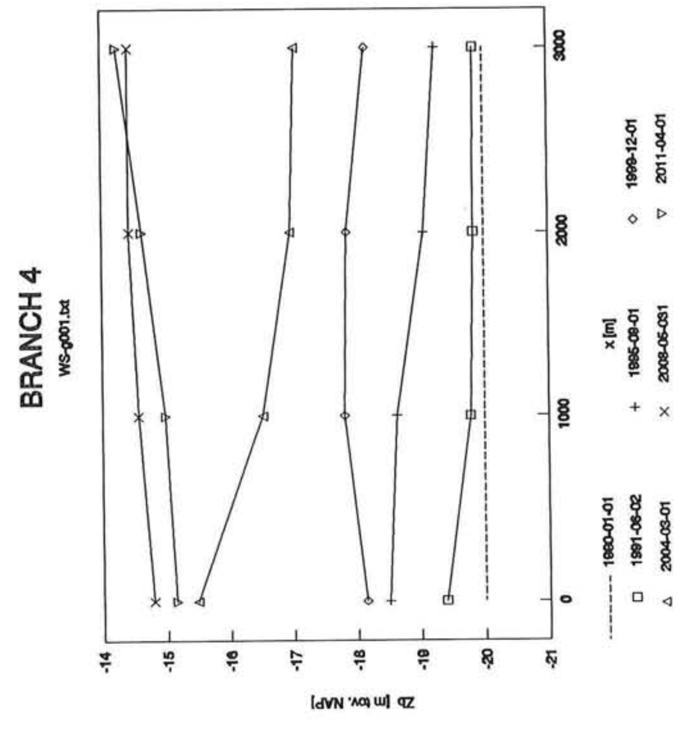

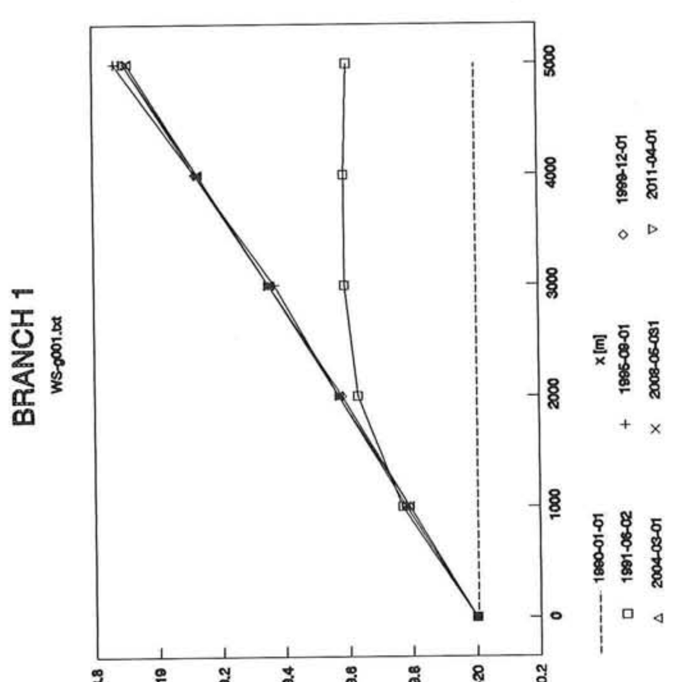

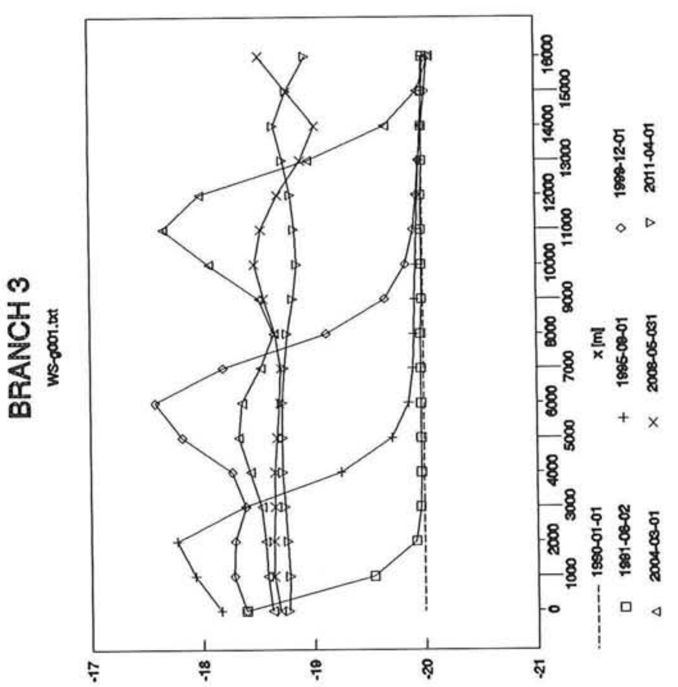

Bed level

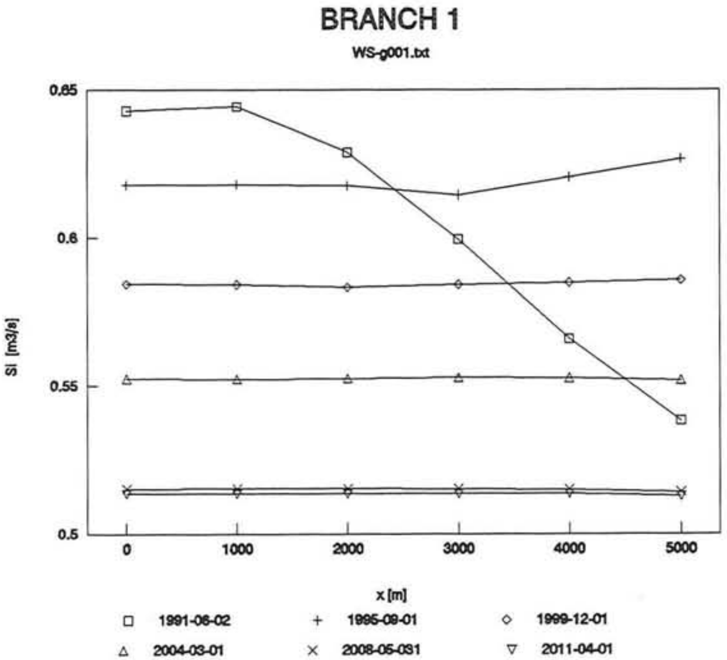

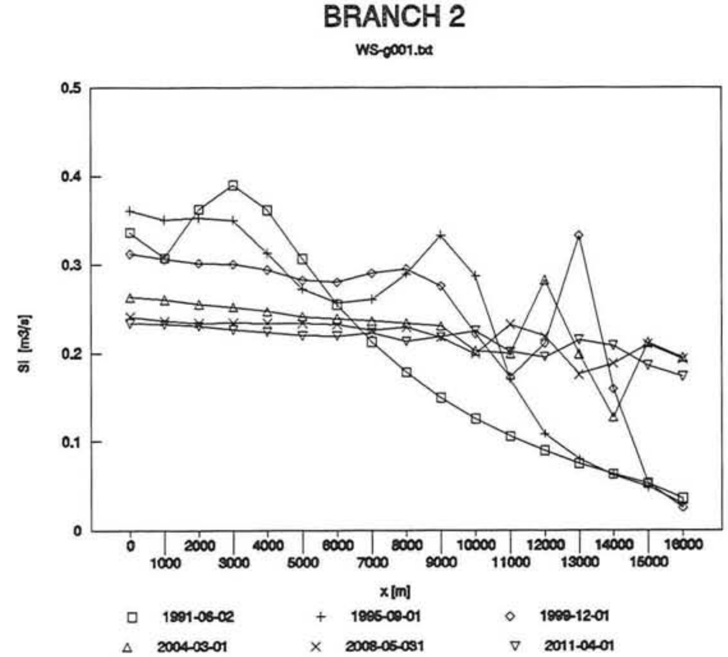

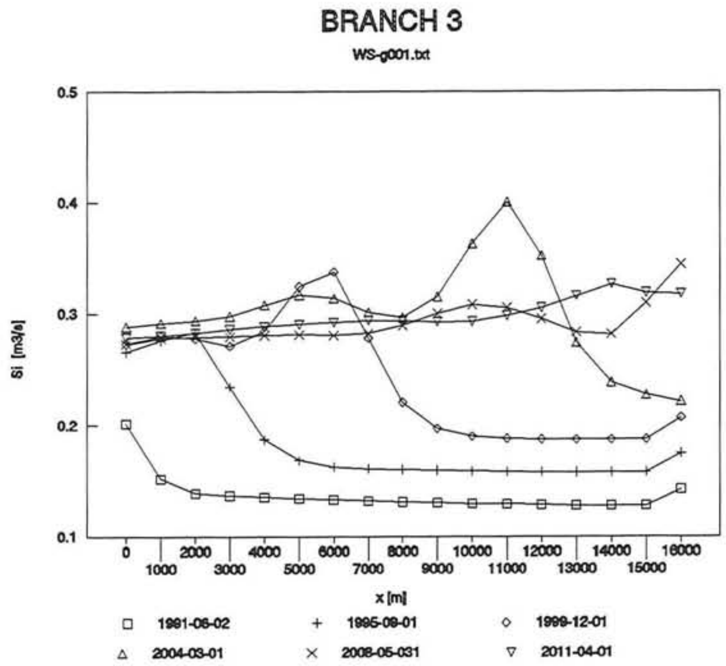

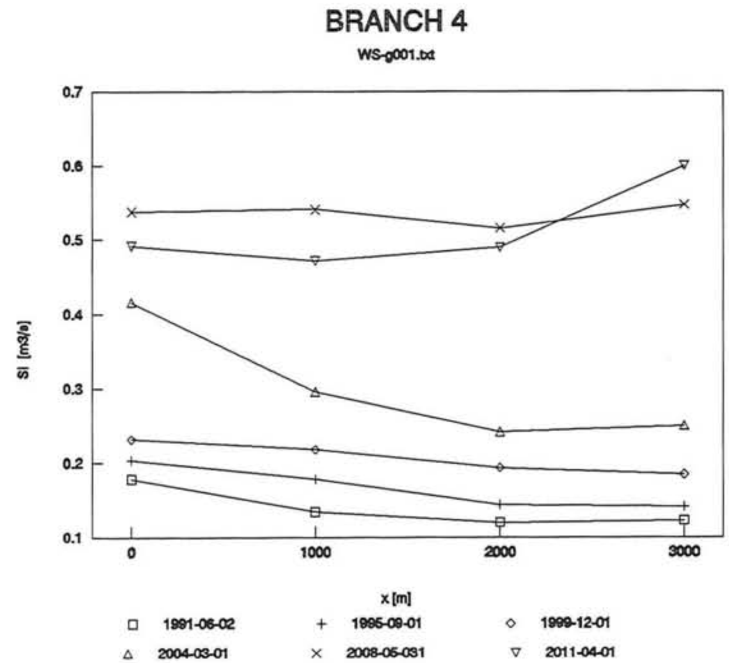

Integrated sediment transport [m^3/s]

Annex 7: SOBEK computations: scenario 1

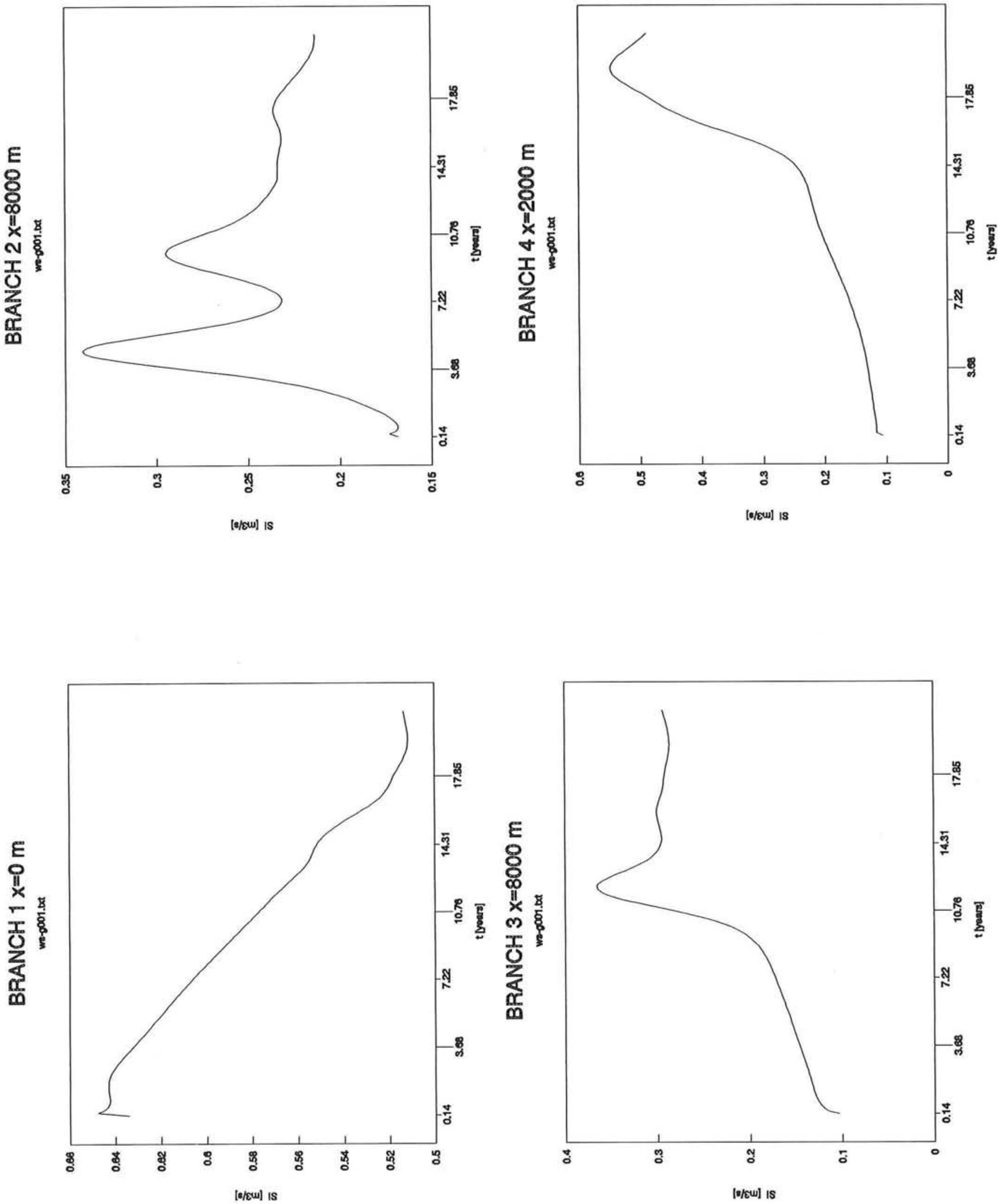

Integrated sediment transport [m^3/s]

WATER STAGES 2011-04-01

ws-g001.txt

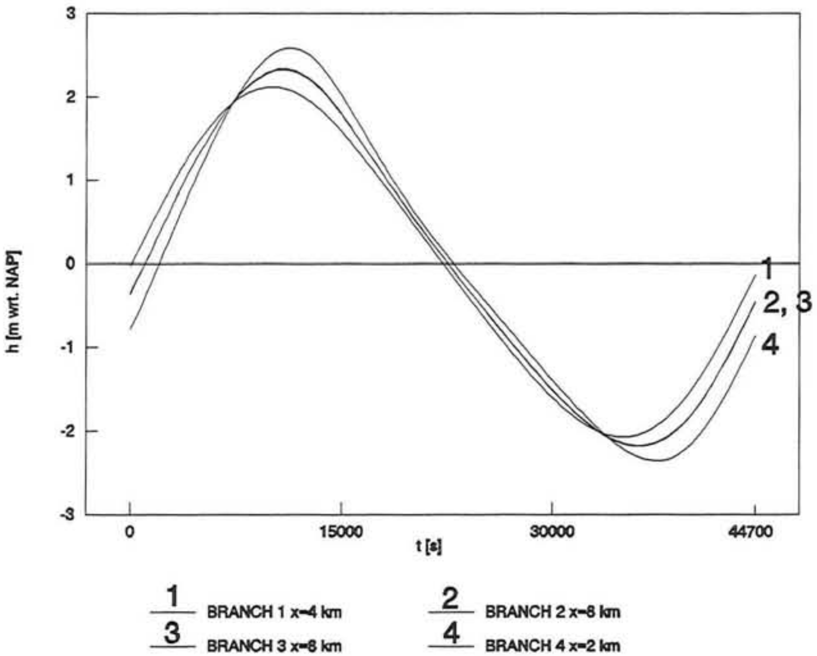

DISCHARGES 2011-04-01

ws-g001.txt

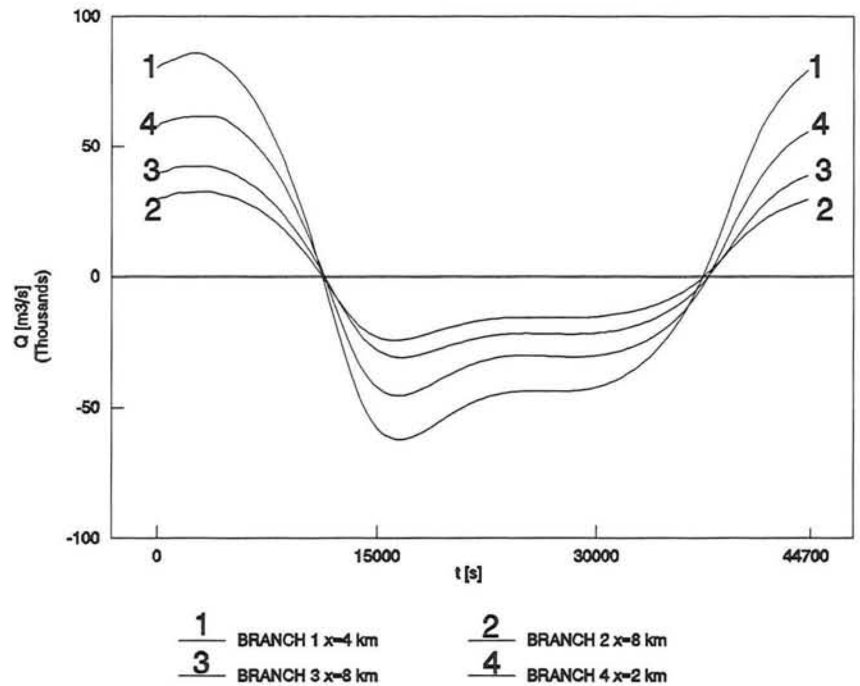

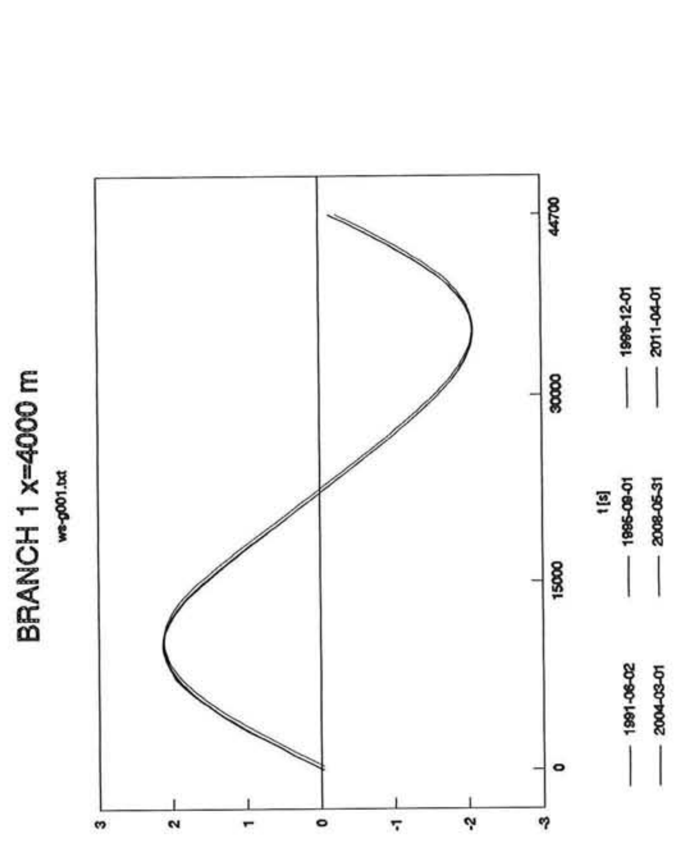

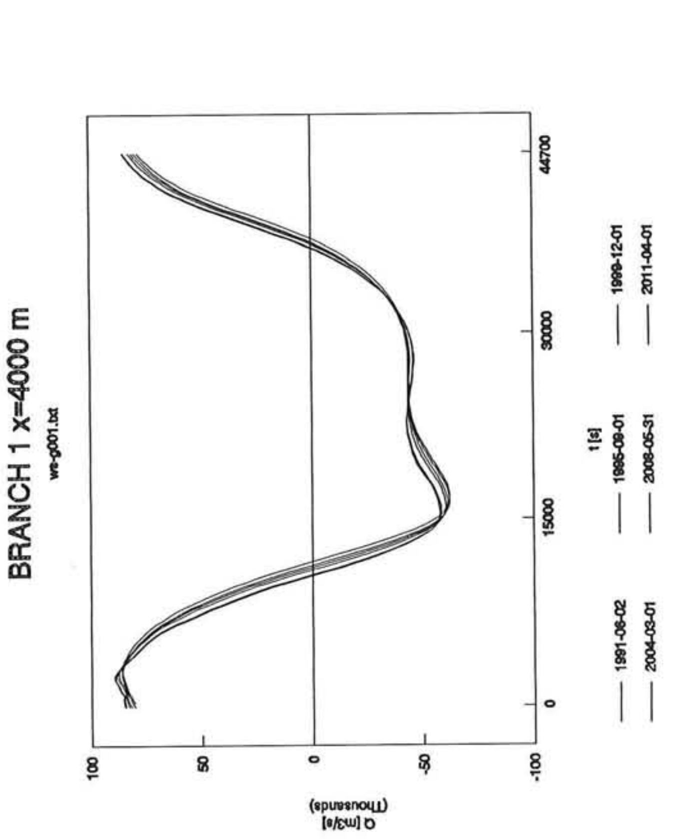

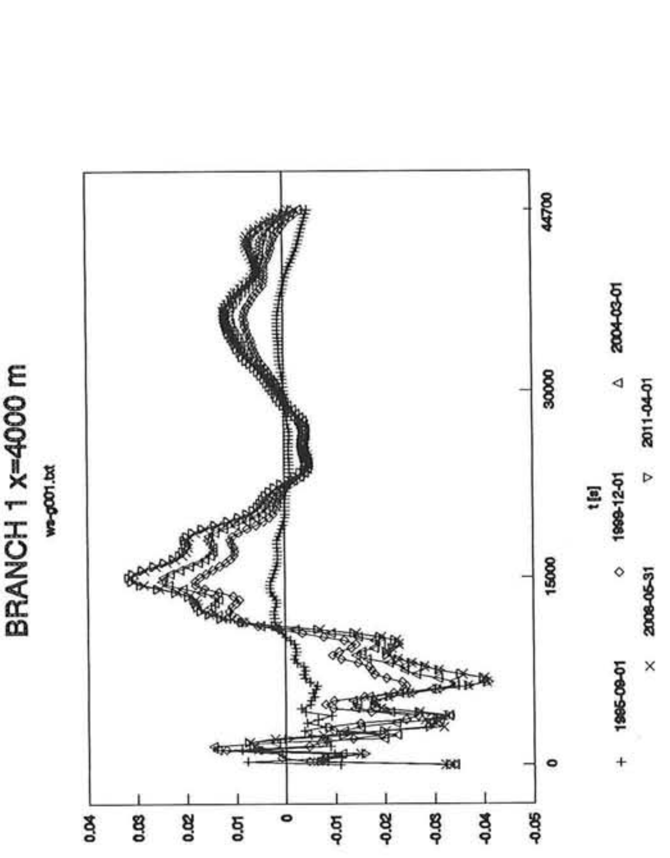

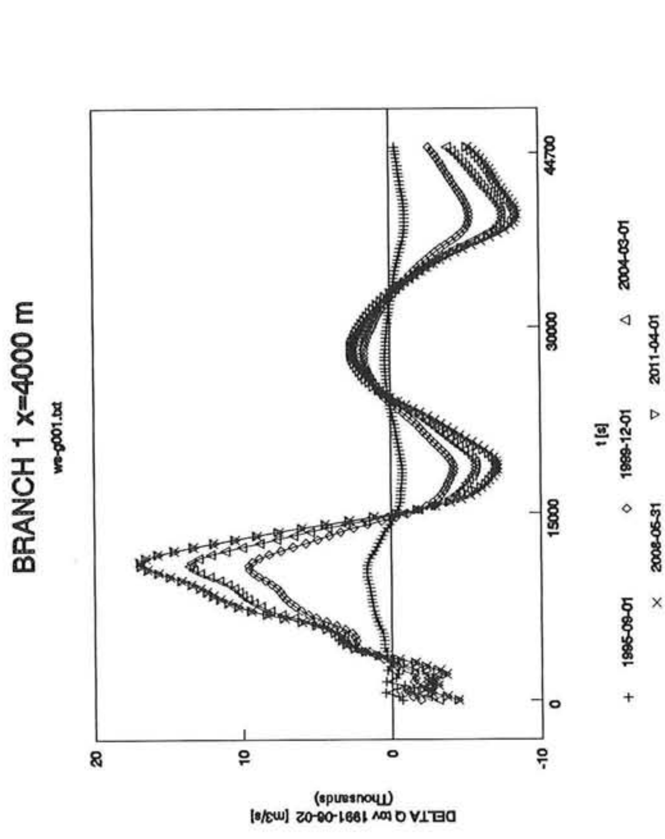

Water levels, discharges and flow velocities

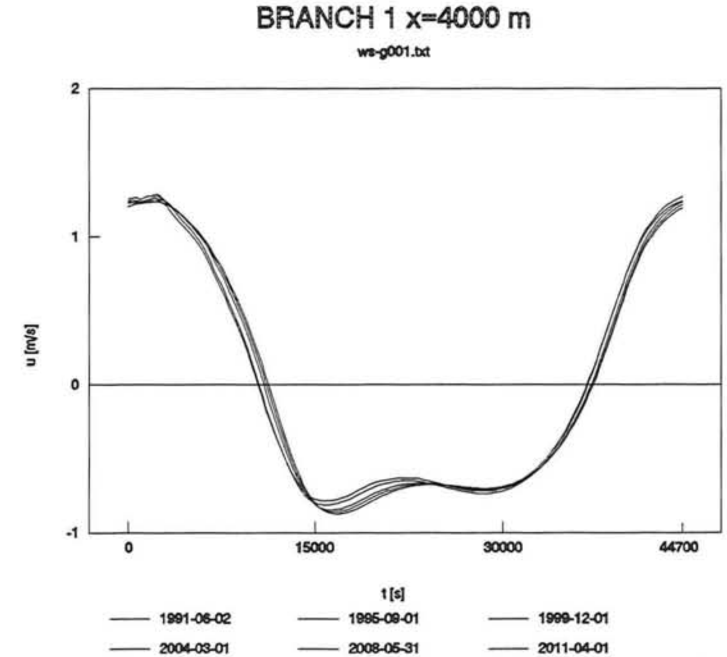
BRANCH 1 x=4000 m
ws-g001.txt
u [m/s]
t [s]
1991-06-02
1995-09-01
1999-12-01
2004-03-01
2008-05-31
2011-04-01

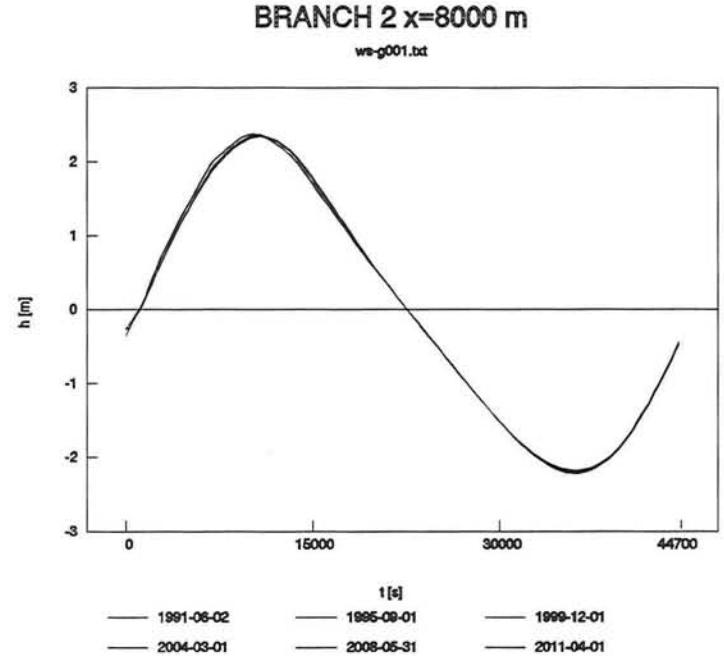
BRANCH 2 x=8000 m
ws-g001.txt
h [m]
t [s]
1991-06-02
1995-09-01
1999-12-01
2004-03-01
2008-05-31
2011-04-01

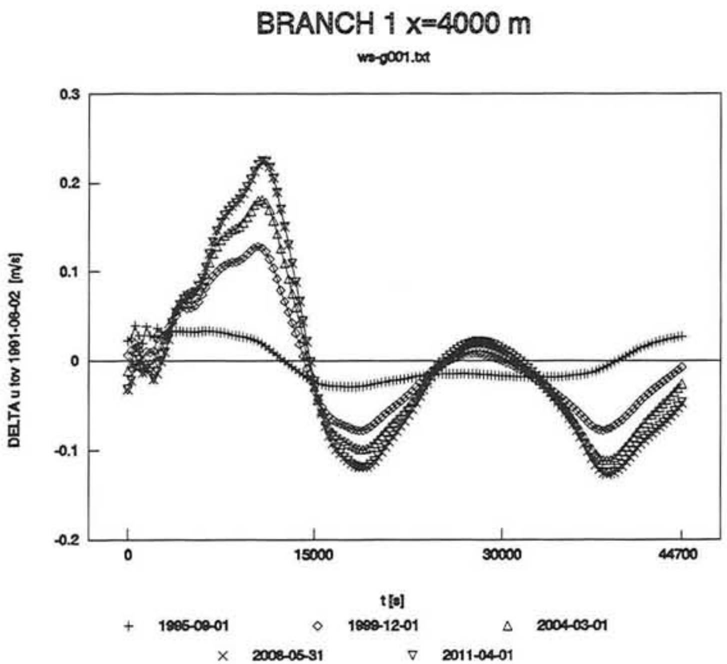
BRANCH 1 x=4000 m
ws-g001.txt
DELTA u tov 1991-06-02 [m/s]
t [s]
1995-09-01
1999-12-01
2004-03-01
2008-05-31
2011-04-01

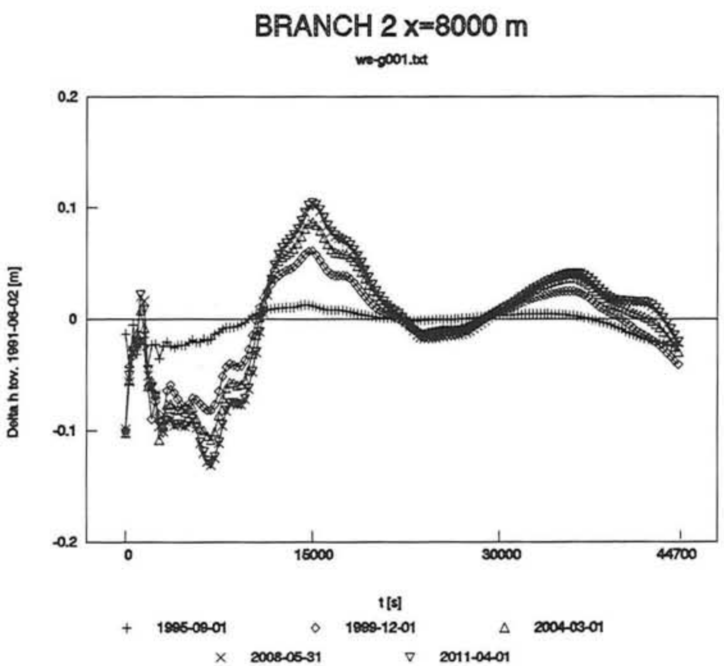
BRANCH 2 x=8000 m
ws-g001.txt
Delta h tov. 1991-06-02 [m]
t [s]
1995-09-01
1999-12-01
2004-03-01
2008-05-31
2011-04-01

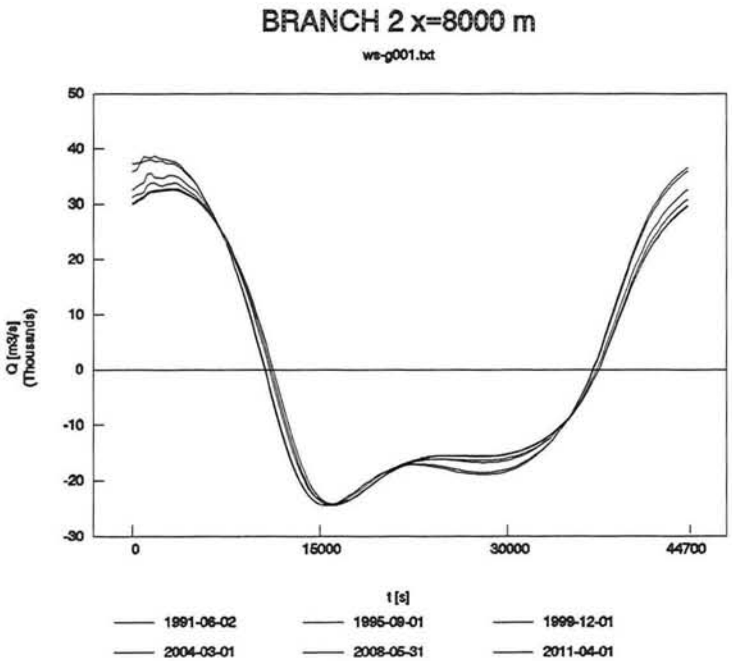
BRANCH 2 x=8000 m
ws-g001.txt
Q [m3/s]
(Thousands)
50
40
30
20
10
0
-10
-20
-30
0
15000
30000
44700
t [s]
1991-06-02
1995-09-01
1999-12-01
2004-03-01
2008-05-31
2011-04-01

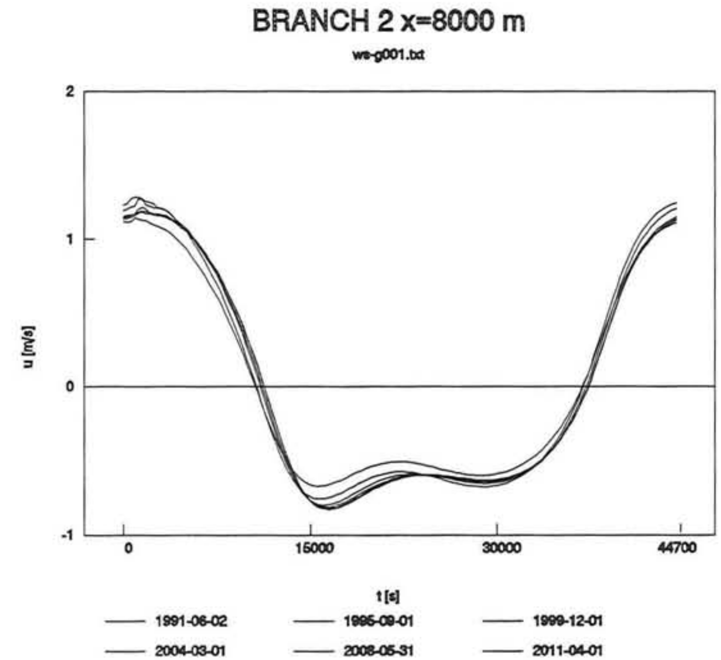
BRANCH 2 x=8000 m
ws-g001.txt
u [m/s]
2
1
0
-1
0
15000
30000
44700
t [s]
1991-06-02
1995-09-01
1999-12-01
2004-03-01
2008-05-31
2011-04-01

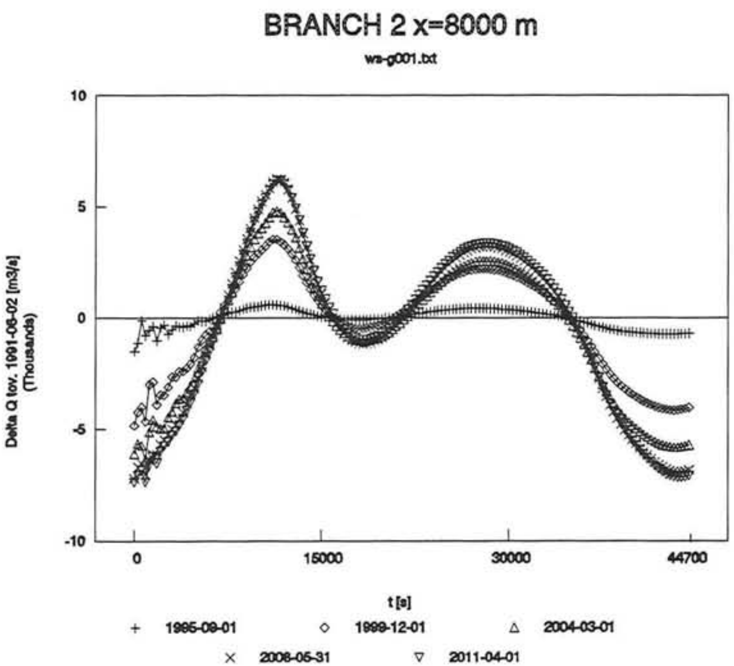
BRANCH 2 x=8000 m
ws-g001.txt
Delta Q tov. 1991-06-02 [m3/s]
(Thousands)
10
5
0
-5
-10
0
15000
30000
44700
t [s]
1995-09-01
1999-12-01
2004-03-01
2008-05-31
2011-04-01

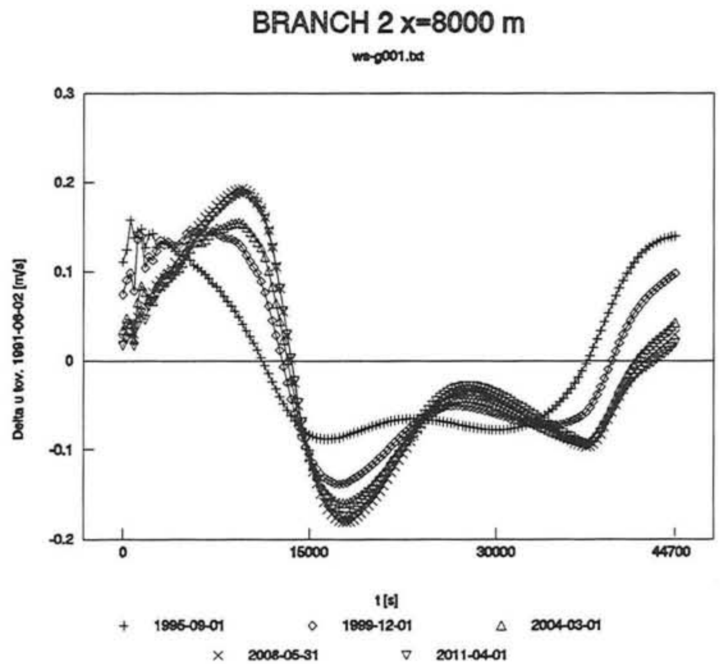
BRANCH 2 x=8000 m
ws-g001.txt
Delta u tov. 1991-06-02 [m/s]
0.3
0.2
0.1
0
-0.1
-0.2
0
15000
30000
44700
t [s]
1995-09-01
1999-12-01
2004-03-01
2008-05-31
2011-04-01

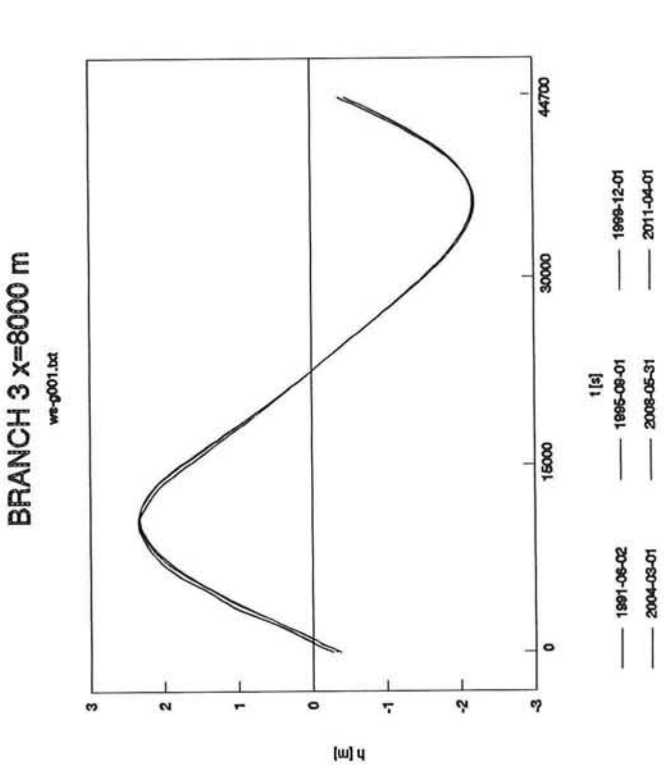
BRANCH 3 x=8000 m
ws-g001.txt
h [m]
t [s]
1991-06-02
1995-09-01
1999-12-01
2004-03-01
2008-05-31
2011-04-01

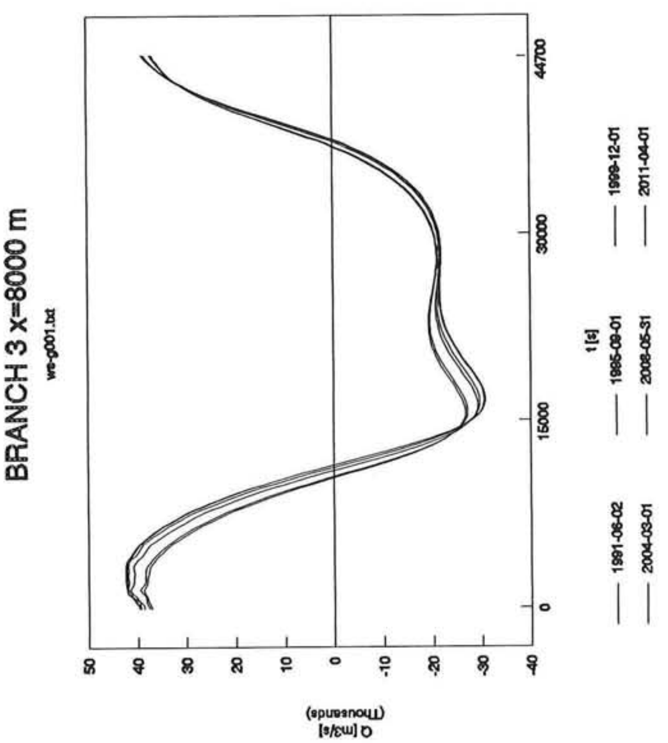
BRANCH 3 x=8000 m
ws-g001.txt
Q [m3/s]
(Thousands)
t [s]
1991-06-02
1995-09-01
1999-12-01
2004-03-01
2008-05-31
2011-04-01

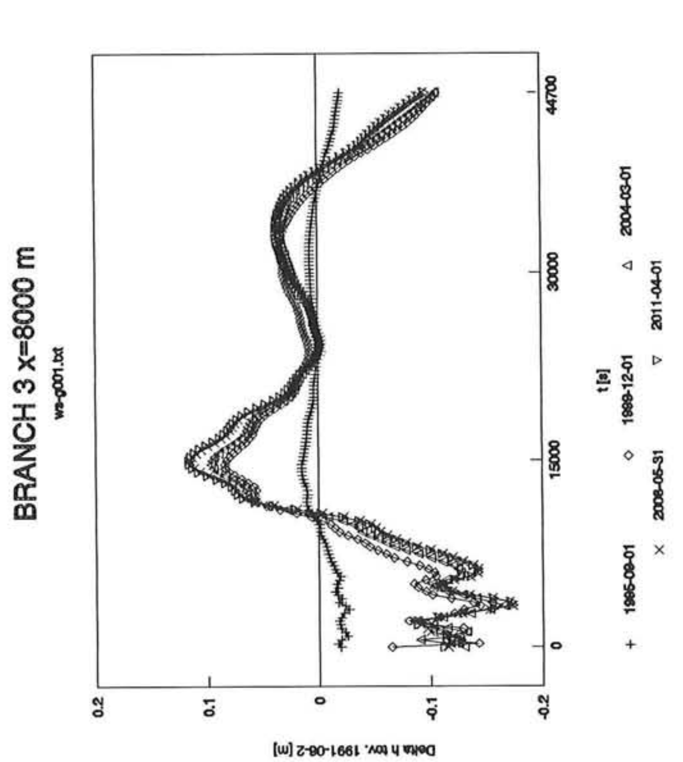
BRANCH 3 x=8000 m
ws-g001.txt
Delta h tov. 1991-06-2 [m]
t [s]
+ 1995-09-01
◇ 1999-12-01
△ 2004-03-01
× 2008-05-31
▽ 2011-04-01

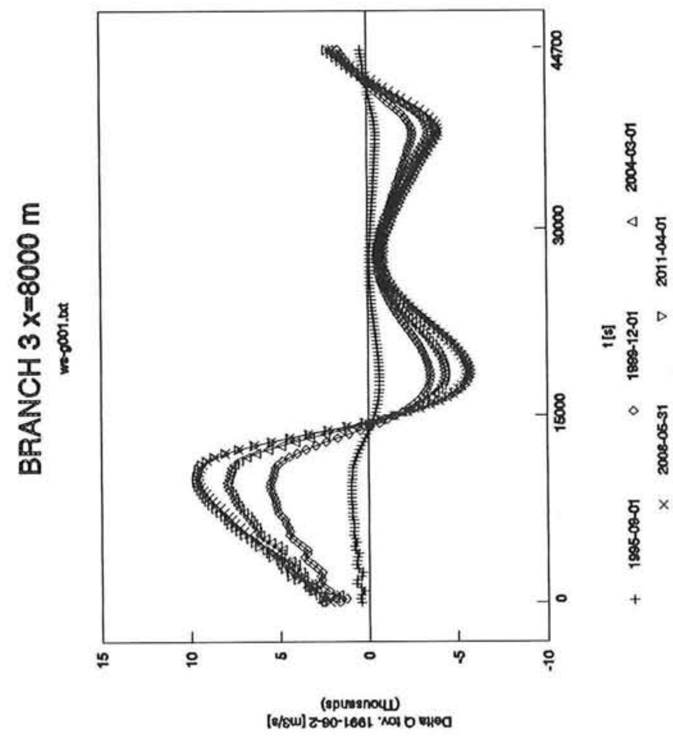
BRANCH 3 x=8000 m
ws-g001.txt
Delta Q tov. 1991-06-2 [m3/s]
(Thousands)
t [s]
+ 1995-09-01
◇ 1999-12-01
△ 2004-03-01
× 2008-05-31
▽ 2011-04-01

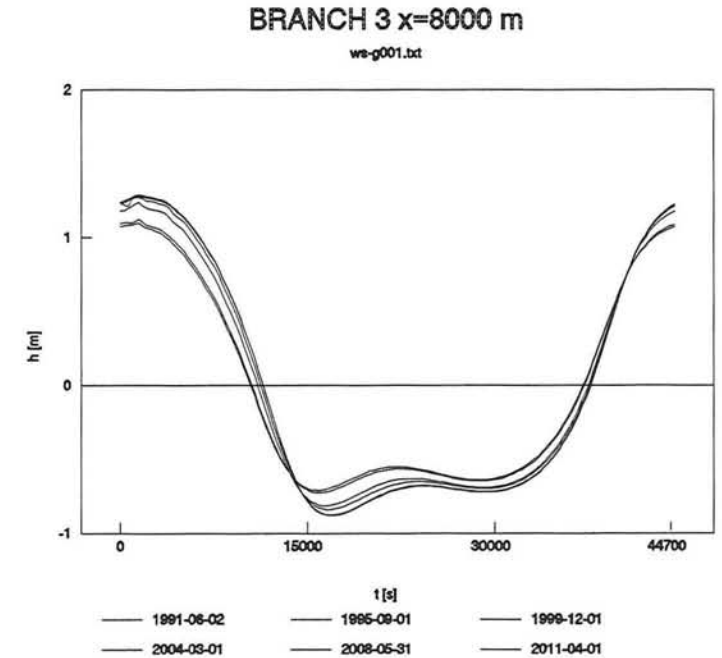
BRANCH 3 x=8000 m
ws-g001.txt
h [m]
t [s]
1991-06-02
1995-09-01
1999-12-01
2004-03-01
2008-05-31
2011-04-01

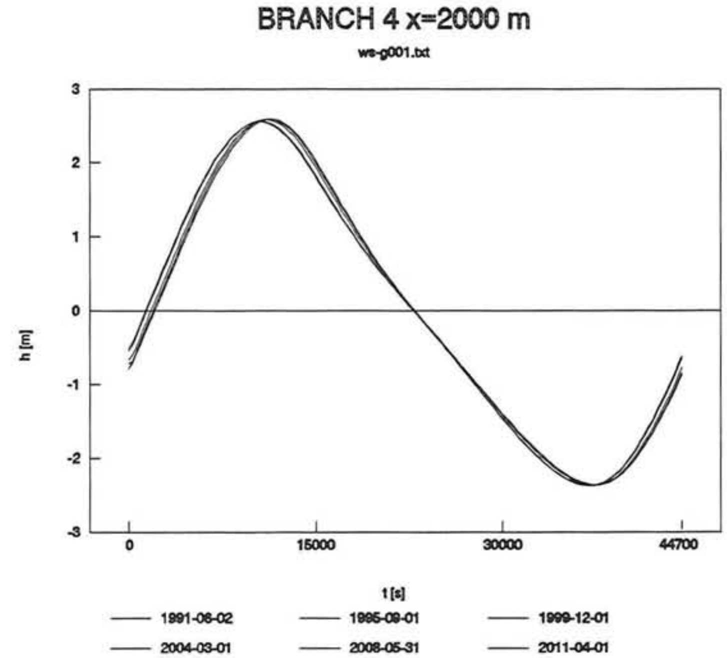
BRANCH 4 x=2000 m
ws-g001.txt
h [m]
t [s]
1991-06-02
1995-09-01
1999-12-01
2004-03-01
2008-05-31
2011-04-01

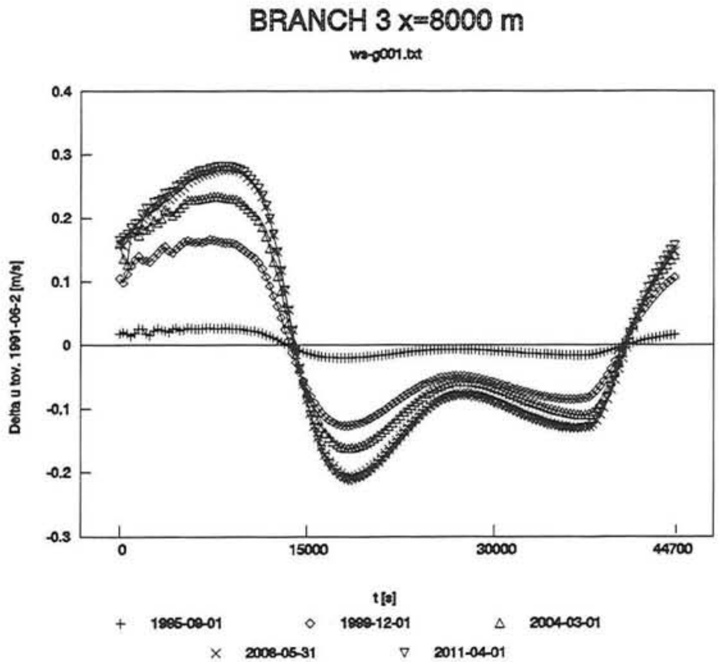
BRANCH 3 x=8000 m
ws-g001.txt
Delta u tov. 1991-06-2 [m/s]
t [s]
1995-09-01
1999-12-01
2004-03-01
2008-05-31
2011-04-01

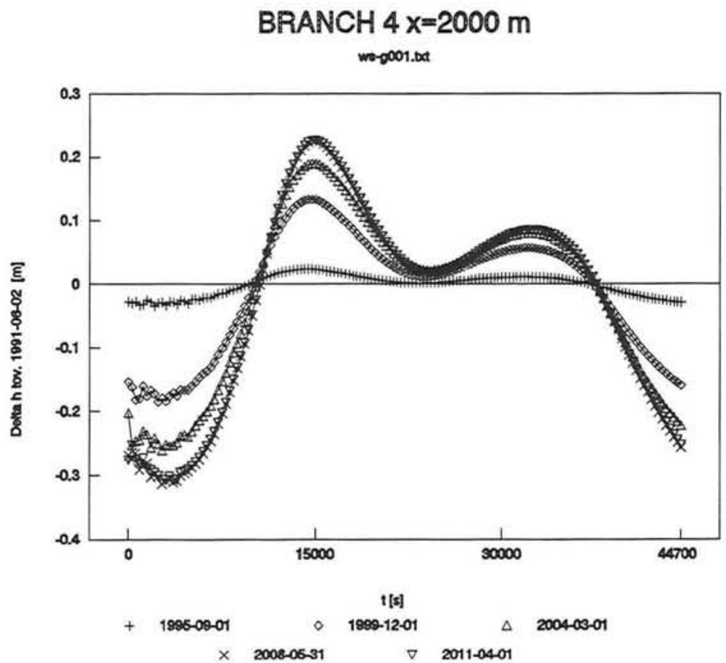
BRANCH 4 x=2000 m
ws-g001.txt
Delta h tov. 1991-06-02 [m]
t [s]
1995-09-01
1999-12-01
2004-03-01
2008-05-31
2011-04-01

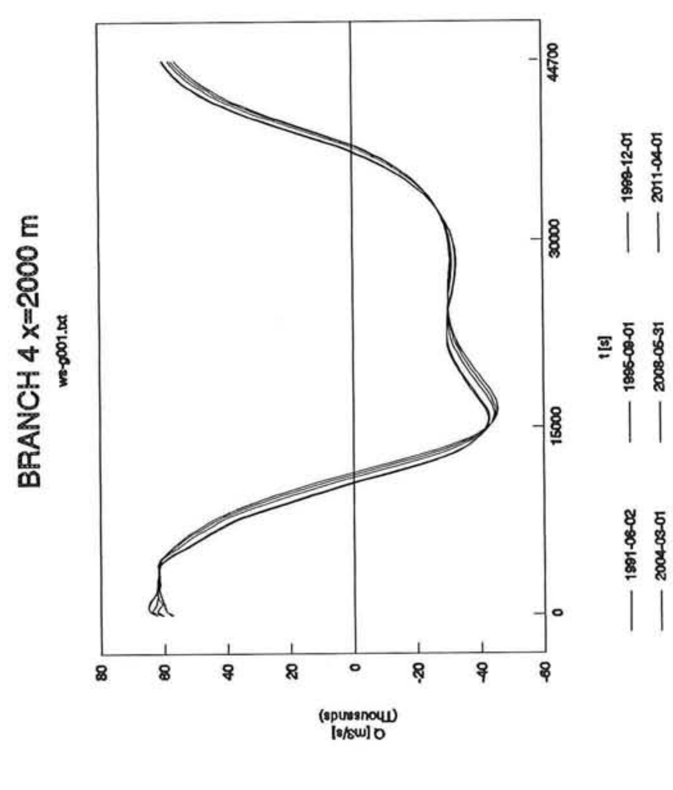

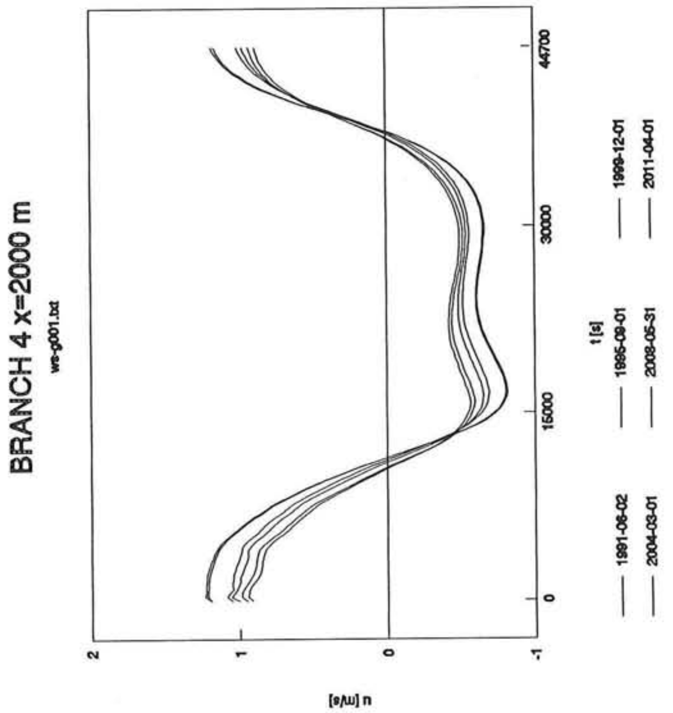

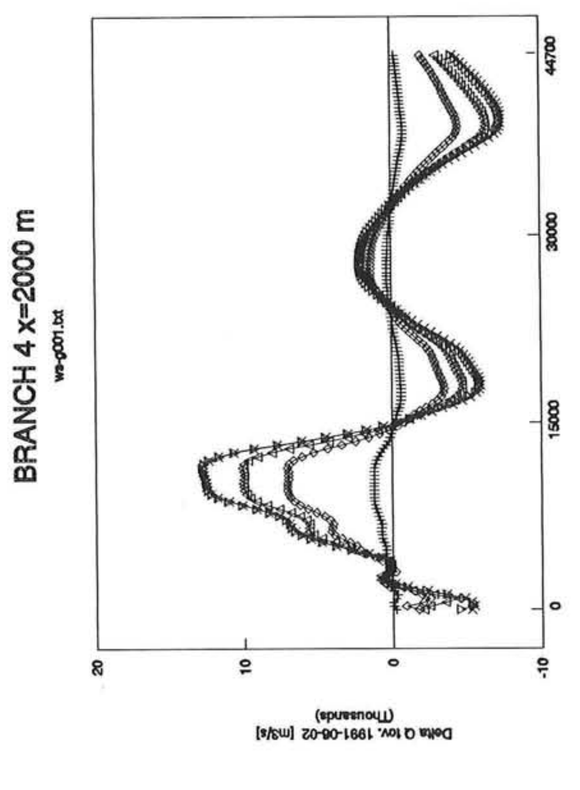

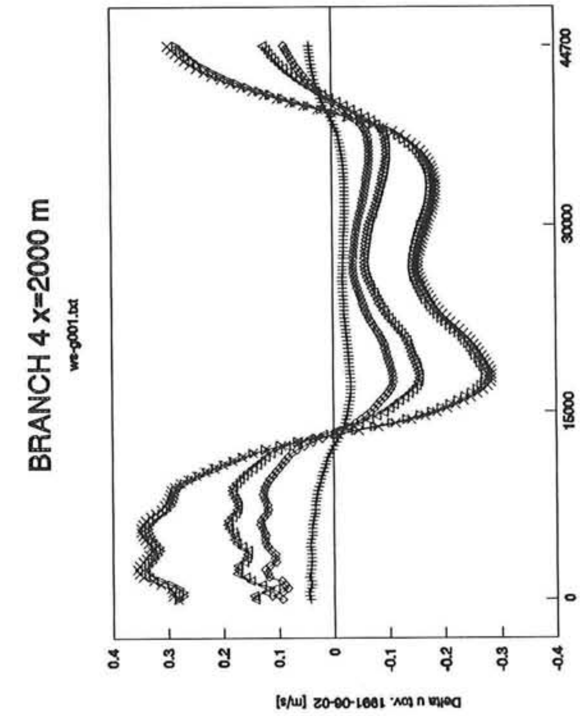

Water levels, discharges and flow velocities

Sediment transport [m^3/s]

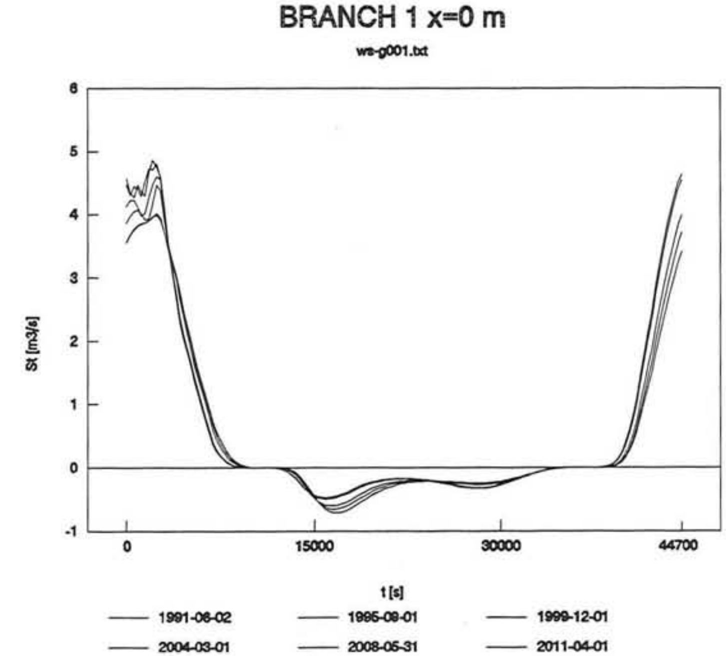

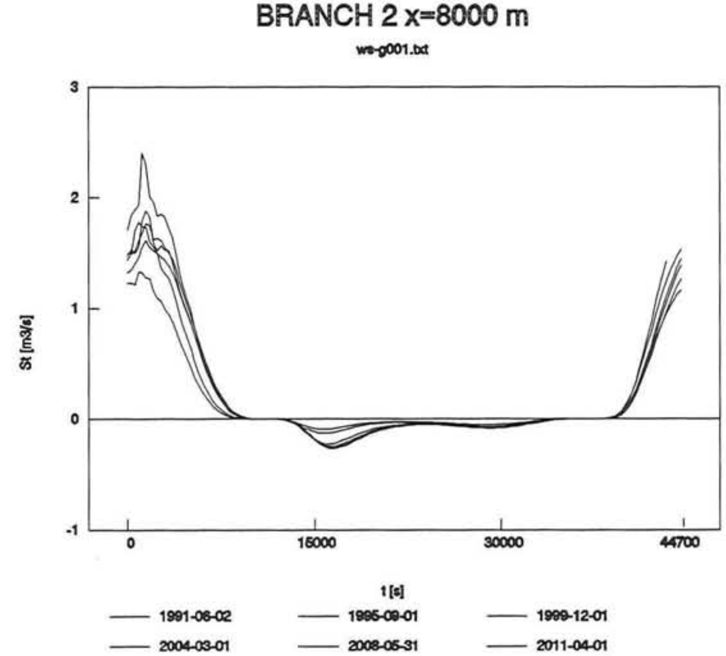

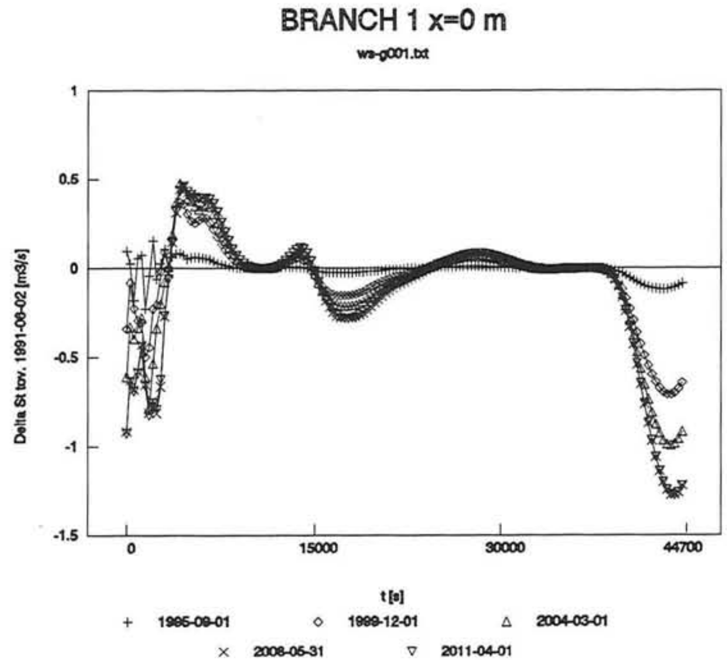

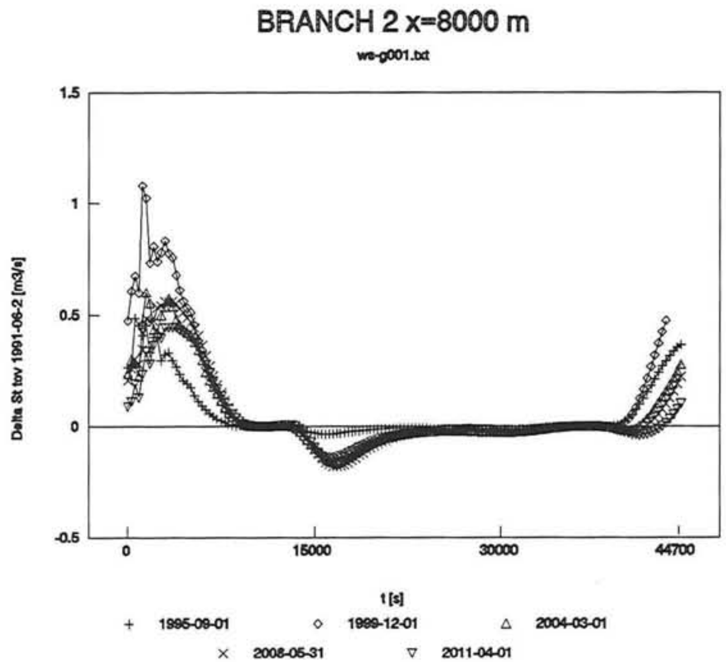

Sediment transport [m^3/s]

BRANCH 3 x=8000 m

ws-g001.txt

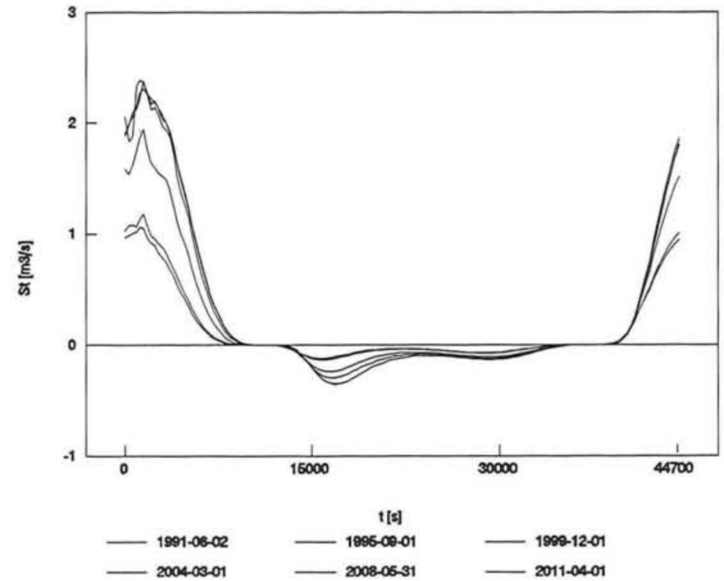

BRANCH 4 x=2000 m

ws-g001.txt

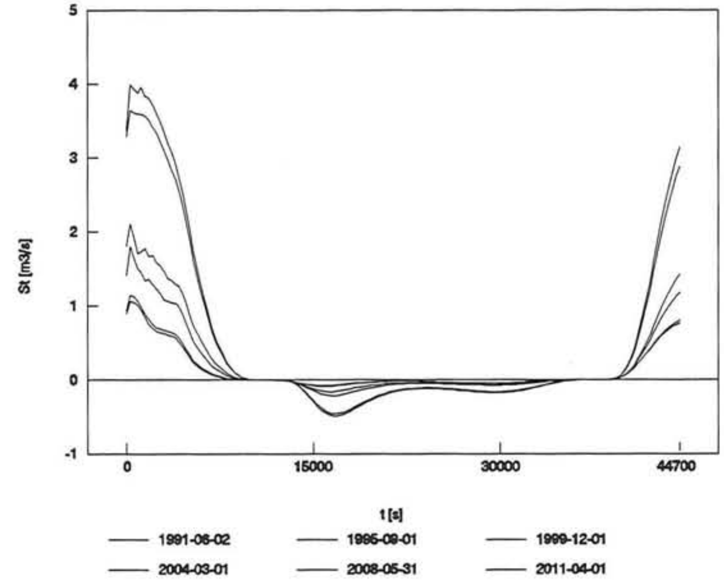

BRANCH 3 x=8000 m

ws-g001.txt

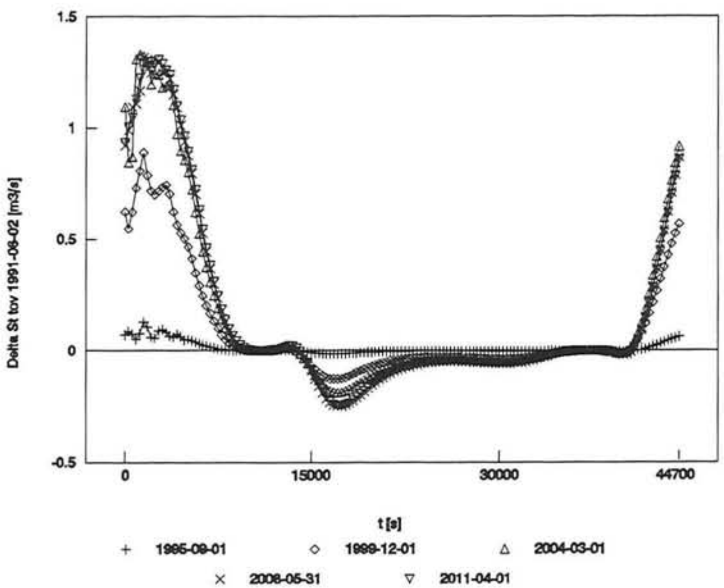

BRANCH 4 x=2000 m

ws-g001.txt

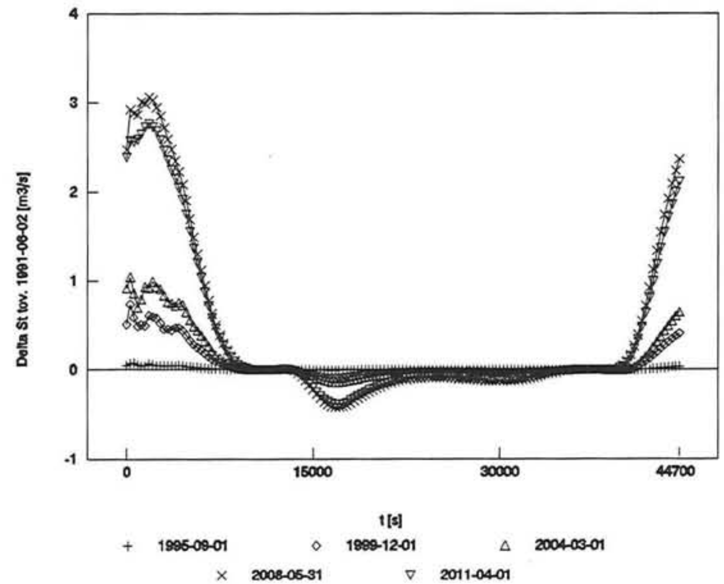

Annex 7: SOBEK computations: scenario 1

	V_{flood} $\cdot 10^6$ m^3	V_{ebb} $\cdot 10^6$ m^3	V_{flood}-V_{ebb} $\cdot 10^6$ m^3
BRANCH 1 x=4000 m			
1991-06-02	1076	1070	7
1995-09-01	1077	1071	6
1999-12-01	1079	1072	7
2004-03-01	1077	1071	6
2008-05-31	1077	1069	8
2011-04-01	1077	1070	7
BRANCH 2 x=8000 m			
1991-06-02	473	441	32
1995-09-01	467	436	31
1999-12-01	438	414	24
2004-03-01	421	412	9
2008-05-31	415	402	13
2011-04-01	411	398	13
BRANCH 3 x=8000 m			
1991-06-02	467	492	-25
1995-09-01	474	498	-24
1999-12-01	505	523	-18
2004-03-01	522	524	-2
2008-05-31	528	534	-6
2011-04-01	532	538	-6
BRANCH 4 x=2000 m			
1991-06-02	775	767	8
1995-09-01	776	768	8
1999-12-01	779	771	8
2004-03-01	779	771	8
2008-05-31	778	771	7
2011-04-01	778	771	7

The volumes have been determined as follows:

$$V_{flood} = \int_{flood} Q(t)\ dt = \Sigma Q_i \cdot \Delta t \qquad \forall\ Q_i > 0$$

$$V_{ebb} = \int_{ebb} Q(t)\ dt = \Sigma Q_i \cdot \Delta t \qquad \forall\ Q_i < 0$$

Table I: Volumes of water that passes a channel during the ebb and flood period

Annex 7: SOBEK computations: scenario 1

$$h(t) = a_0 + h_1\sin(\omega_1 t-\alpha_1) + h_2\sin(\omega_2 t-\alpha_2) + h_3\sin(\omega_3 t-\alpha_3)$$

	a_0 [m]	h_1 [m]	α_1 [°]	h_2 [m]	α_2 [°]	h_3 [m]	α_3 [°]
BRANCH 1 x=4000 m							
1991-06-02	-0.008	2.048	90.028	0.232	97.384	0.014	260.119
1995-09-01	-0.009	2.047	90.092	0.230	97.910	0.014	261.436
1999-12-01	-0.008	2.045	90.171	0.223	98.595	0.014	-81.925
2004-03-01	-0.008	2.044	90.218	0.219	98.765	0.014	-74.777
2008-05-31	-0.007	2.043	90.256	0.216	98.732	0.014	-65.840
2011-04-01	-0.007	2.044	0.000	0.216	-81.778	0.014	-336.698
BRANCH 2 x=8000 m							
1991-06-02	-0.027	2.164	95.005	0.329	114.637	0.043	261.813
1995-09-01	-0.031	2.164	95.338	0.328	116.452	0.044	262.633
1999-12-01	-0.032	2.158	95.796	0.309	120.642	0.046	-82.687
2004-03-01	-0.027	2.155	95.892	0.296	121.639	0.046	-73.039
2008-05-31	-0.027	2.152	95.930	0.286	122.431	0.047	-64.839
2011-04-01	-0.026	2.152	95.929	0.286	122.356	0.048	-64.684
BRANCH 3 x=8000 m							
1991-06-02	-0.018	2.151	94.035	0.316	111.332	0.038	266.967
1995-09-01	-0.019	2.152	94.373	0.315	112.909	0.038	269.406
1999-12-01	-0.027	2.154	95.885	0.308	120.095	0.042	-79.647
2004-03-01	-0.029	2.149	95.927	0.296	121.599	0.043	-74.514
2008-05-31	-0.027	2.147	95.977	0.286	122.199	0.044	-64.573
2011-04-01	-0.027	2.147	96.019	0.286	122.284	0.044	-64.580
BRANCH 4 x=2000 m							
1991-06-02	-0.033	2.270	97.745	0.420	120.015	0.062	267.364
1995-09-01	-0.034	2.273	98.211	0.421	121.885	0.063	-89.790
1999-12-01	-0.044	2.282	100.397	0.419	130.655	0.068	-77.267
2004-03-01	-0.048	2.285	101.582	0.416	134.993	0.069	-71.445
2008-05-31	-0.057	2.284	102.234	0.407	138.267	0.074	-65.834
2011-04-01	-0.056	2.284	102.205	0.407	138.101	0.074	-65.407

Table II: Results of a harmonic analysis

	a_0 [m]	h_1 [m]	α_1 [°]	h_2 [m]	α_2 [°]	h_3 [m]	α_3 [°]
BRANCH 1 x=4000 m							
1991-06-02	-0.008	2.048	0.000	0.232	-82.673	0.014	-9.966
1995-09-01	-0.009	2.047	0.000	0.230	-82.274	0.014	-8.841
1999-12-01	-0.008	2.045	0.000	0.223	-81.747	0.014	-352.439
2004-03-01	-0.008	2.044	0.000	0.219	-81.672	0.014	-345.431
2008-05-31	-0.007	2.043	0.000	0.216	-81.780	0.014	-336.608
2011-04-01	-0.007	2.044	0.000	0.216	-81.778	0.014	-336.698
BRANCH 2 x=8000 m							
1991-06-02	-0.027	2.164	0.000	0.329	-75.373	0.043	-23.201
1995-09-01	-0.031	2.164	0.000	0.328	-74.224	0.044	-23.381
1999-12-01	-0.032	2.158	0.000	0.309	-70.950	0.046	-10.075
2004-03-01	-0.027	2.155	0.000	0.296	-70.144	0.046	-0.713
2008-05-31	-0.027	2.152	0.000	0.286	-69.429	0.047	-352.628
2011-04-01	-0.026	2.152	0.000	0.286	-69.501	0.048	-352.470
BRANCH 3 x=8000 m							
1991-06-02	-0.018	2.151	0.000	0.316	-76.738	0.038	-15.137
1995-09-01	-0.019	2.152	0.000	0.315	-75.838	0.038	-13.714
1999-12-01	-0.027	2.154	0.000	0.308	-71.675	0.042	-7.302
2004-03-01	-0.029	2.149	0.000	0.296	-70.254	0.043	-2.293
2008-05-31	-0.027	2.147	0.000	0.286	-69.754	0.044	-352.503
2011-04-01	-0.027	2.147	0.000	0.286	-69.754	0.044	-352.636
BRANCH 4 x=2000 m							
1991-06-02	-0.033	2.270	0.000	0.420	-75.474	0.062	-25.870
1995-09-01	-0.034	2.273	0.000	0.421	-74.538	0.063	-24.424
1999-12-01	-0.044	2.282	0.000	0.419	-70.139	0.068	-18.457
2004-03-01	-0.048	2.285	0.000	0.416	-68.171	0.069	-16.191
2008-05-31	-0.057	2.284	0.000	0.407	-66.201	0.074	-12.535
2011-04-01	-0.056	2.284	0.000	0.407	-66.308	0.074	-12.021

Table III: Phase difference of the M4 and M6 component compared the M2 component at that point.

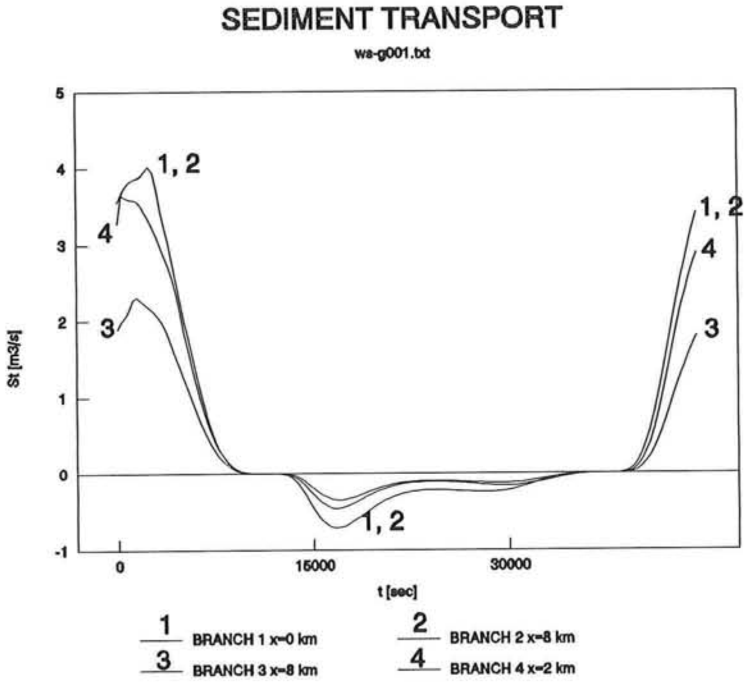

	S_{flood} [m^3]	S_{ebb} [m^3]
BRANCH 1 x=0 km	29314	6361
BRANCH 2 x=8 km	29306	6363
BRANCH 3 x=8 km	16284	3145
BRANCH 4 x=2 km	25828	3954

Table VI: Sediment transport during the flood and ebb period at the end of the calculation (2023-12-30)

Annex 8: SOBEK computations: scenario 2

BRANCH 1

ws-k001.txt

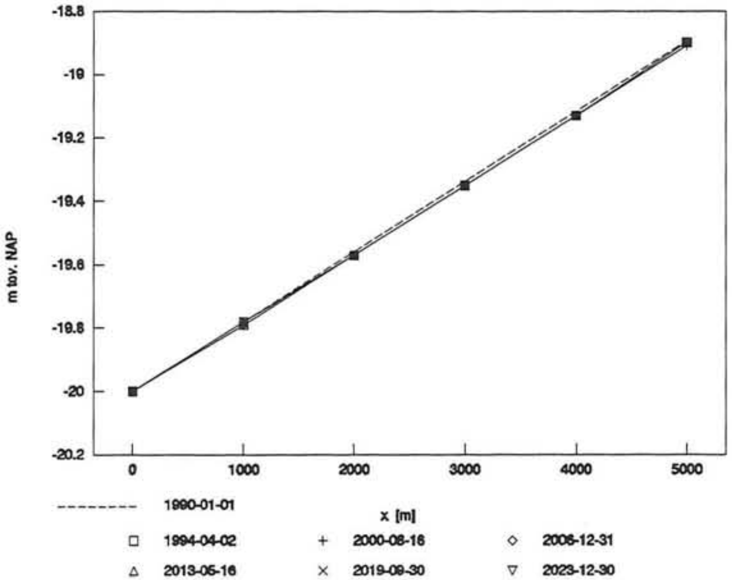

BRANCH 2

ws-k001.txt

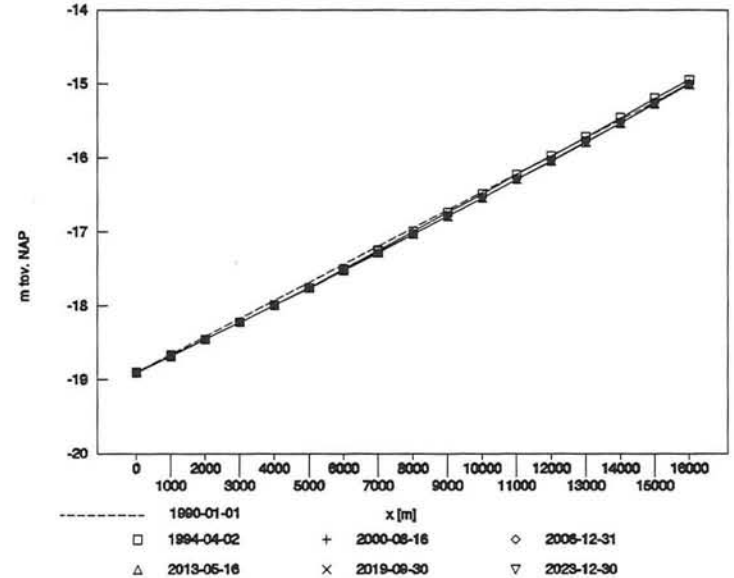

BRANCH 3

ws-k001.txt

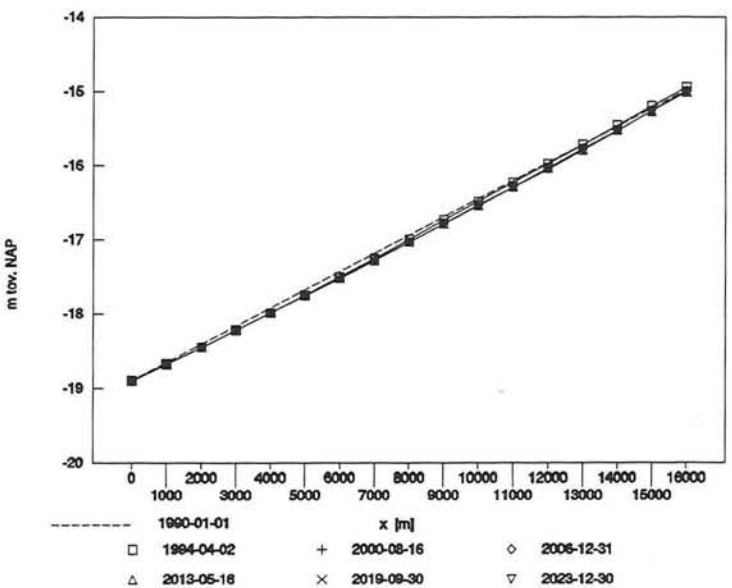

BRANCH 4

ws-k001.txt

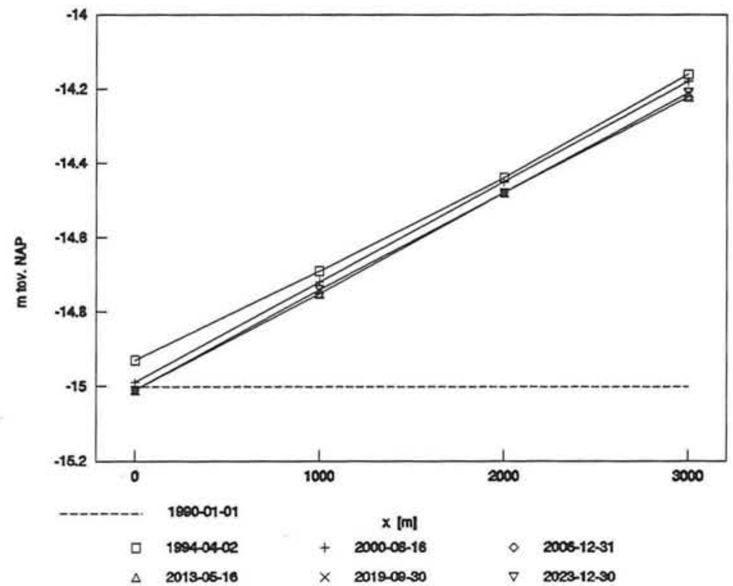

Integrated sediment transport [m^3/s]

BRANCH 1

ws-k001.txt

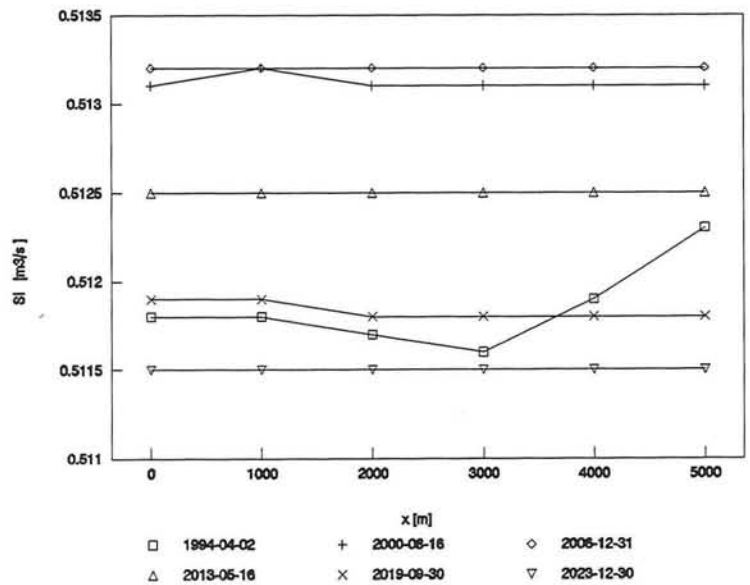

BRANCH 2

ws-k001.txt

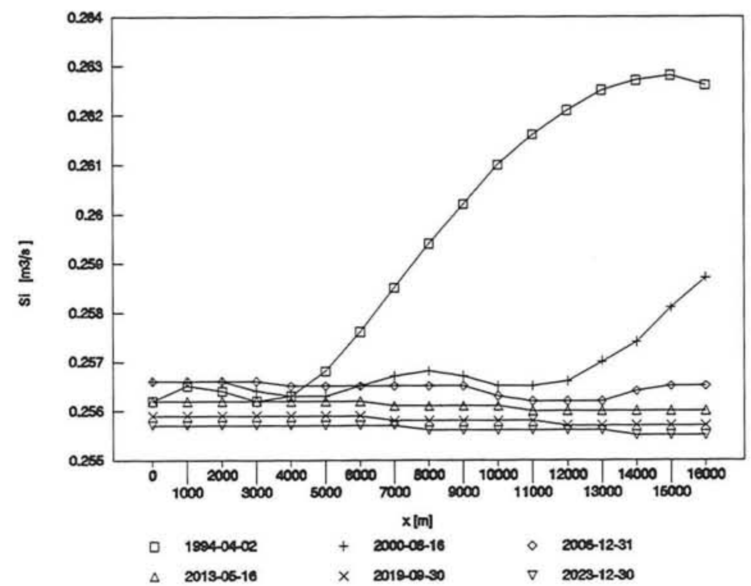

BRANCH 3

ws-k001.txt

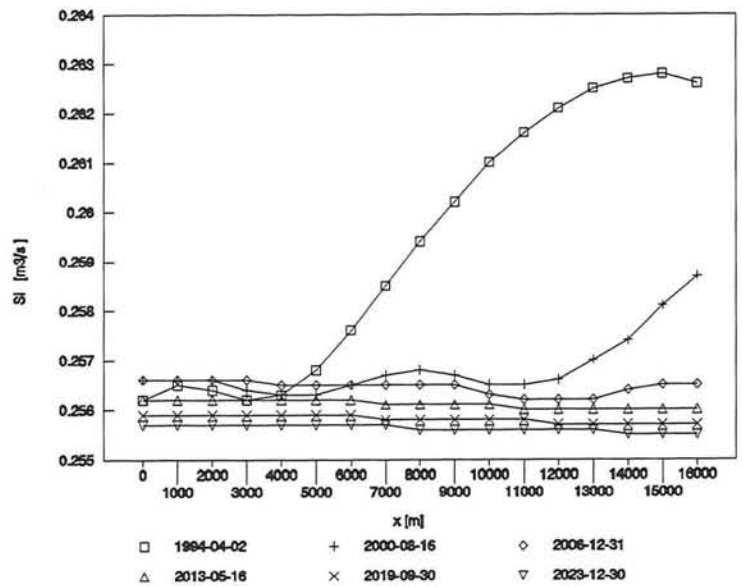

BRANCH 4

ws-k001.txt

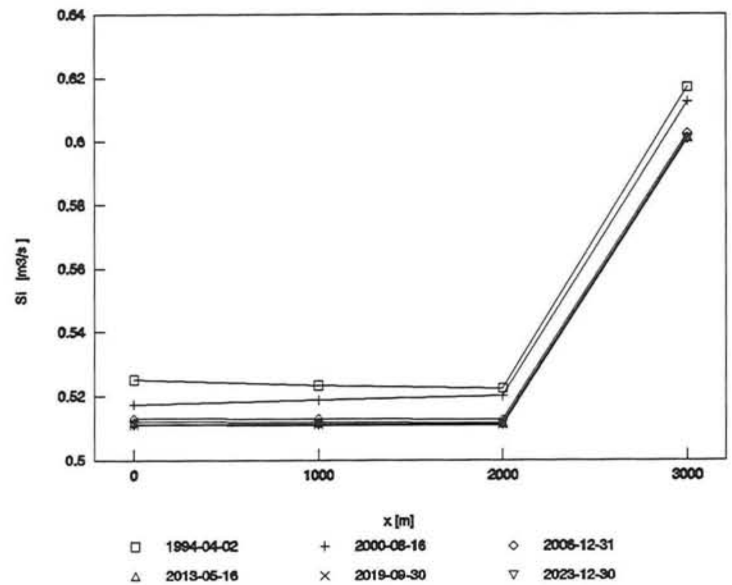

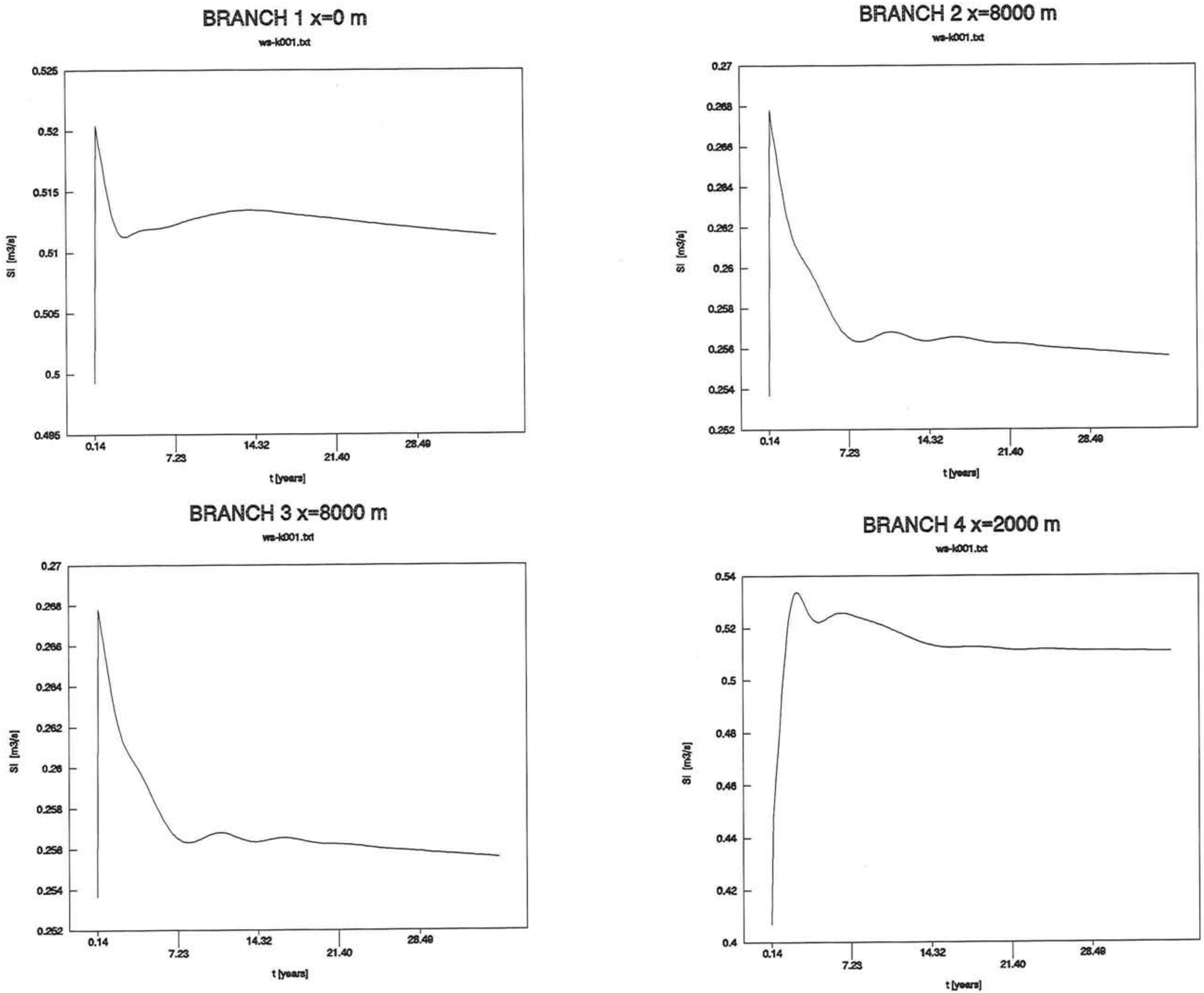

Integrated sediment transport [m^3/s]

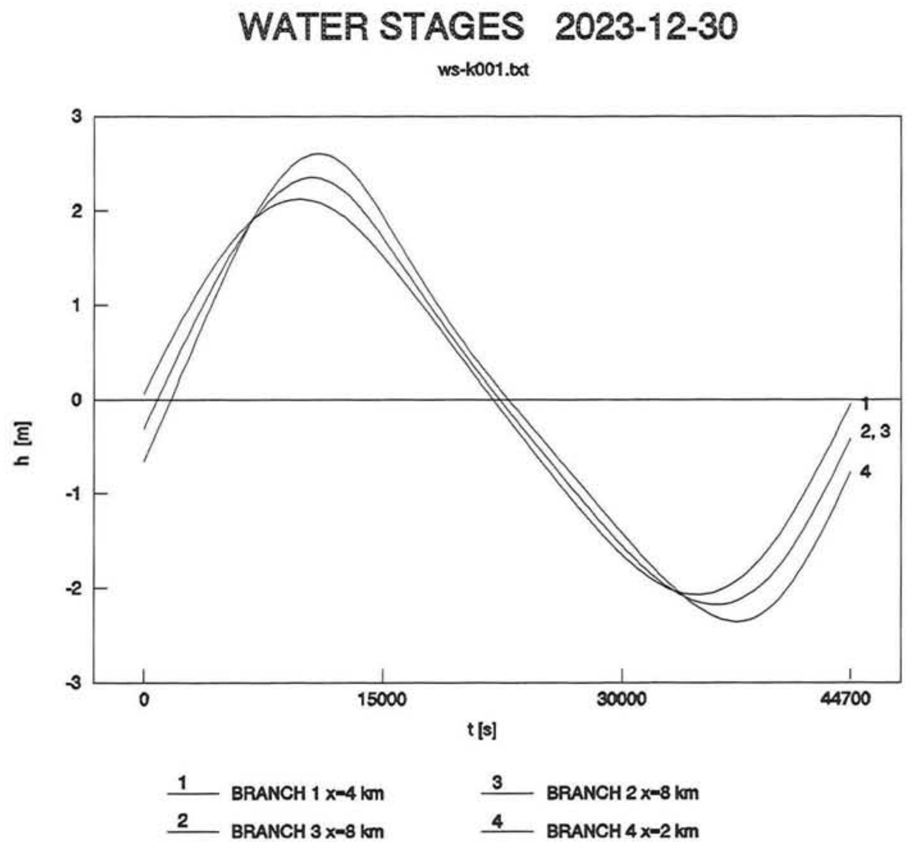
WATER STAGES 2023-12-30
ws-k001.txt
h [m]
3
2
1
0
-1
-2
-3
0
15000
30000
44700
t [s]
1
2, 3
4
1 BRANCH 1 x=4 km
2 BRANCH 3 x=8 km
3 BRANCH 2 x=8 km
4 BRANCH 4 x=2 km

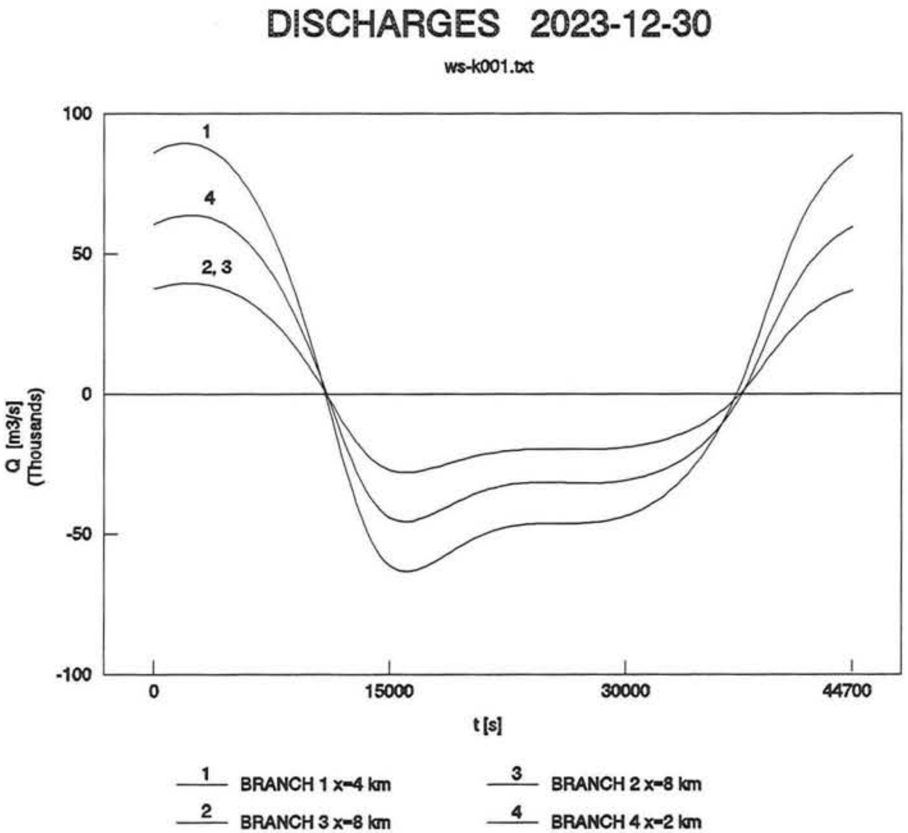
DISCHARGES 2023-12-30
ws-k001.txt
Q [m3/s] (Thousands)
100
50
0
-50
-100
0
15000
30000
44700
t [s]
1
4
2, 3
1 BRANCH 1 x=4 km
2 BRANCH 3 x=8 km
3 BRANCH 2 x=8 km
4 BRANCH 4 x=2 km

Annex 8: SOBEK computations: scenario 2

	V_{flood} $\cdot 10^6$ [m^3]	V_{ebb} $\cdot 10^6$ [m^3]
BRANCH 1 x=4 km	1118	1118
BRANCH 2 x=8 km	492	492
BRANCH 3 x=8 km	492	492
BRANCH 4 x=2 km	769	769

There is no net transport of water over a tidal period for this computation as the water motion has been recalculated with a fixed bed (no dredging activities).

Table I: Volumes of water that passes a channel during the ebb and flood period (2023-12-30)

	a0 [m]	h1 [m]	alfa1 [°]	h2 [m]	alfa2 [°]	h3 [m]	alfa3 [°]
1992-02-16							
BRANCH 1 x=0 m	-0.000	2.000	85.122	0.200	80.290	0.000	22.323
BRANCH 1 x=4 km	-0.008	2.044	87.895	0.217	94.678	0.014	-83.448
BRANCH 2 x=8 km	-0.031	2.153	94.207	0.297	119.746	0.043	-83.965
BRANCH 3 x=8 km	-0.031	2.153	94.207	0.297	119.746	0.043	-83.965
BRANCH 4 x=2 km	-0.036	2.289	100.144	0.417	132.041	0.061	-75.090
2006-12-31							
BRANCH 1 x=0 m	-0.000	2.000	85.122	0.200	80.290	0.000	22.323
BRANCH 1 x=4 km	-0.008	2.044	87.889	0.218	94.617	0.014	-83.998
BRANCH 2 x=8 km	-0.031	2.154	94.167	0.299	119.378	0.043	-84.399
BRANCH 3 x=8 km	-0.031	2.154	94.167	0.299	119.378	0.043	-84.399
BRANCH 4 x=2 km	-0.036	2.290	100.041	0.418	131.452	0.061	-75.474
2023-12-30							
BRANCH 1 x=0 m	-0.000	2.000	85.122	0.200	80.290	0.000	22.323
BRANCH 1 x=4 km	-0.008	2.044	87.885	0.218	94.571	0.014	-84.074
BRANCH 2 x=8 km	-0.031	2.154	94.152	0.299	119.199	0.044	-84.479
BRANCH 3 x=8 km	-0.031	2.154	94.152	0.299	119.199	0.044	-84.479
BRANCH 4 x=2 km	-0.036	2.290	100.014	0.419	131.201	0.062	-75.596

Table II: Results of the harmonic analysis

	a0 [m]	h1 [m]	alfa1 [°]	h2 [m]	alfa2 [°]	h3 [m]	alfa3 [°]
1992-02-16							
BRANCH 1 x=0 m	-0.000	2.000	0.000	0.200	-89.955	0.000	-233.044
BRANCH 1 x=4 km	-0.008	2.044	0.000	0.217	-81.111	0.014	-347.131
BRANCH 2 x=8 km	-0.031	2.153	0.000	0.297	-68.668	0.043	-6.586
BRANCH 3 x=8 km	-0.031	2.153	0.000	0.297	-68.668	0.043	-6.586
BRANCH 4 x=2 km	-0.036	2.289	0.000	0.417	-68.246	0.061	-15.521
2006-12-31							
BRANCH 1 x=0 m	-0.000	2.000	0.000	0.200	-89.955	0.000	-233.044
BRANCH 1 x=4 km	-0.008	2.044	0.000	0.218	-81.160	0.014	-347.664
BRANCH 2 x=8 km	-0.031	2.154	0.000	0.299	-68.956	0.043	-6.899
BRANCH 3 x=8 km	-0.031	2.154	0.000	0.299	-68.956	0.043	-6.899
BRANCH 4 x=2 km	-0.036	2.290	0.000	0.418	-68.630	0.061	-15.597
2023-12-30							
BRANCH 1 x=0 m	-0.000	2.000	0.000	0.200	-89.955	0.000	-233.044
BRANCH 1 x=4 km	-0.008	2.044	0.000	0.218	-81.198	0.014	-347.727
BRANCH 2 x=8 km	-0.031	2.154	0.000	0.299	-69.105	0.044	-6.934
BRANCH 3 x=8 km	-0.031	2.154	0.000	0.299	-69.105	0.044	-6.934
BRANCH 4 x=2 km	-0.036	2.290	0.000	0.419	-68.827	0.062	-15.638

Table III: Phase difference of the M4 and M6 component compared the M2 component at that point

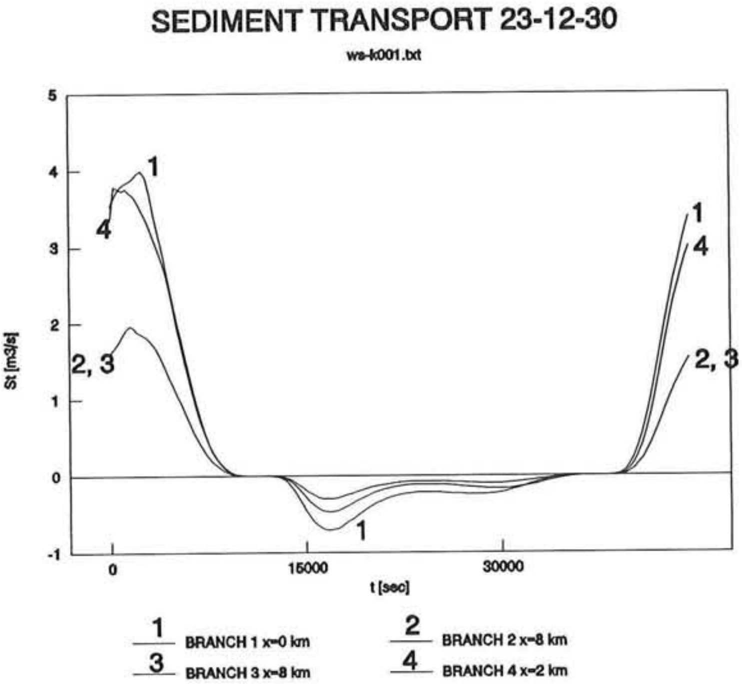

	S_{flood} [m^3]	S_{ebb} [m^3]
BRANCH 1 x=0 km	29218	6356
BRANCH 2 x=8 km	14010	2583
BRANCH 3 x=8 km	14010	2583
BRANCH 4 x=2 km	26963	4128

Table IV: Sediment transport during the flood and ebb period at the end of the calculation (2023-12-30)

Annex 9:SOBEK computations; scenario 3

BRANCH 1

ws-l001.txt

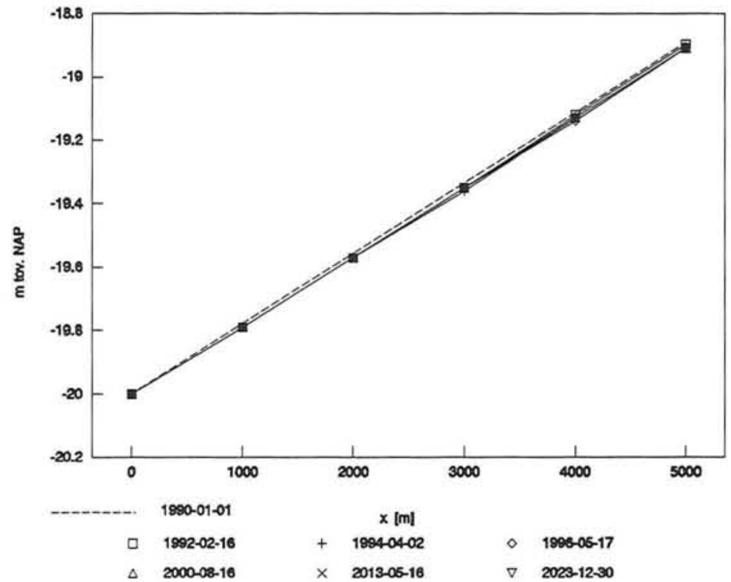

BRANCH 2

ws-l001.txt

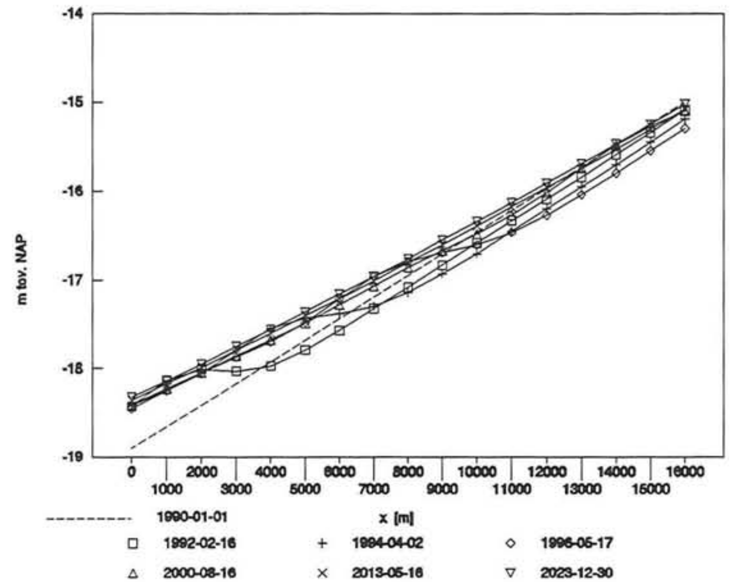

BRANCH 3

ws-l001.txt

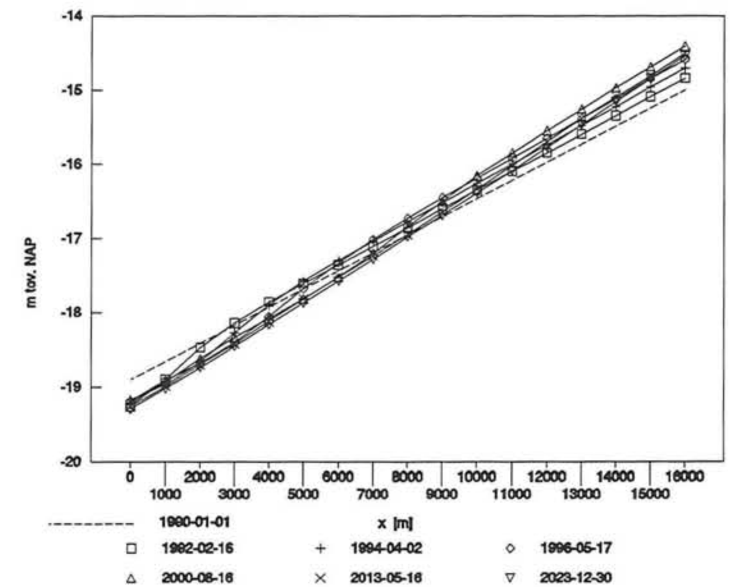

BRANCH 4

ws-l001.txt

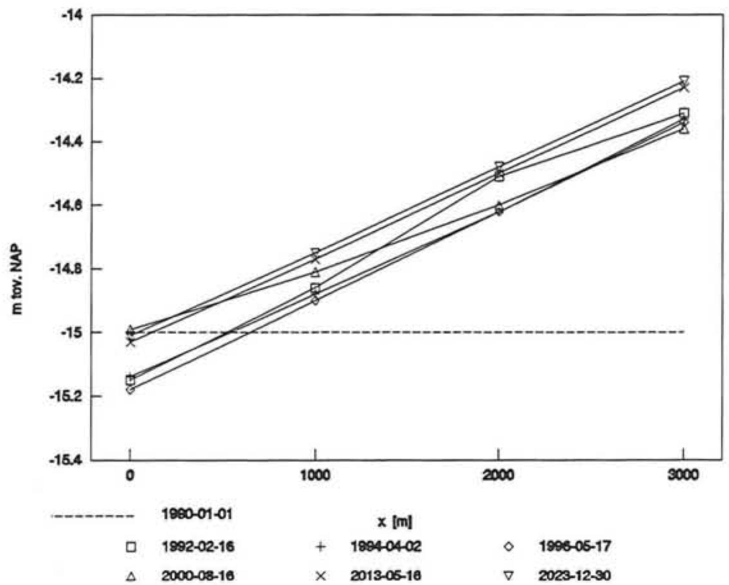

Integrated sediment transport [m^3/s]

BRANCH 1

ws-l001.txt

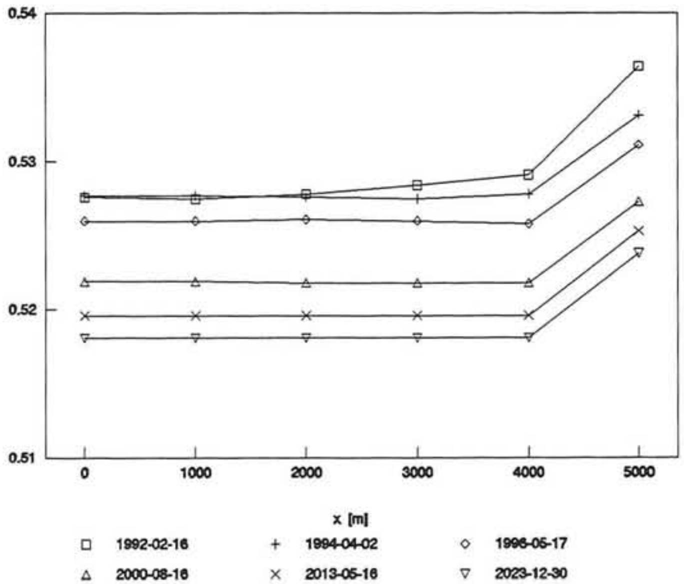

BRANCH 2

ws-l001.txt

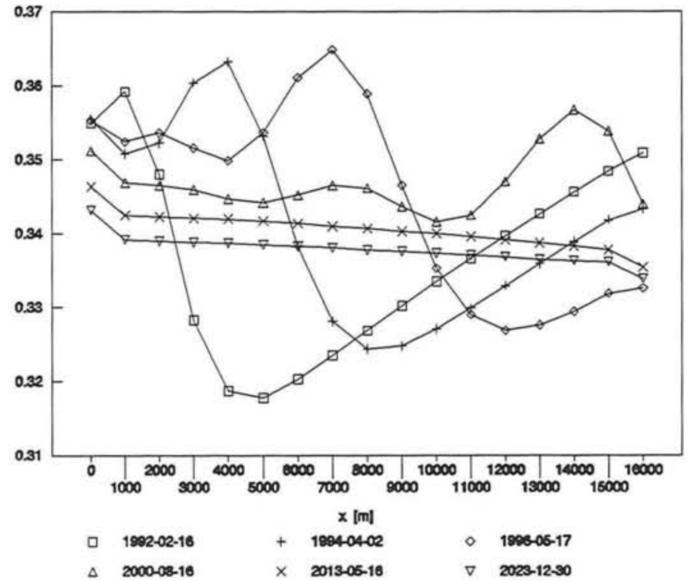

BRANCH 3

ws-l001.txt

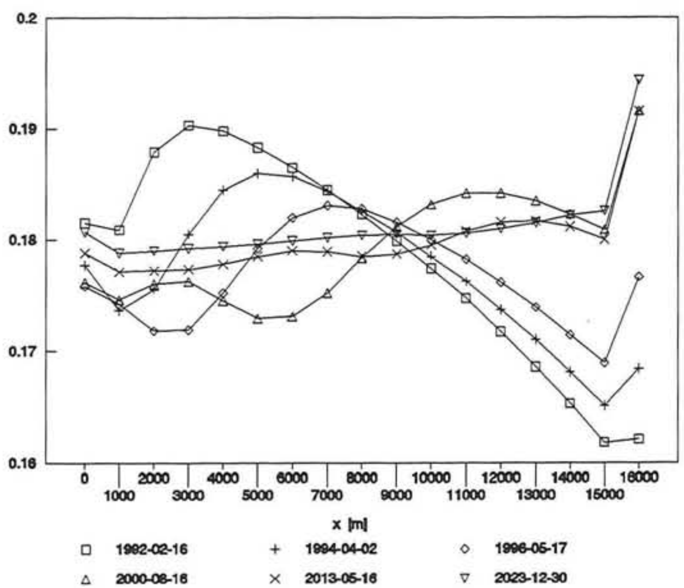

BRANCH 4

ws-l001.txt

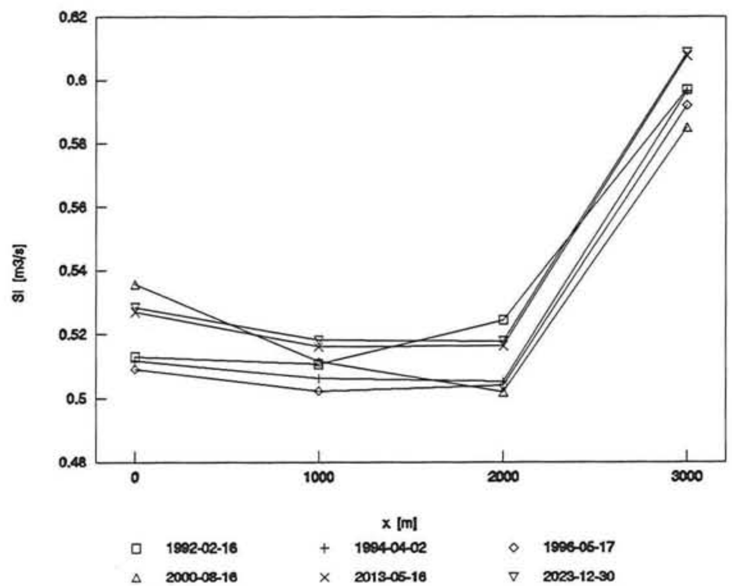

Integrated sediment transport [m^3/s]

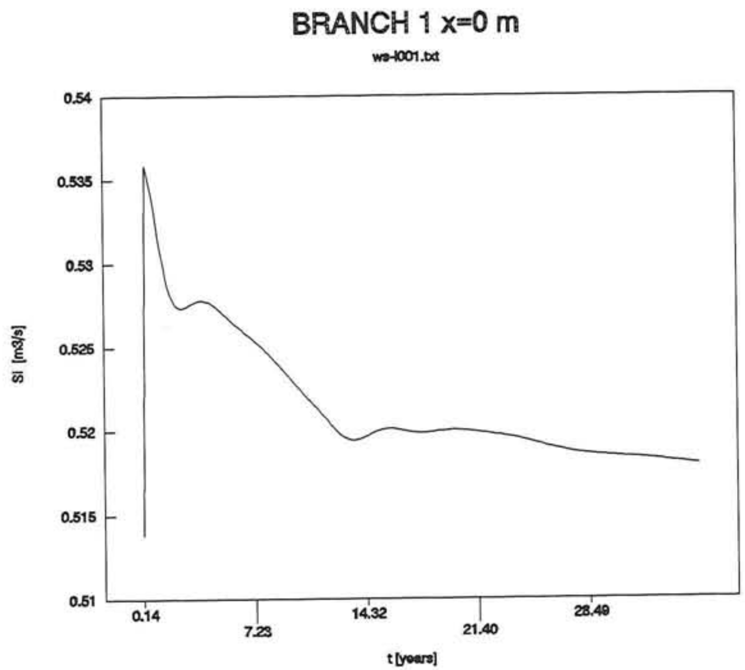

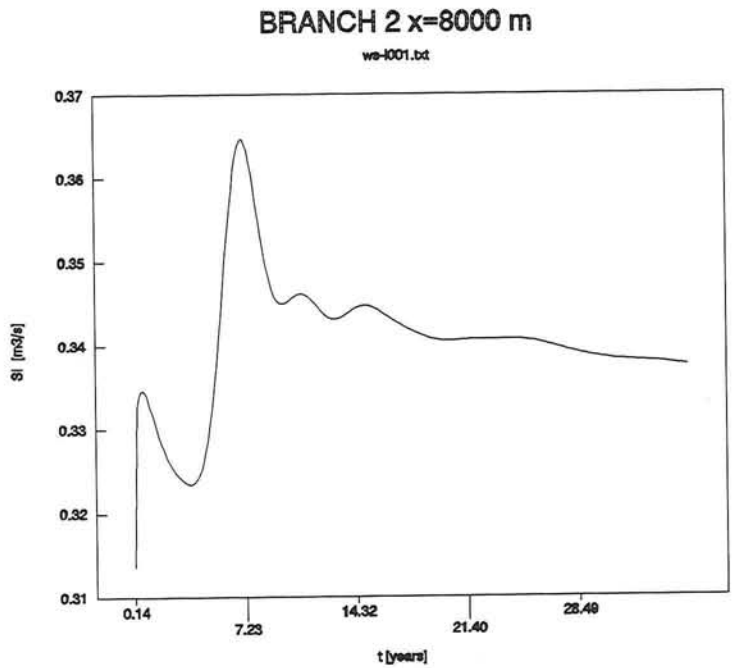

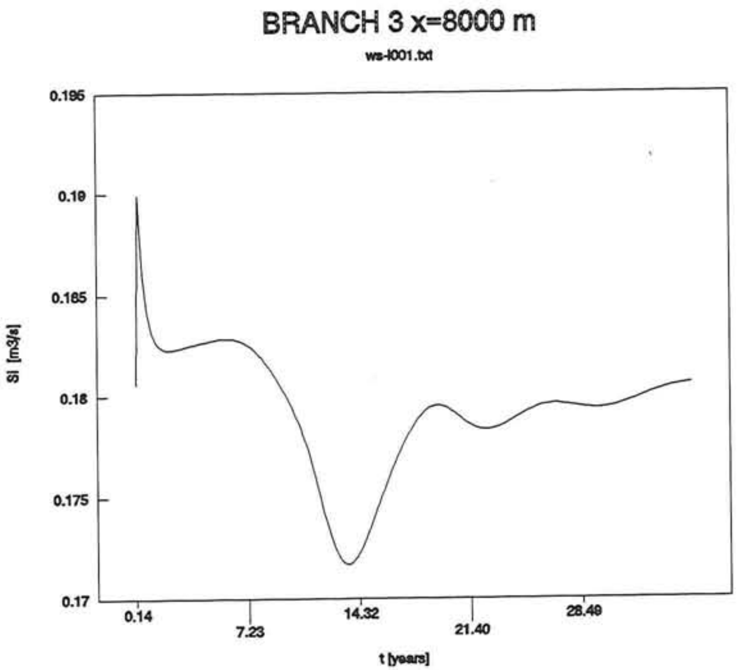

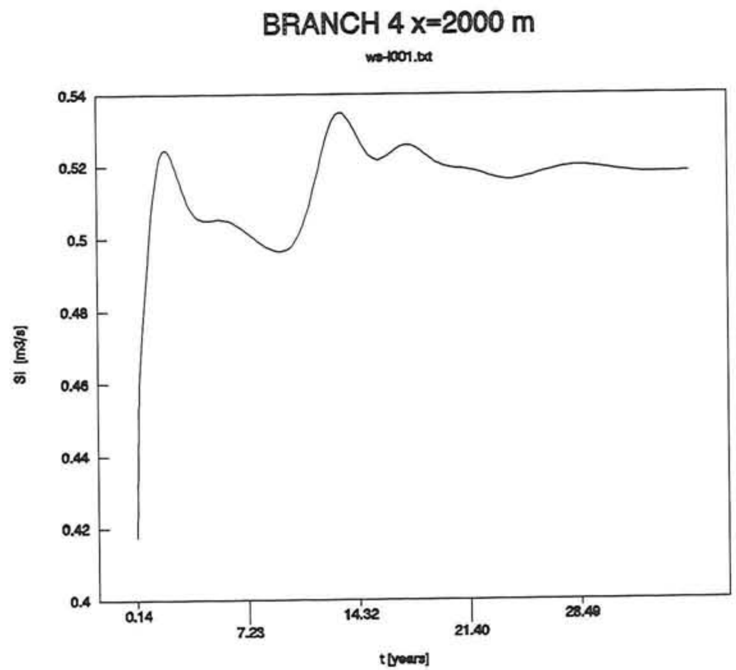

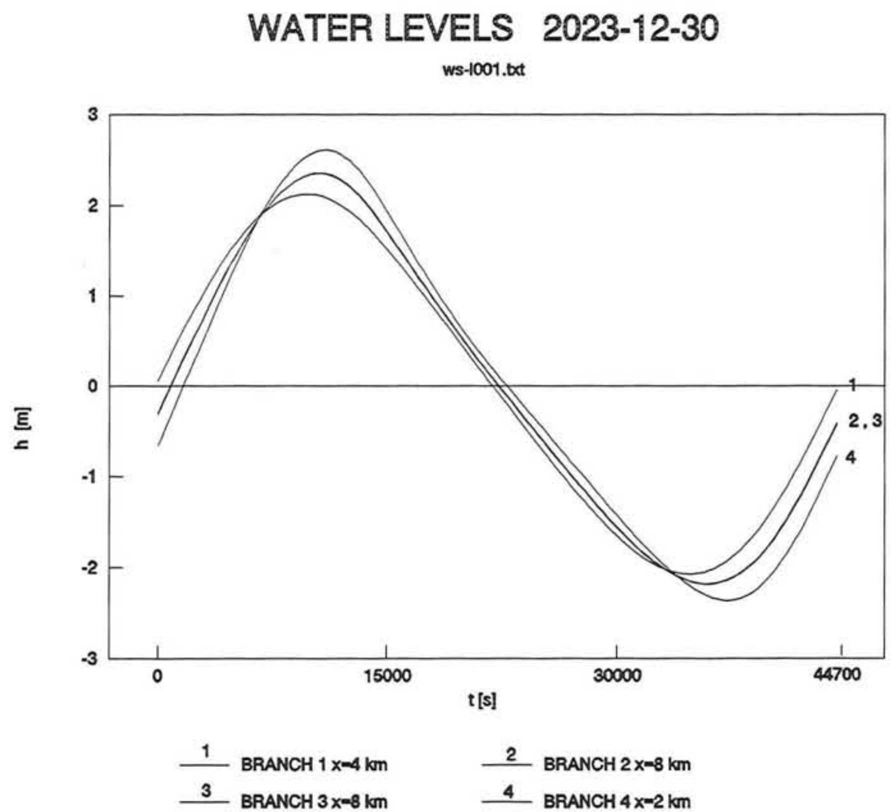
WATER LEVELS 2023-12-30
ws-l001.txt
h [m]
3
2
1
0
-1
-2
-3
0
15000
30000
44700
t [s]
1
2, 3
4
1 BRANCH 1 x=4 km
2 BRANCH 2 x=8 km
3 BRANCH 3 x=8 km
4 BRANCH 4 x=2 km

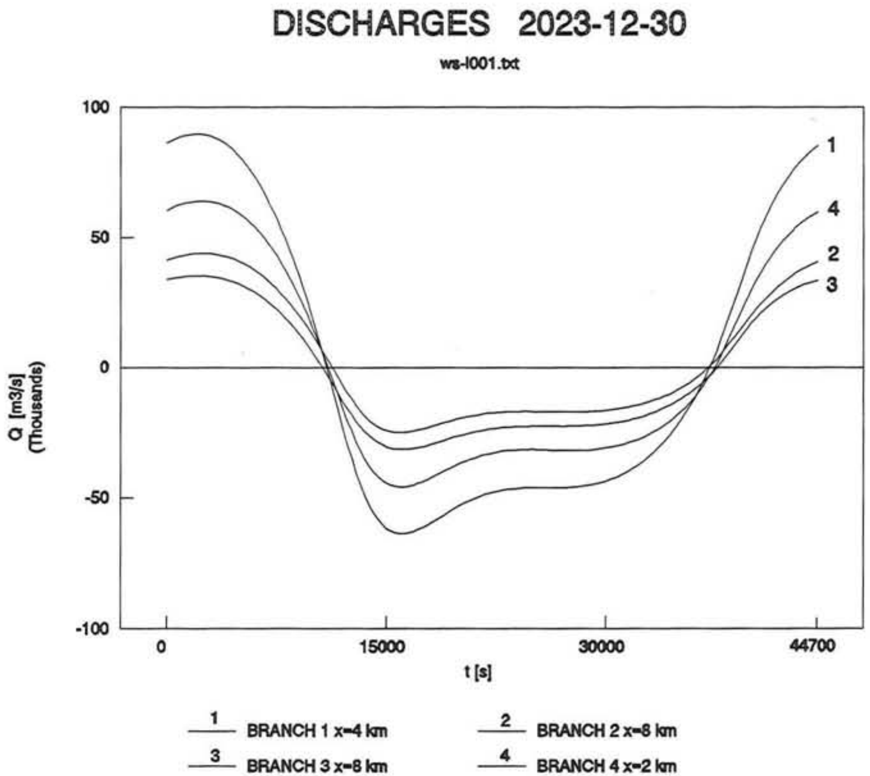
DISCHARGES 2023-12-30
ws-l001.txt
Q [m3/s]
(Thousands)
100
50
0
-50
-100
0
15000
30000
44700
t [s]
1
4
2
3
1 BRANCH 1 x=4 km
2 BRANCH 2 x=8 km
3 BRANCH 3 x=8 km
4 BRANCH 4 x=2 km

Annex 9: SOBEK computations: scenario 3

	Vflood $\cdot 10^6$ [m^3]	Vebb $\cdot 10^6$ [m^3]	Vflood-Vebb $\cdot 10^6$ [m^3]
BRANCH 1 x=4 km	1078	1071	7
BRANCH 2 x=8 km	532	399	132
BRANCH 3 x=8 km	415	540	-125
BRANCH 4 x=2 km	780	773	7

Table I: Volumes of water that passes a channel during the ebb and flood period (2023-12-30)

	a0 [m]	h1 [m]	alfa1 [°]	h2 [m]	alfa2 [°]	h3 [m]	alfa3 [°]
BRANCH 1							
1992-02-16	-0.007	2.044	90.128	0.216	98.700	0.014	-67.168
2013-05-16	-0.007	2.044	90.309	0.216	98.981	0.014	-65.727
2023-12-30	-0.007	2.044	90.399	0.216	99.136	0.014	-65.422
BRANCH 2							
1992-02-16	-0.025	2.152	95.829	0.288	122.260	0.045	-64.397
2013-05-16	-0.026	2.152	96.097	0.288	122.861	0.045	-63.844
2023-12-30	-0.026	2.152	96.175	0.288	122.940	0.046	-63.573
BRANCH 3							
1992-02-16	-0.029	2.151	95.705	0.287	122.412	0.045	-67.311
2013-05-16	-0.028	2.150	95.807	0.286	122.340	0.046	-65.383
2023-12-30	-0.028	2.150	95.897	0.286	122.457	0.046	-65.099
BRANCH 4							
1992-02-16	-0.056	2.286	101.958	0.410	138.122	0.072	-66.878
2013-05-16	-0.056	2.286	102.258	0.411	138.620	0.074	-65.756
2023-12-30	-0.057	2.286	102.338	0.411	138.695	0.074	-65.508

Table II: Results of the harmonic analysis

	a0 [m]	h1 [m]	alfa1 [°]	h2 [m]	alfa2 [°]	h3 [m]	alfa3 [°]
BRANCH 1							
1992-02-16	-0.007	2.044	0.000	0.216	-81.555	0.014	-337.551
2013-05-16	-0.007	2.044	0.000	0.216	-81.638	0.014	-336.654
2023-12-30	-0.007	2.044	0.000	0.216	-81.661	0.014	-336.618
BRANCH 2							
1992-02-16	-0.025	2.152	0.000	0.288	-69.398	0.045	-351.885
2013-05-16	-0.026	2.152	0.000	0.288	-69.333	0.045	-352.134
2023-12-30	-0.026	2.152	0.000	0.288	-69.409	0.046	-352.096
BRANCH 3							
1992-02-16	-0.029	2.151	0.000	0.287	-68.997	0.045	-354.425
2013-05-16	-0.028	2.150	0.000	0.286	-69.273	0.046	-352.803
2023-12-30	-0.028	2.150	0.000	0.286	-69.336	0.046	-352.789
BRANCH 4							
1992-02-16	-0.056	2.286	0.000	0.410	-65.794	0.072	-12.753
2013-05-16	-0.056	2.286	0.000	0.411	-65.896	0.074	-12.530
2023-12-30	-0.057	2.286	0.000	0.411	-65.981	0.074	-12.521

Table III: Phase difference of the M4 and M6 component compared the M2 component at that point

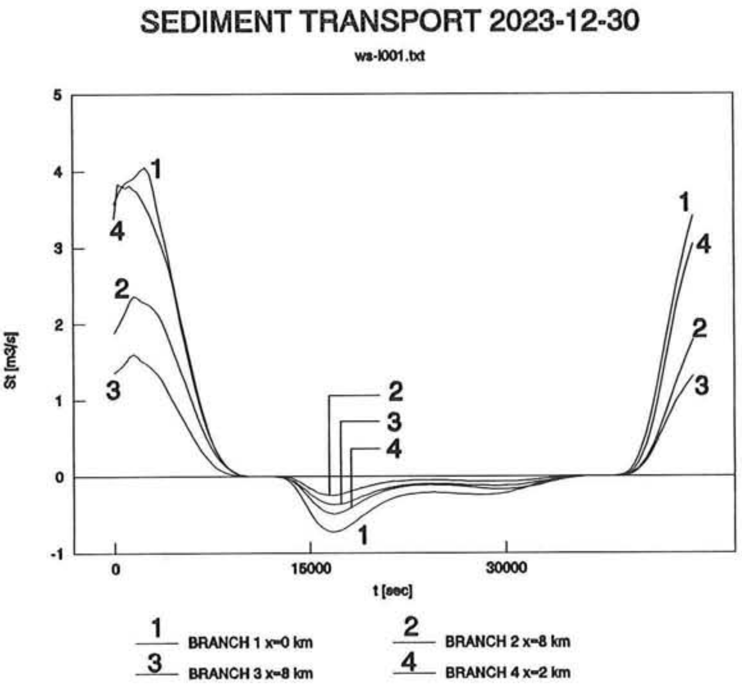

	S_{flood} [m^3]	S_{ebb} [m^3]
BRANCH 1 x=0 km	29580	6422
BRANCH 2 x=8 km	17021	1921
BRANCH 3 x=8 km	11371	3305
BRANCH 4 x=2 km	27329	4177

Table VI: Sediment transport during the flood and ebb period at the end of the calculation (2023-12-30)

Annex 10: SOBEK computations; scenario 4

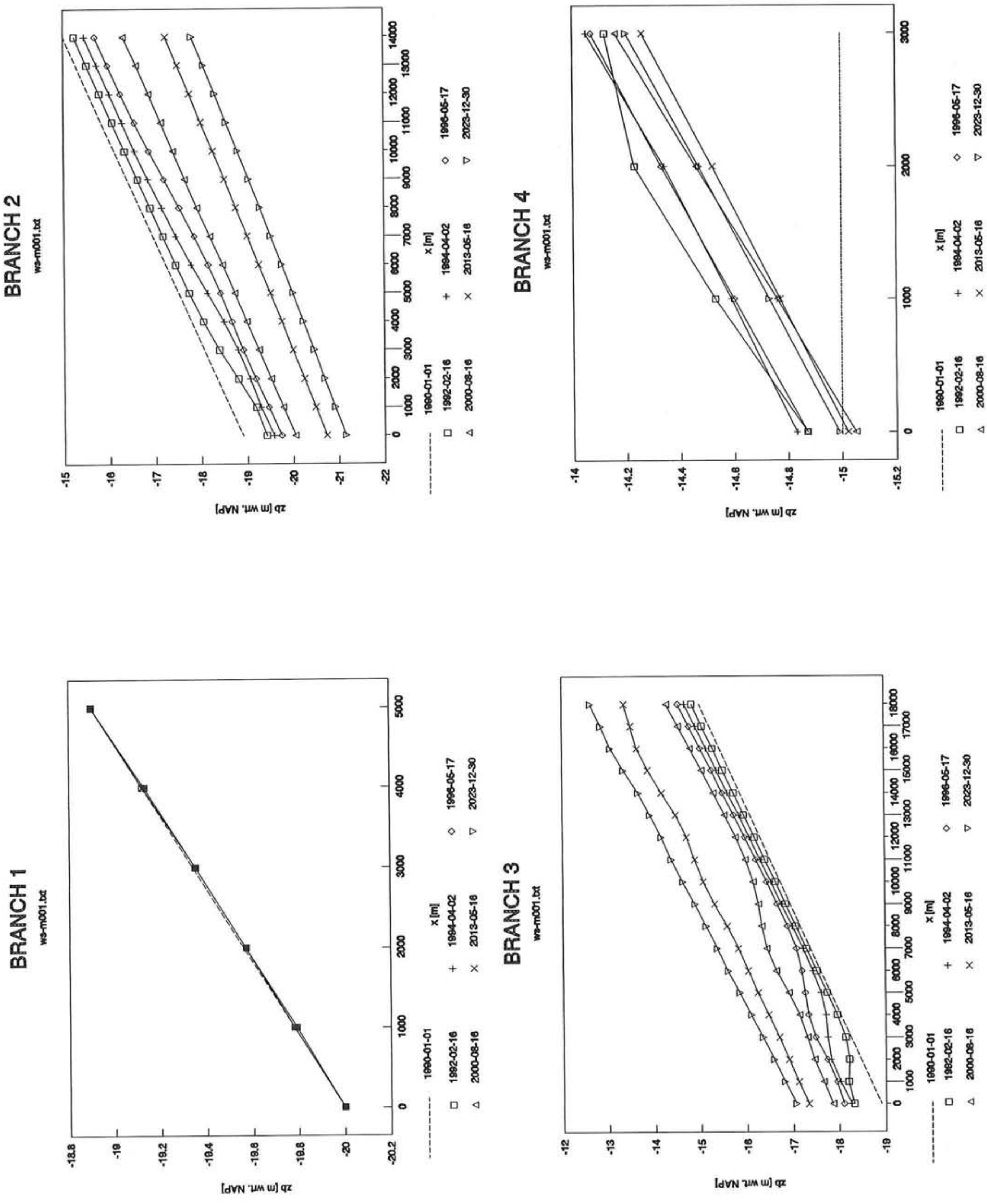
BRANCH 2
ws-m001.txt
BRANCH 4
ws-m001.txt
BRANCH 1
ws-m001.txt
BRANCH 3
ws-m001.txt
zb [m wrt. NAP]
x [m]
1990-01-01
1992-02-16
1994-04-02
1996-05-17
2000-08-16
2013-05-16
2023-12-30

Bed level

Integrated sediment transport [m^3/s]

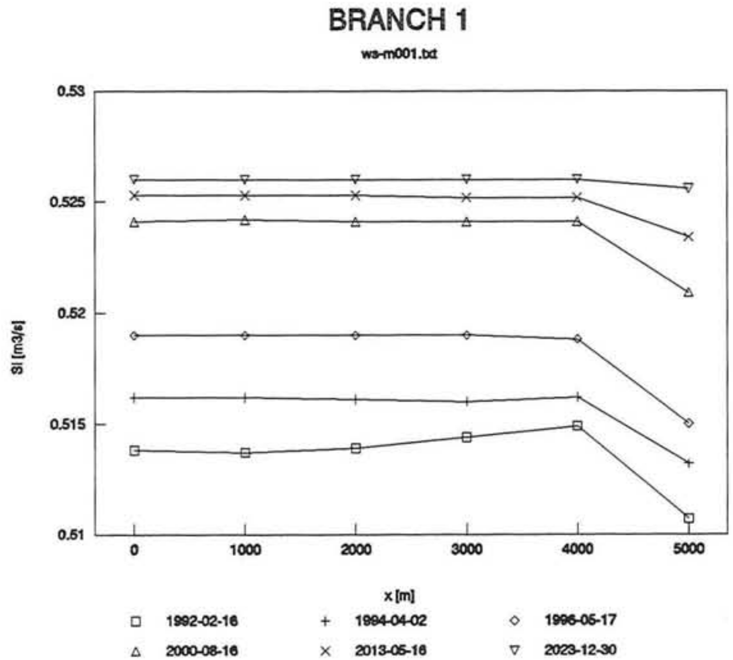

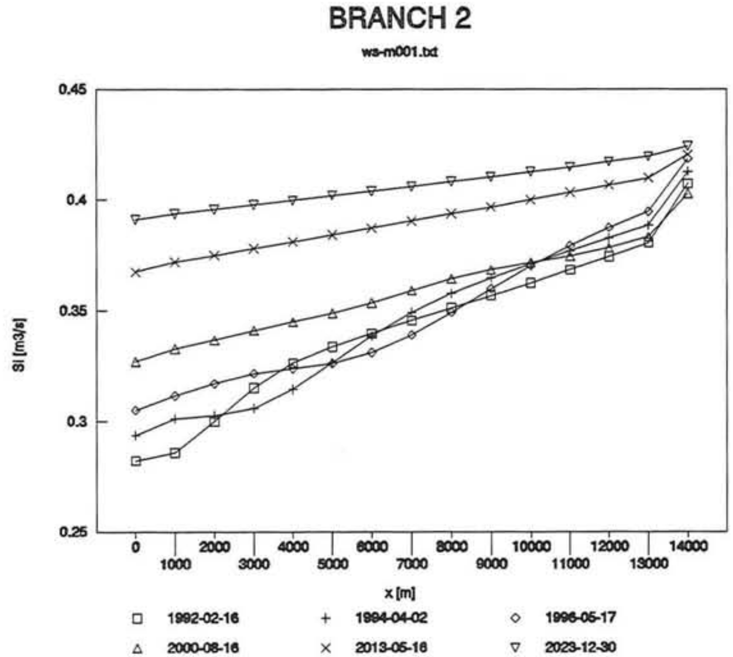

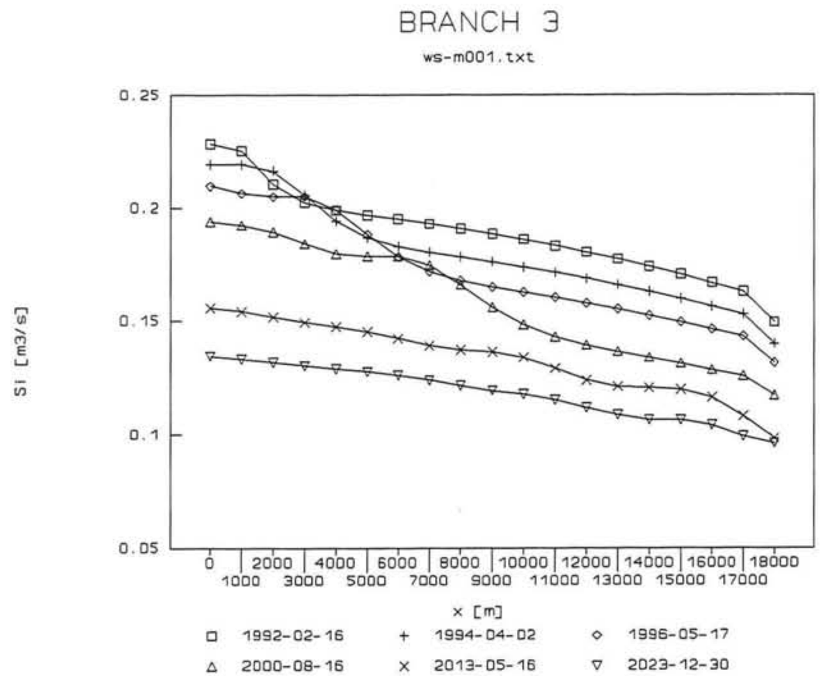

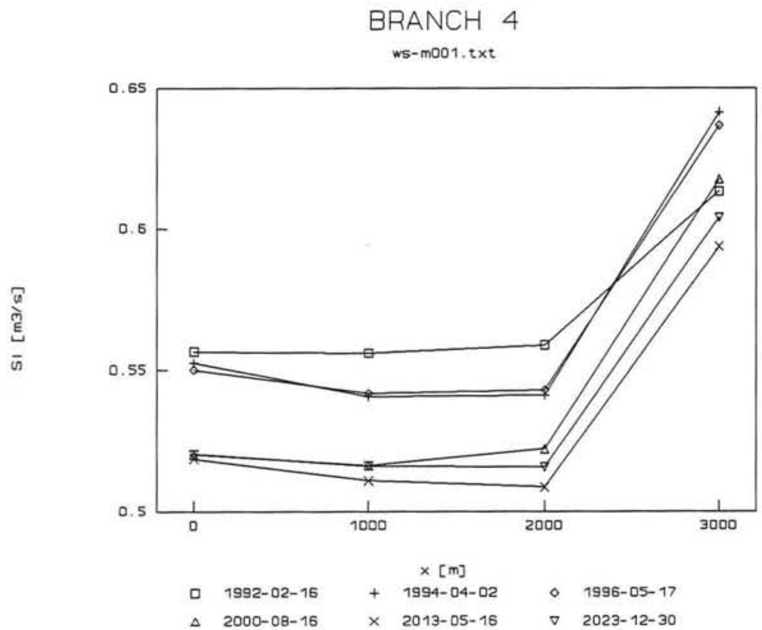

Annex 10: SOBEK computations: scenario 4

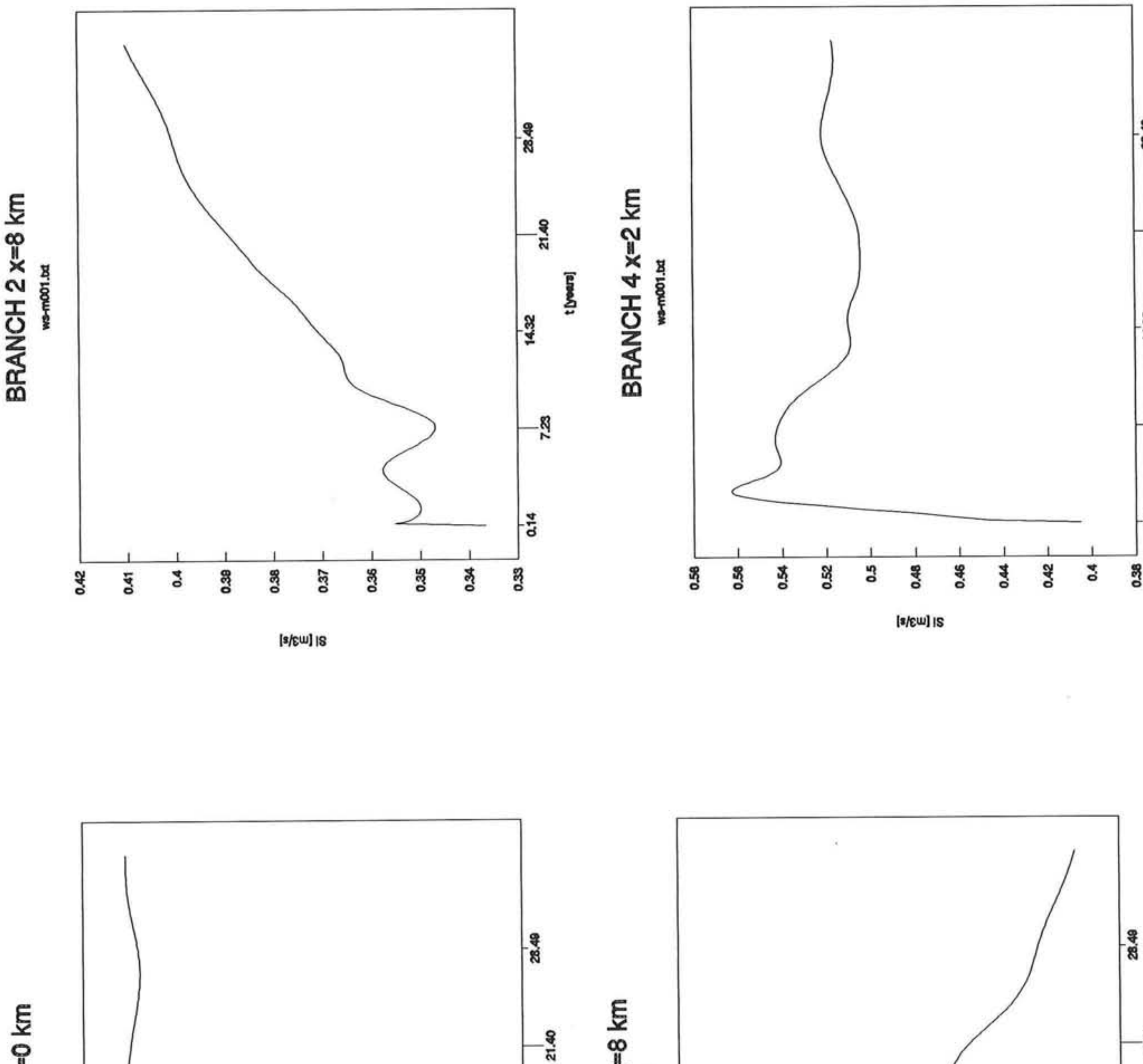

Integrated sediment transport [m^3/s]

Annex 10: SOBEK computations: scenario 4

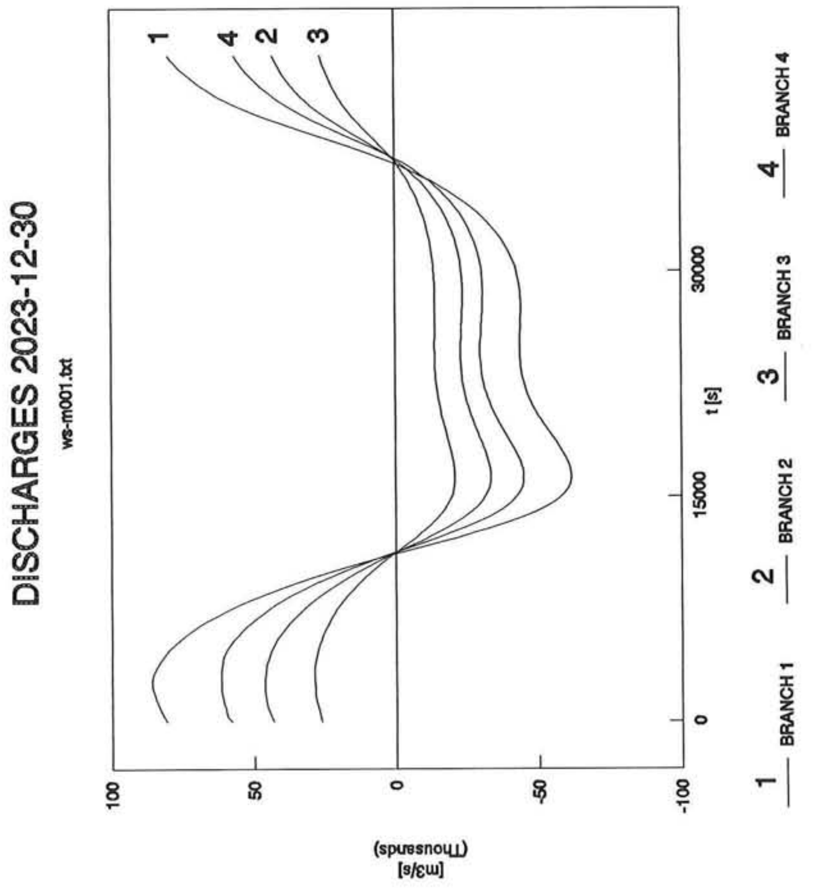

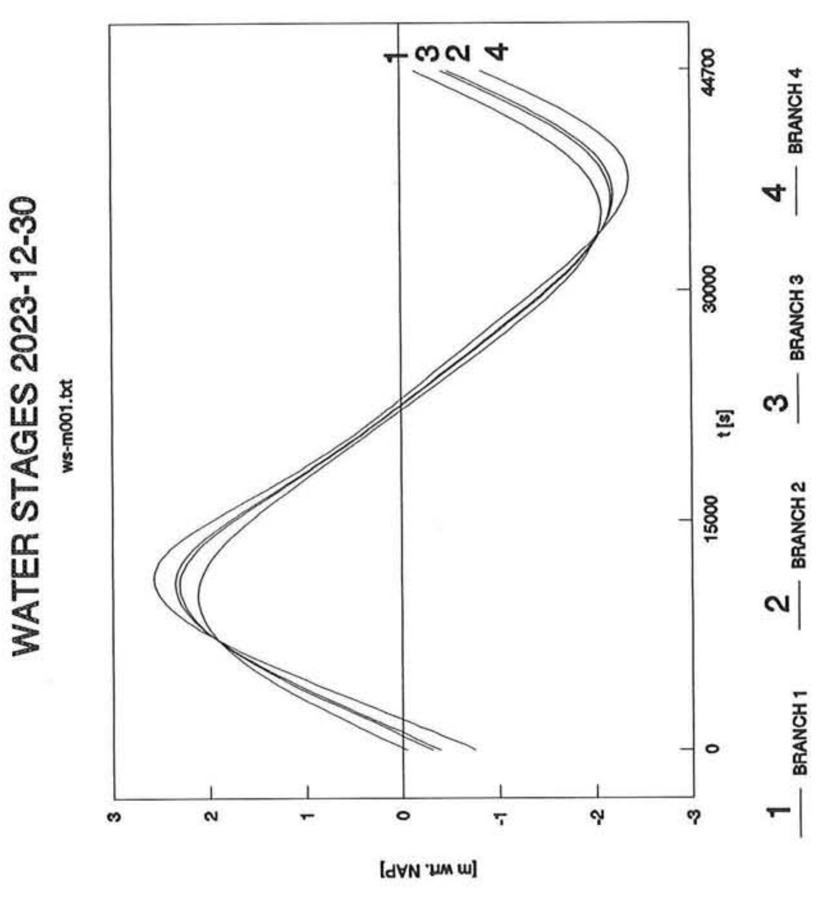

Annex 10: SOBEK computations: scenario 4

	Vflood $\cdot 10^6$ [m^3]	Vebb $\cdot 10^6$ [m^3]	Vflood-Vebb $\cdot 10^6$ [m^3]
BRANCH 1 x=4 km			
1992-02-16	1077	1069	8
2013-05-16	1076	1069	7
2023-12-30	1076	1069	7
BRANCH 2 x=8 km			
1992-02-16	501	513	-12
2013-05-16	563	567	-4
2023-12-30	581	583	-2
BRANCH 3 x=8 km			
1992-02-16	442	423	19
2013-05-16	379	367	12
2023-12-30	361	352	9
BRANCH 4 x=2 km			
1992-02-16	779	772	7
2013-05-16	778	770	8
2023-12-30	777	770	7

Table I: Volumes of water passing a channel during the ebb and flood period

	a0 [m]	h1 [m]	alfa1 [°]	h2 [m]	alfa2 [°]	h3 [m]	alfa3 [°]
BRANCH 1 x=4 km							
1992-02-16	-0.007	2.043	90.115	0.216	98.480	0.014	-66.772
2013-05-16	-0.008	2.044	90.289	0.218	98.760	0.014	-69.576
2023-12-30	-0.008	2.044	90.379	0.218	98.908	0.014	-69.871
BRANCH 2 x=8 km							
1992-02-16	-0.030	2.159	96.314	0.294	123.952	0.048	-65.729
2013-05-16	-0.029	2.160	96.306	0.300	122.905	0.048	-68.055
2023-12-30	-0.029	2.161	96.351	0.301	122.785	0.049	-68.292
BRANCH 3 x=8 km							
1992-02-16	-0.025	2.139	95.351	0.277	120.362	0.042	-65.606
2013-05-16	-0.025	2.140	95.250	0.281	119.209	0.043	-68.874
2023-12-30	-0.025	2.140	95.228	0.282	118.882	0.043	-69.140
BRANCH 4 x=2 km							
1992-02-16	-0.056	2.279	102.067	0.404	138.170	0.073	-66.782
2013-05-16	-0.053	2.277	101.618	0.407	135.839	0.073	-68.934
2023-12-30	-0.053	2.277	101.585	0.407	135.509	0.074	-69.170

Table II: Results of the harmonic analysis

Annex 10: SOBEK computations: scenario 4

	a0 [m]	h1 [m]	alfa1 [°]	h2 [m]	alfa2 [°]	h3 [m]	alfa3 [°]
BRANCH 1 x=4 km							
1992-02-16	-0.007	2.043	0.000	0.216	-81.749	0.014	-337.116
2013-05-16	-0.008	2.044	0.000	0.218	-81.819	0.014	-340.445
2023-12-30	-0.008	2.044	0.000	0.218	-81.850	0.014	-341.007
BRANCH 2 x=8 km							
1992-02-16	-0.030	2.159	0.000	0.294	-68.677	0.048	-354.672
2013-05-16	-0.029	2.160	0.000	0.300	-69.707	0.048	-356.973
2023-12-30	-0.029	2.161	0.000	0.301	-69.917	0.049	-357.346
BRANCH 3 x=8 km							
1992-02-16	-0.025	2.139	0.000	0.277	-70.339	0.042	-351.658
2013-05-16	-0.025	2.140	0.000	0.281	-71.290	0.043	-354.623
2023-12-30	-0.025	2.140	0.000	0.282	-71.573	0.043	-354.822
BRANCH 4 x=2 km							
1992-02-16	-0.056	2.279	0.000	0.404	-65.964	0.073	-12.983
2013-05-16	-0.053	2.277	0.000	0.407	-67.397	0.073	-13.788
2023-12-30	-0.053	2.277	0.000	0.407	-67.662	0.074	-13.927

Table III: The following table shows the phase difference of the M4 and M6 component compared the M2 component at that point.

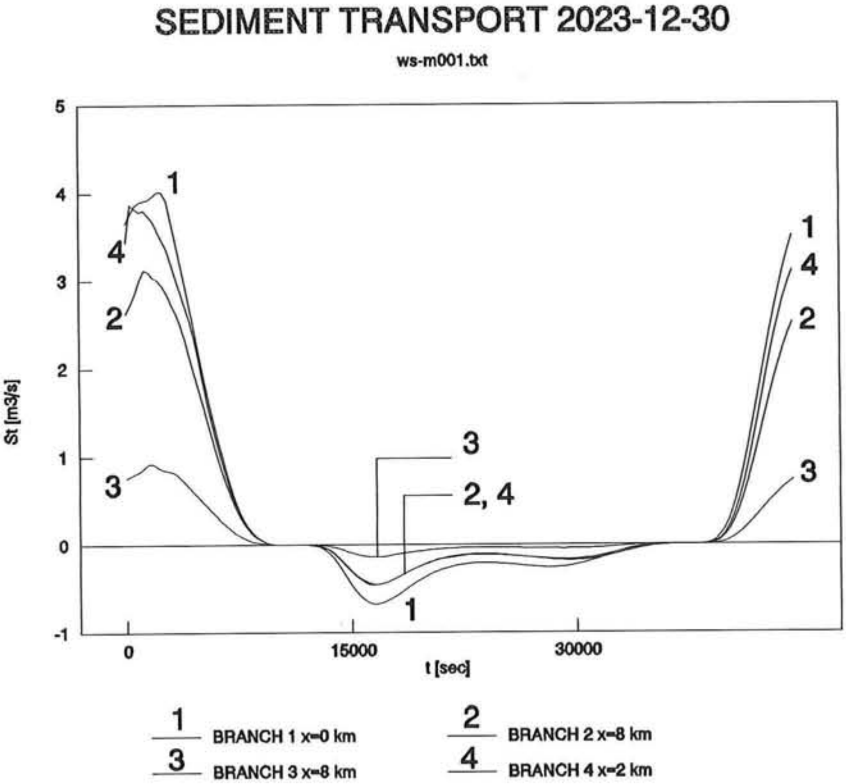

	S_{flood} [m^3]	S_{ebb} [m^3]
BRANCH 1 x=0 km	29689	6175
BRANCH 2 x=8 km	22246	3991
BRANCH 3 x=8 km	6559	1137
BRANCH 4 x=2 km	27098	4041

Table IV: Sediment transport during the flood and ebb period at the end of the calculation (2023-12-30)

Annex 11: SOBEK computations; scenario 5

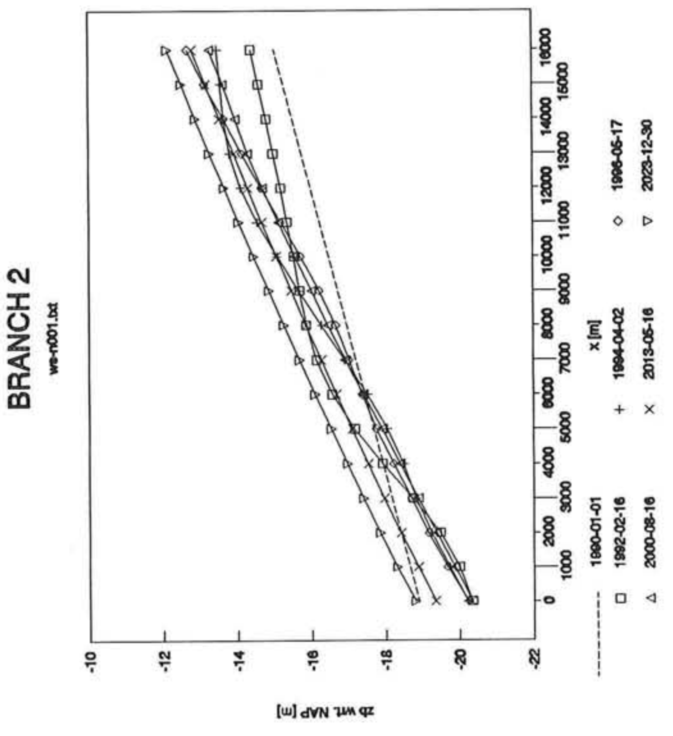
BRANCH 2
ws-n001.txt
zb wrt. NAP [m]
x [m]
1990-01-01
1992-02-16
2000-08-16
1994-04-02
2013-05-16
1996-05-17
2023-12-30

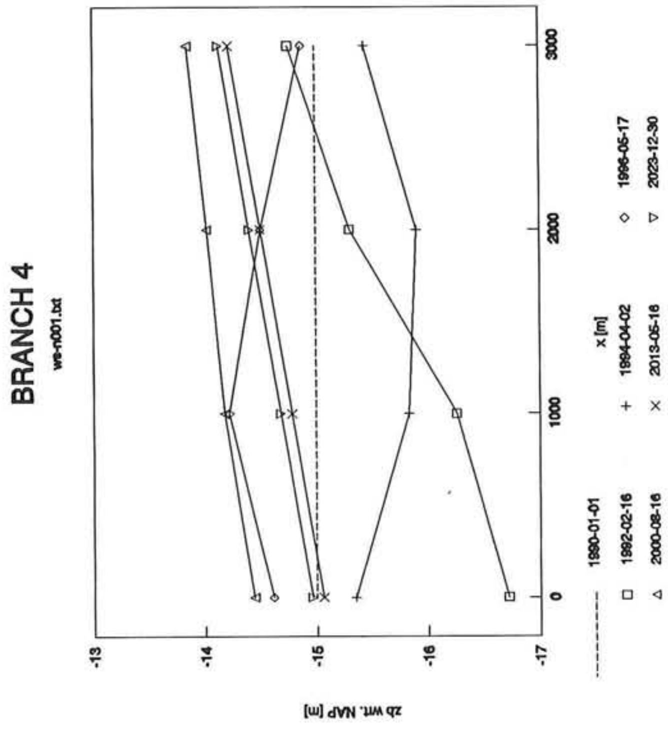
BRANCH 4
ws-n001.txt
zb wrt. NAP [m]
x [m]
1990-01-01
1992-02-16
2000-08-16
1994-04-02
2013-05-16
1996-05-17
2023-12-30

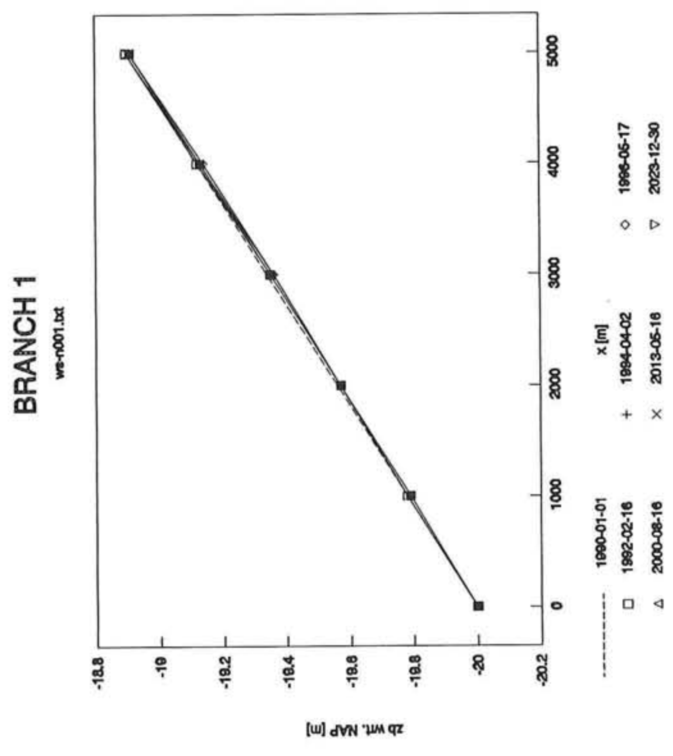
BRANCH 1
ws-n001.txt
zb wrt. NAP [m]
x [m]
1990-01-01
1992-02-16
2000-08-16
1994-04-02
2013-05-16
1996-05-17
2023-12-30

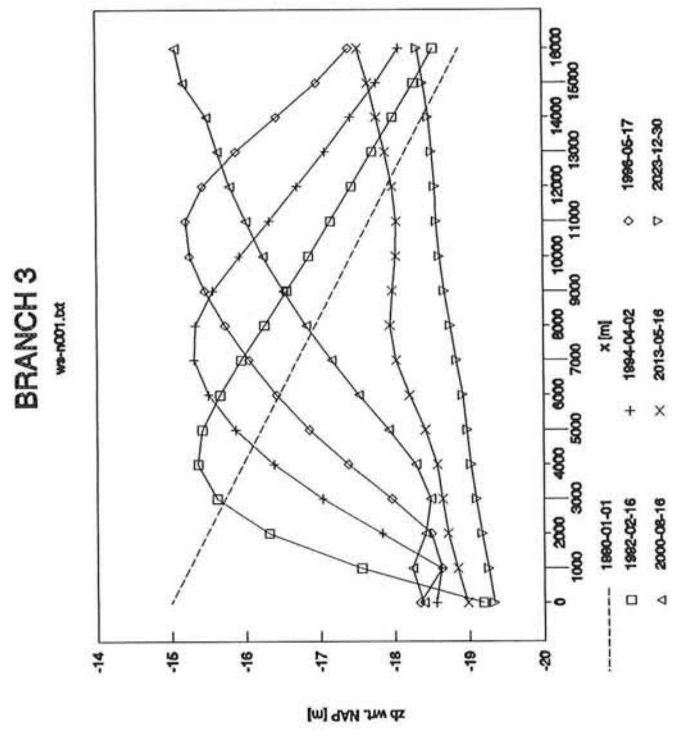
BRANCH 3
ws-n001.txt
zb wrt. NAP [m]
x [m]
1990-01-01
1992-02-16
2000-08-16
1994-04-02
2013-05-16
1996-05-17
2023-12-30

Bed level

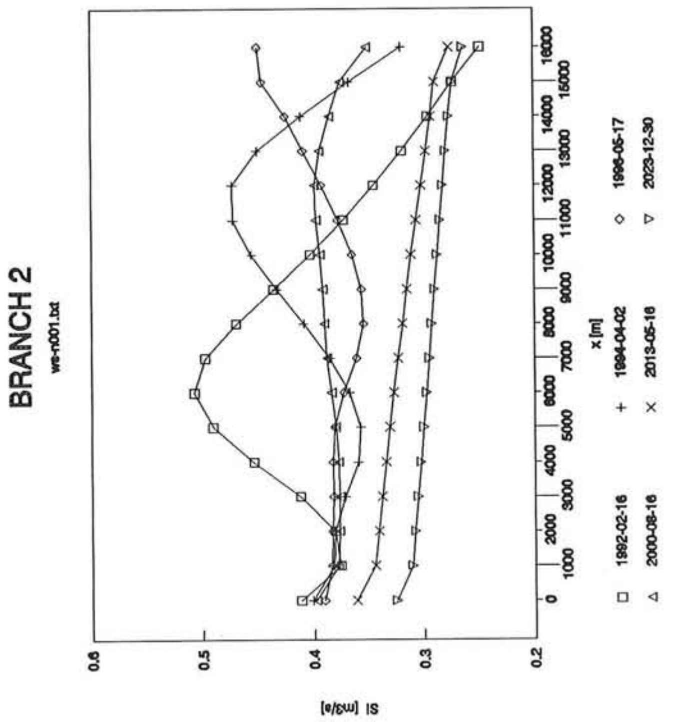

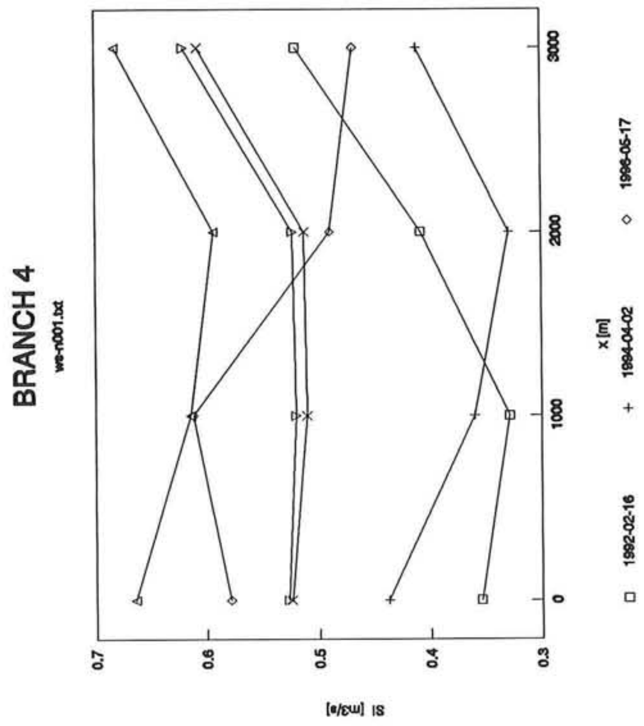

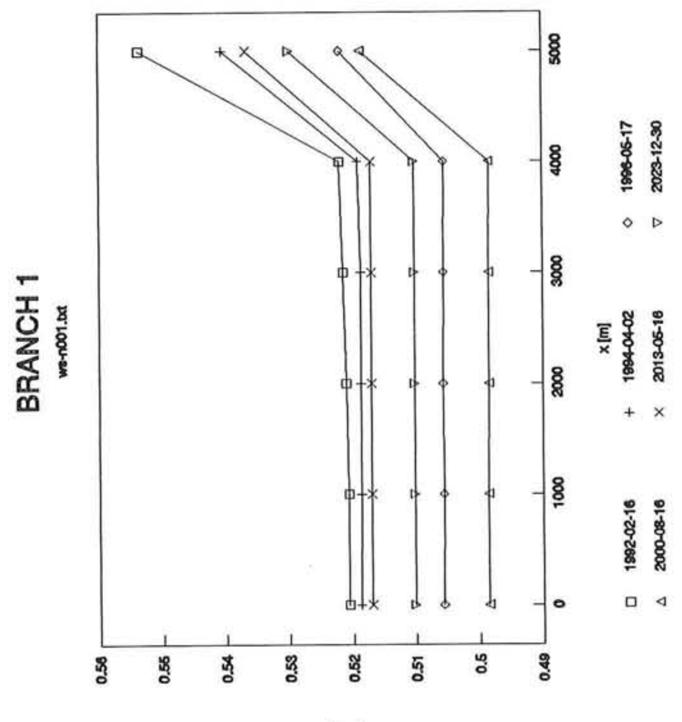

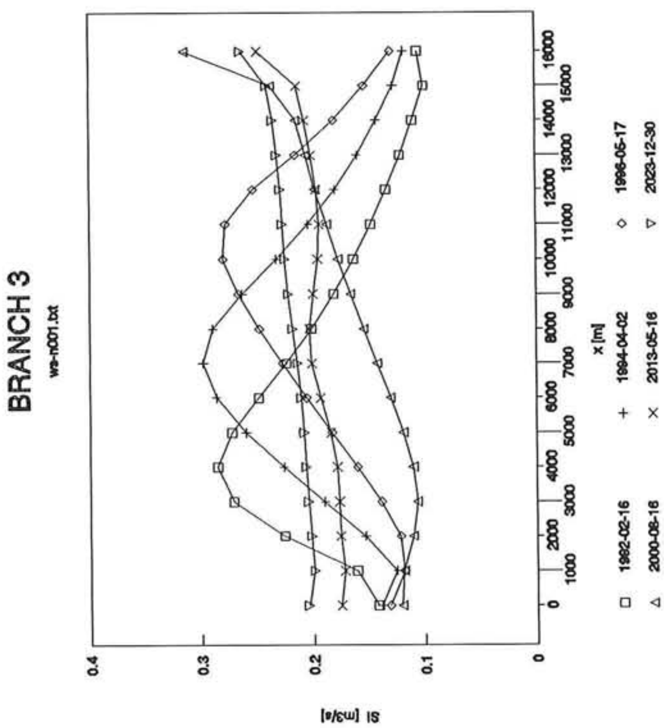

Integrated sediment transport [m^3/s]

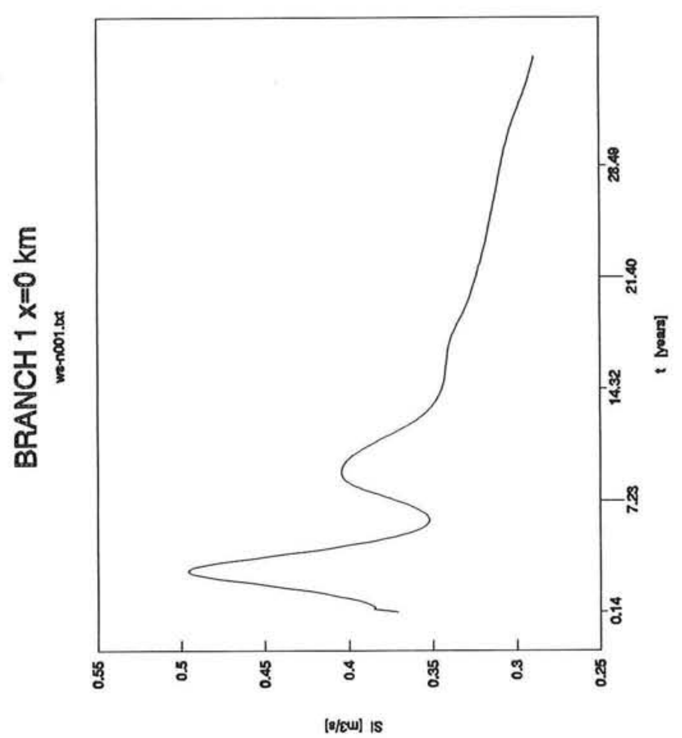

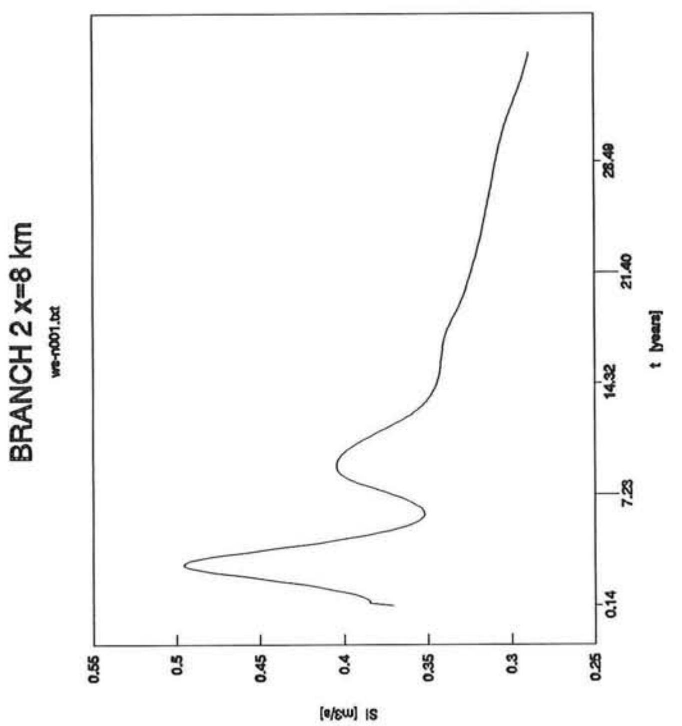

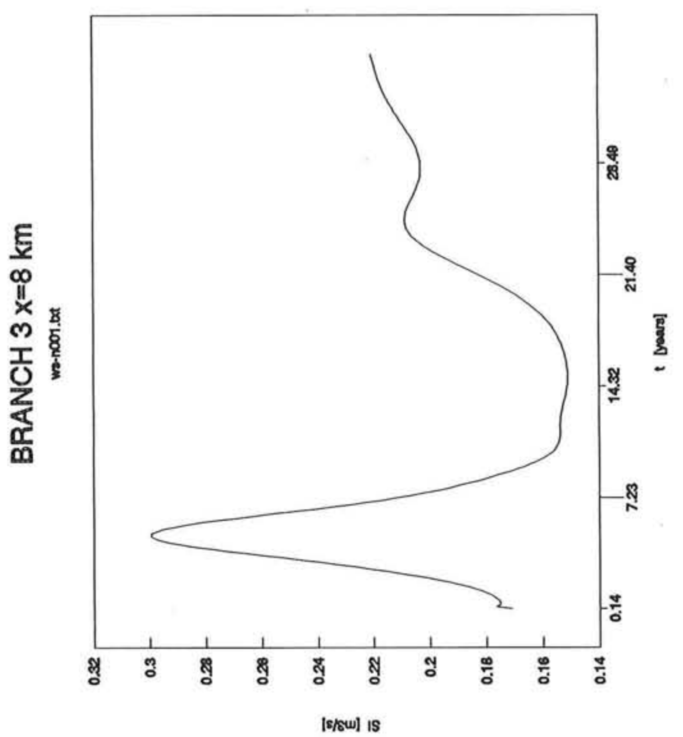

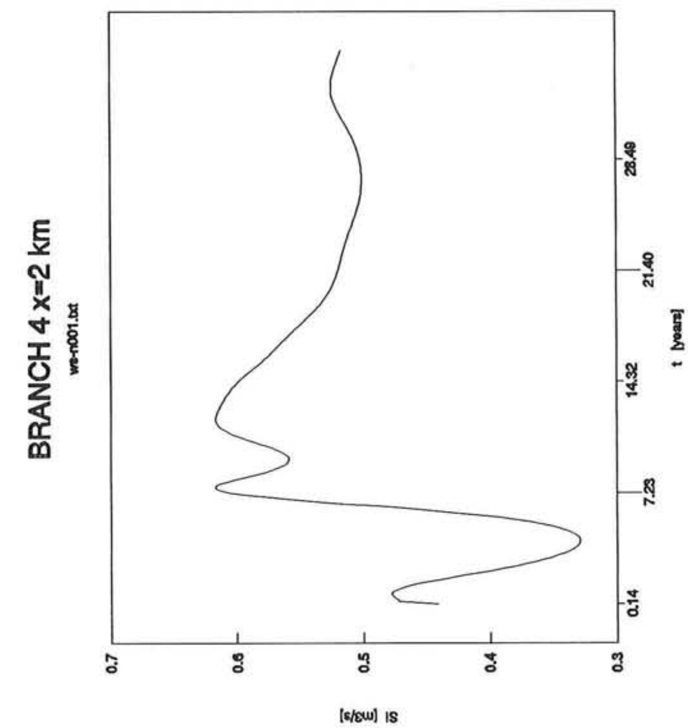

Integrated sediment transport [m^3/s]

WATER STAGES 2023-12-30

ws-n001.txt

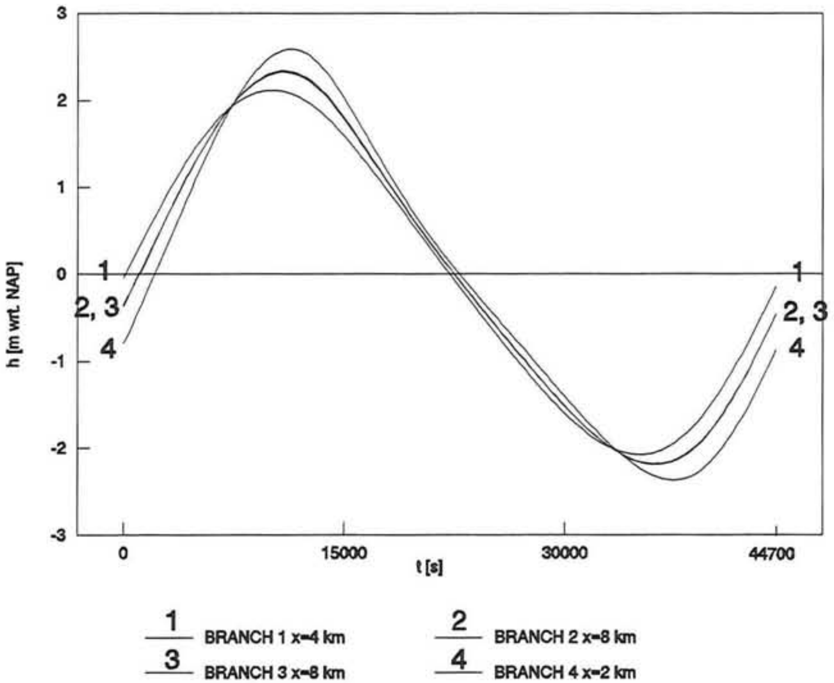

DISCHARGES 2023-12-30

ws-n001.txt

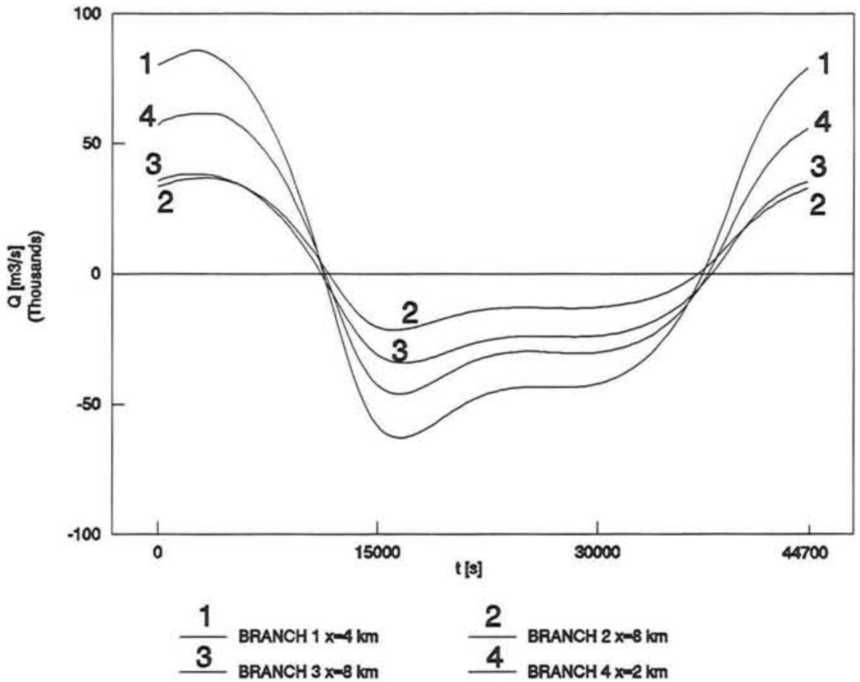

	Vflood $\cdot 10^6$ m^3	Vebb $\cdot 10^6$ m^3	Vflood-Vebb $\cdot 10^6$ m^3
BRANCH 1 x=4000 m			
1992-02-16	1080	1073	7
2013-05-16	1080	1073	7
2023-12-30	1079	1072	7
BRANCH 2 x=8000 m			
1992-02-16	538	395	143
2013-05-16	498	354	144
2023-12-30	473	334	139
BRANCH 3 x=8000 m			
1992-02-16	410	546	-46
2013-05-16	450	586	-136
2023-12-30	474	606	-132
BRANCH 4 x=2000 m			
1992-02-16	782	775	7
2013-05-16	781	774	7
2023-12-30	781	773	8

Table I: Volumes of water that passes a channel during the ebb and flood period

	a0 [m]	h1 [m]	alfa1 [°]	h2 [m]	alfa2 [°]	h3 [m]	alfa3 [°]
BRANCH 1 x=4 km							
1992-02-16	-0.007	2.043	90.132	0.214	98.748	0.014	-65.366
2013-05-16	-0.007	2.044	90.305	0.216	98.939	0.014	-63.970
2023-12-30	-0.007	2.044	90.396	0.216	99.057	0.015	-62.420
BRANCH 2 x=8 km							
1992-02-16	-0.031	2.154	96.331	0.289	124.829	0.048	-65.931
2013-05-16	-0.028	2.156	95.922	0.288	122.711	0.048	-63.247
2023-12-30	-0.028	2.156	95.959	0.286	122.764	0.049	-62.142
BRANCH 3 x=8 km							
1992-02-16	-0.040	2.151	96.715	0.294	126.242	0.045	-71.799
2013-05-16	-0.031	2.149	95.681	0.286	122.041	0.045	-65.286
2023-12-30	-0.031	2.149	95.791	0.285	122.253	0.045	-63.567
BRANCH 4 x=2 km							
1992-02-16	-0.056	2.287	102.249	0.410	139.201	0.073	-64.957
2013-05-16	-0.061	2.288	101.936	0.410	138.231	0.076	-65.283
2023-12-30	-0.064	2.288	102.048	0.408	138.631	0.077	-64.232

Table II: Results of the harmonic analysis

Annex 11: SOBEK computations: scenario 5

	a0 [m]	h1 [m]	alfa1 [°]	h2 [m]	alfa2 [°]	h3 [m]	alfa3 [°]
BRANCH 1 x=4 km							
1992-02-16	-0.007	2.043	0.000	0.214	-81.515	0.014	-335.760
2013-05-16	-0.007	2.044	0.000	0.216	-81.672	0.014	-334.885
2023-12-30	-0.007	2.044	0.000	0.216	-81.734	0.015	-333.606
BRANCH 2 x=8 km							
1992-02-16	-0.031	2.154	0.000	0.289	-67.833	0.048	-354.924
2013-05-16	-0.028	2.156	0.000	0.288	-69.133	0.048	-351.013
2023-12-30	-0.028	2.156	0.000	0.286	-69.153	0.049	-350.018
BRANCH 3 x=8 km							
1992-02-16	-0.040	2.151	0.000	0.294	-67.188	0.045	-1.945
2013-05-16	-0.031	2.149	0.000	0.286	-69.321	0.045	-352.329
2023-12-30	-0.031	2.149	0.000	0.285	-69.329	0.045	-350.940
BRANCH 4 x=2 km							
1992-02-16	-0.056	2.287	0.000	0.410	-65.296	0.073	-11.703
2013-05-16	-0.061	2.288	0.000	0.410	-65.642	0.076	-11.092
2023-12-30	-0.064	2.288	0.000	0.408	-65.464	0.077	-10.375

Table III: The following table shows the phase difference between the M4 and M2, and M6 and M2 component at that point.

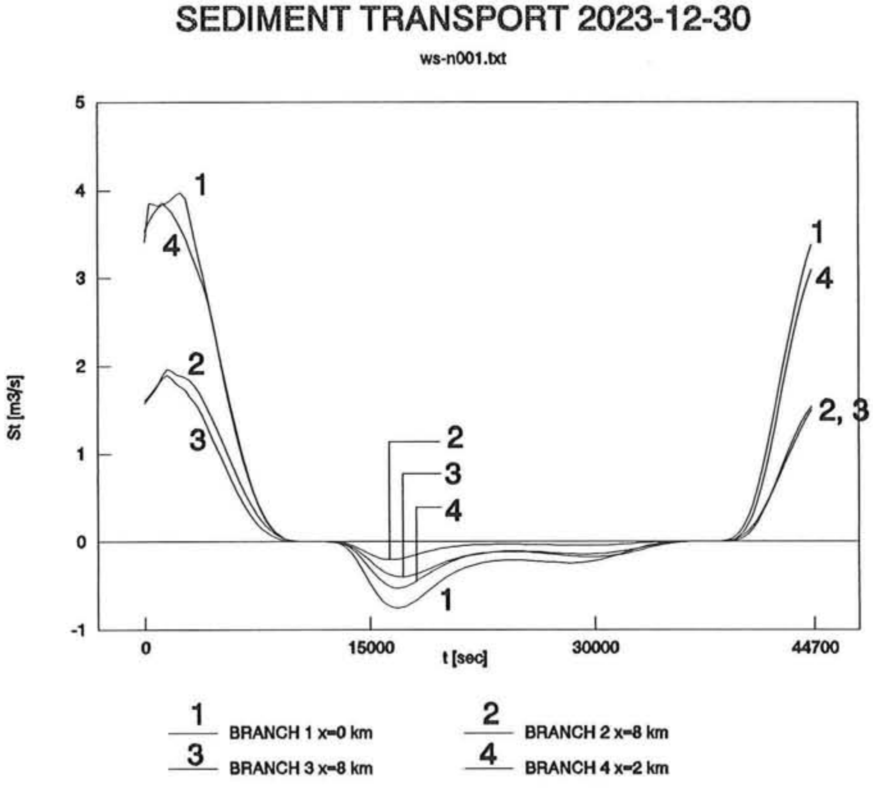

	S_{flood} [m^3]	S_{ebb} [m^3]
BRANCH 1 x=0 km	29340	6532
BRANCH 2 x=8 km	14426	1372
BRANCH 3 x=8 km	13393	3624
BRANCH 4 x=2 km	27758	4396

Table IV: Sediment transport during the flood and ebb period at the end of the calculation (2023-12-30)

Annex 12: SOBEK computations; scenario 6

Annex 12: SOBEK computations: scenario 6

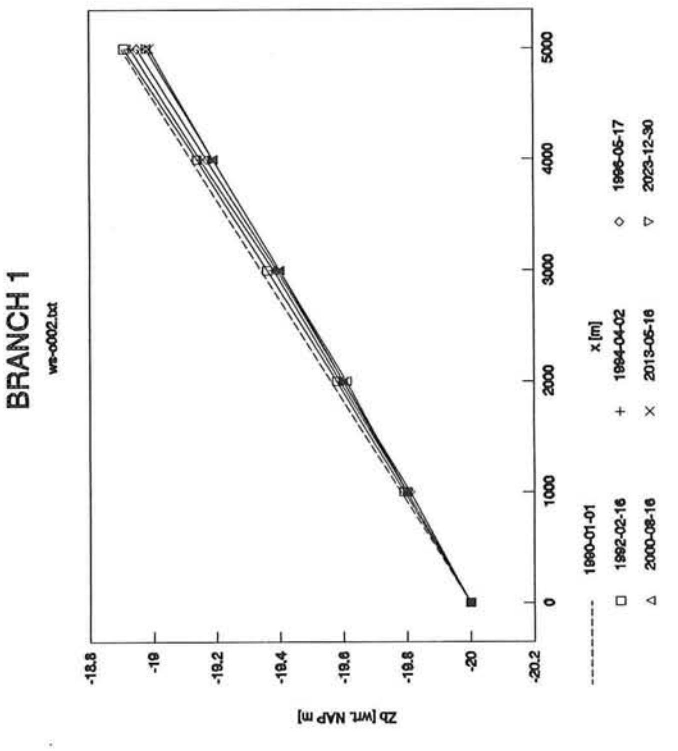

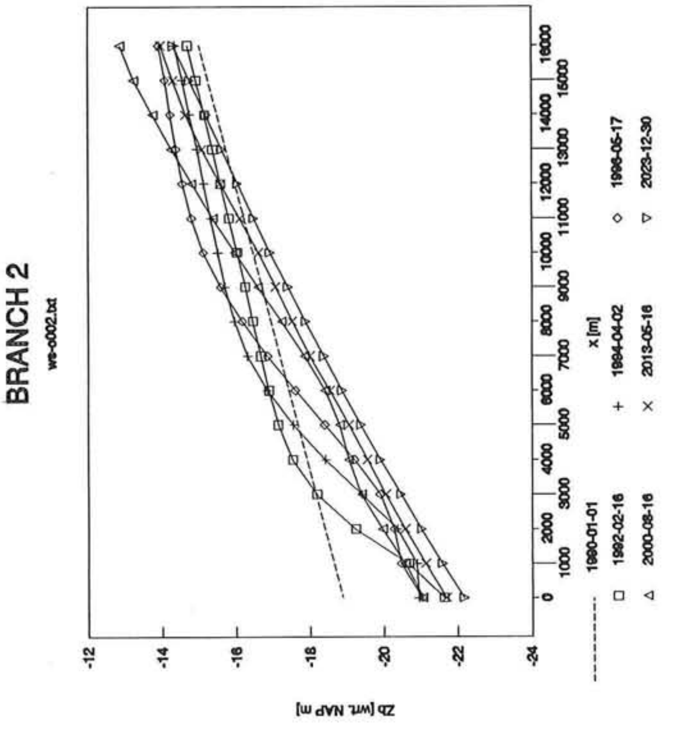

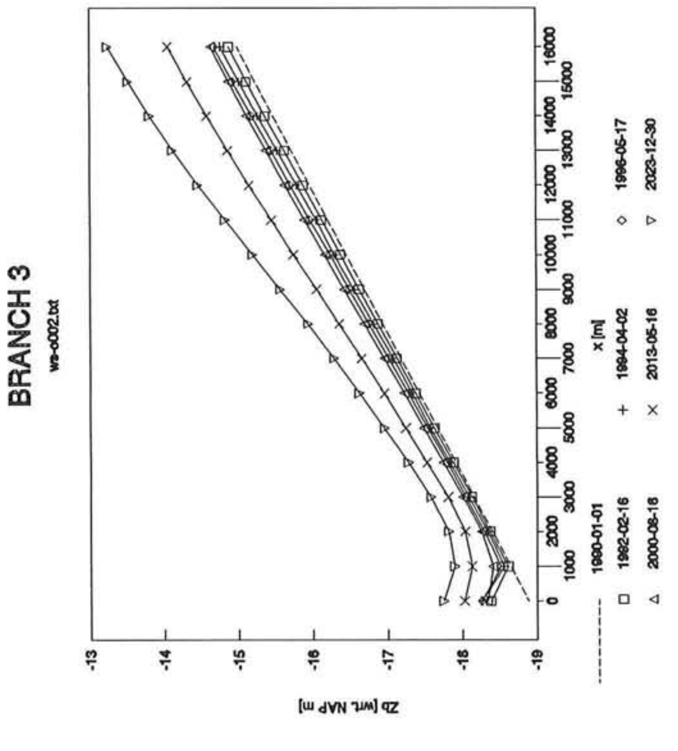

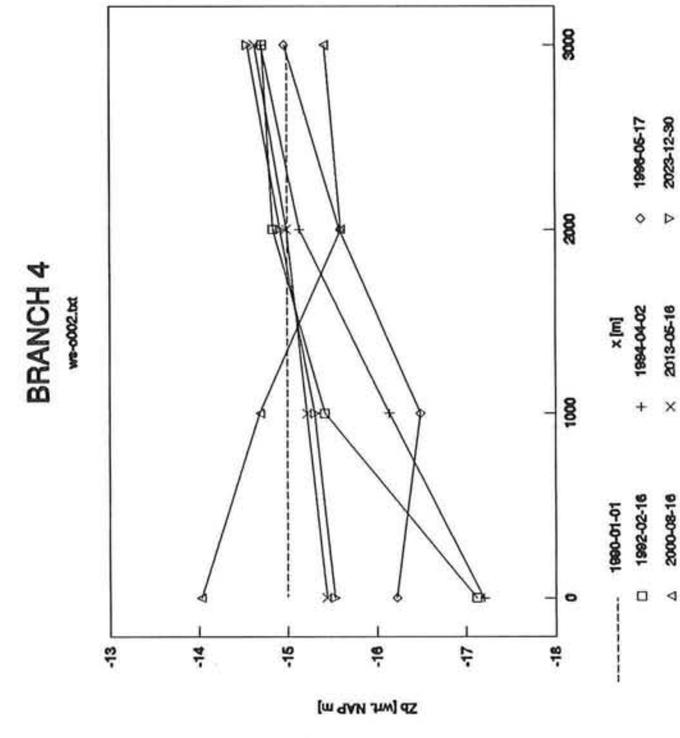

Bed level

Integrated sediment transport [m^3/s]

BRANCH 1

ws-o002.txt

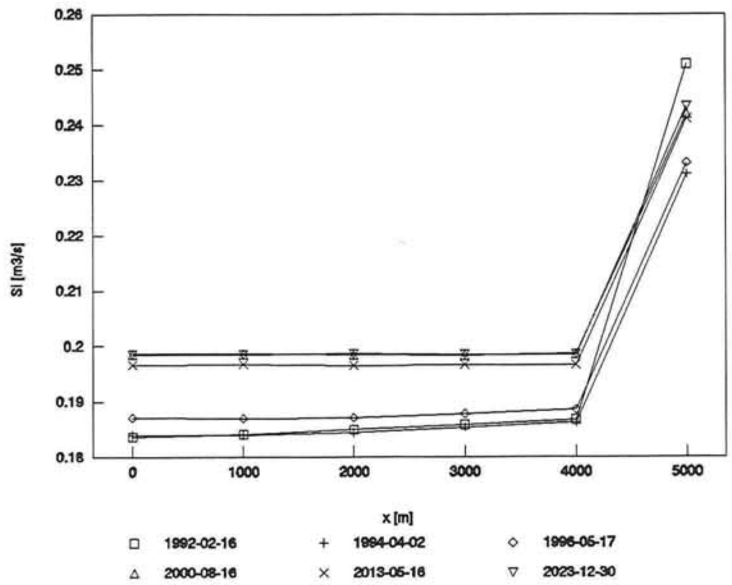

BRANCH 2

ws-o002.txt

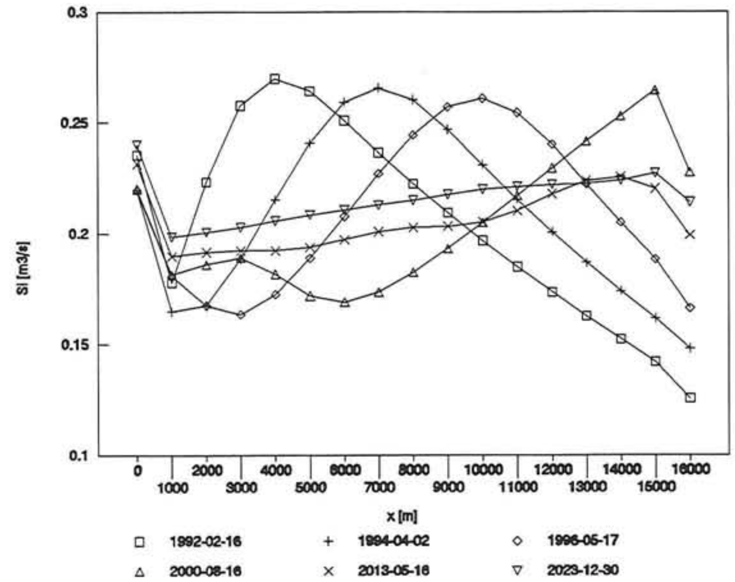

BRANCH 3

ws-o002.txt

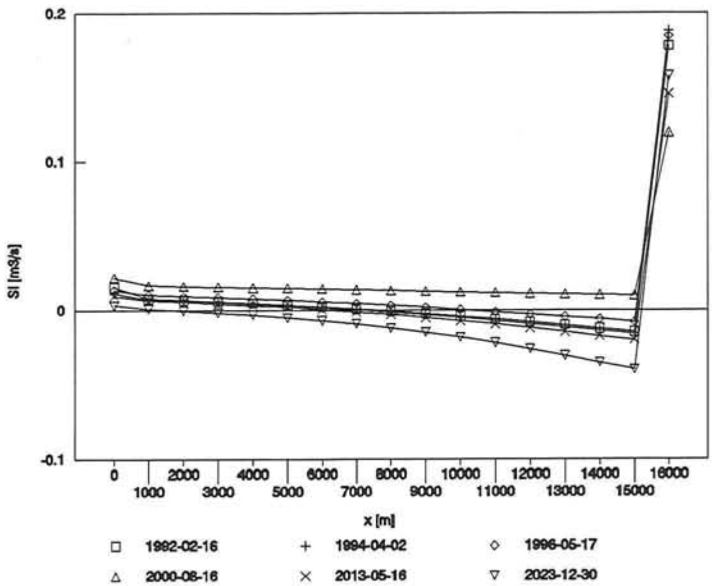

BRANCH 4

ws-o002.txt

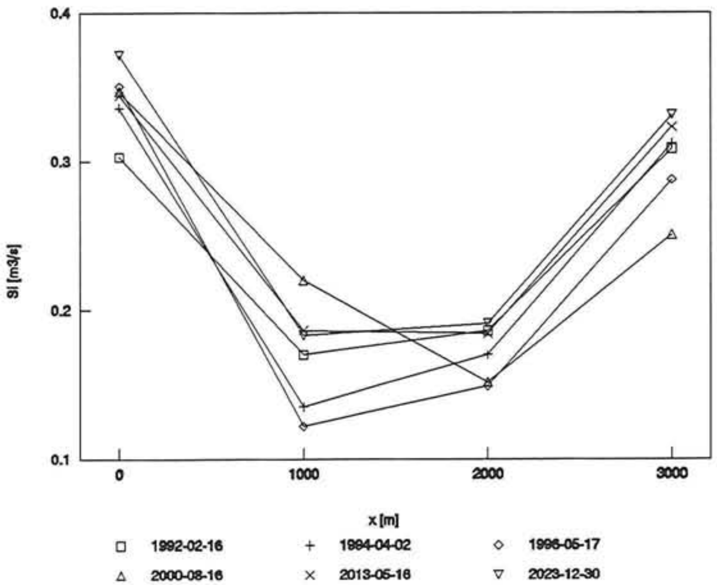

Annex 12: SOBEK computations: scenario 6

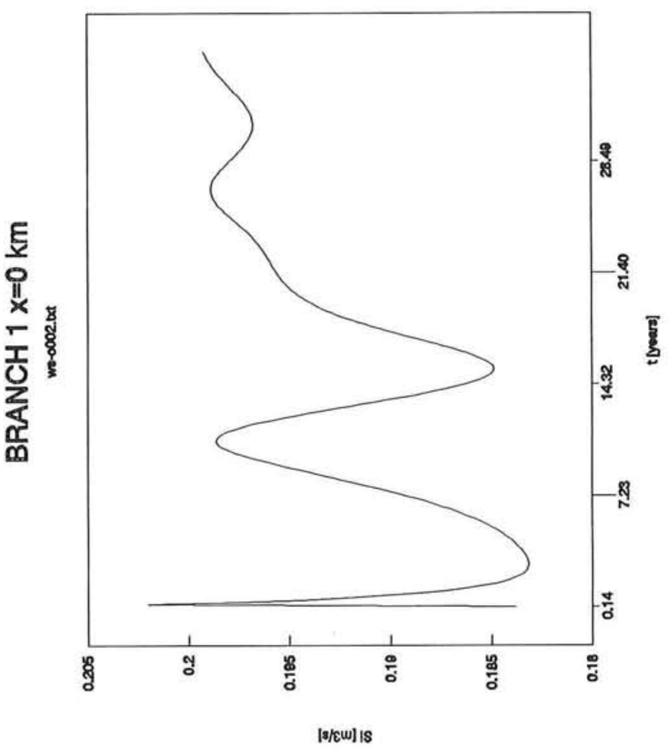

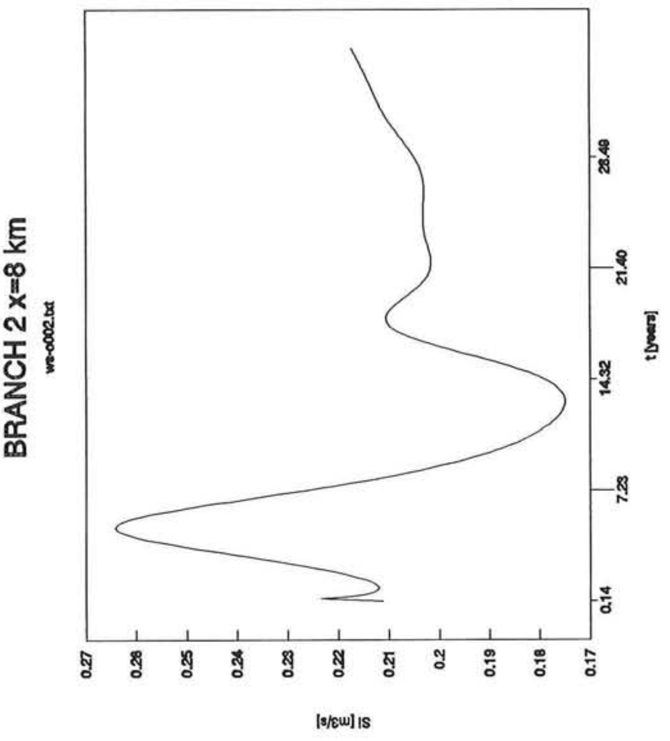

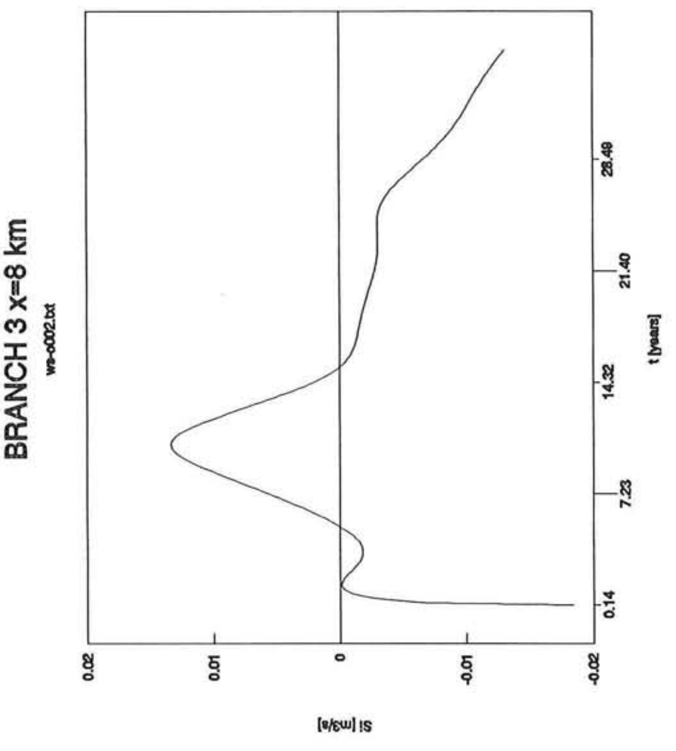

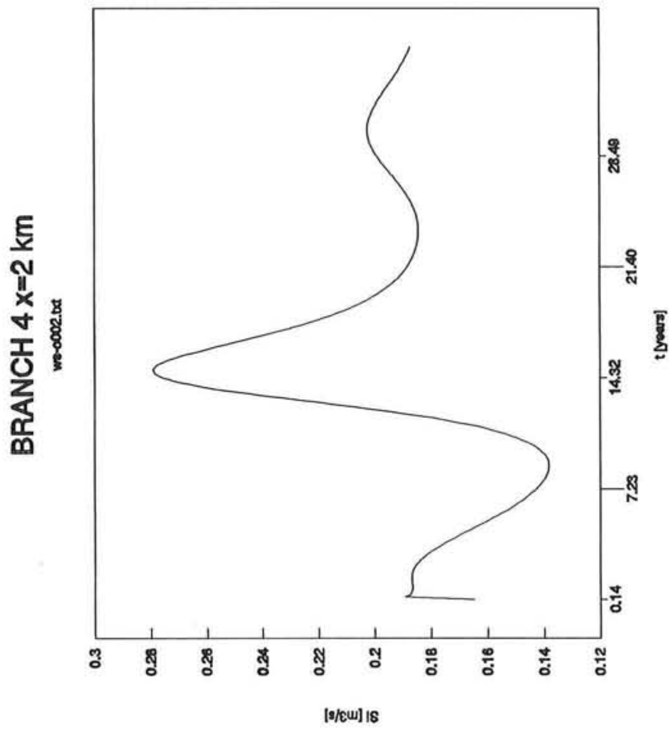

Integrated sediment transport [m^3/s]

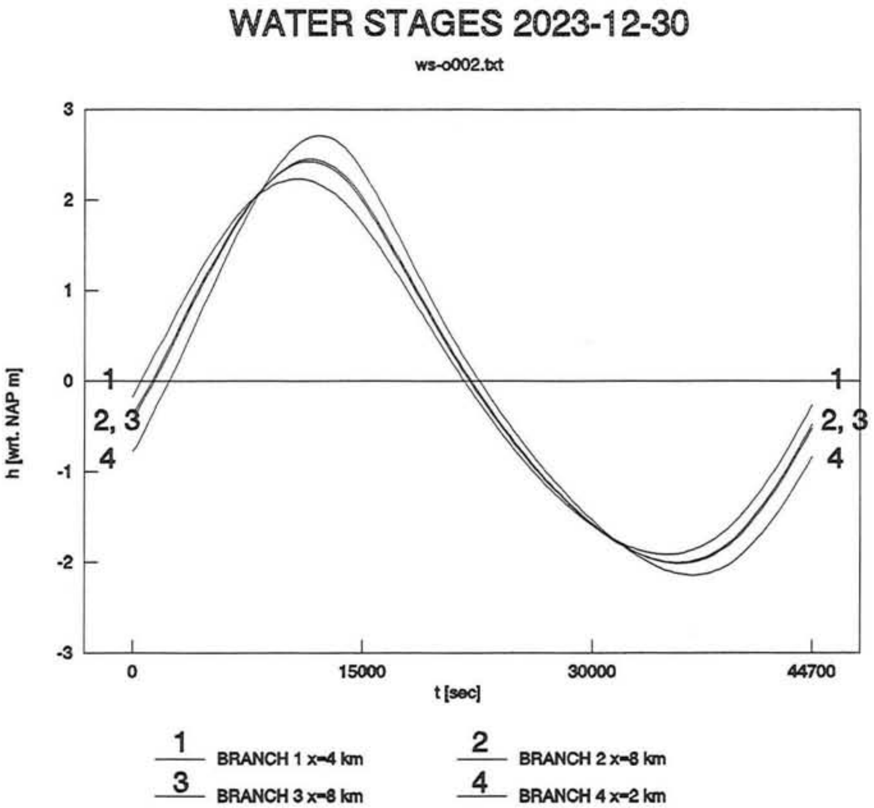
WATER STAGES 2023-12-30
ws-o002.txt
h [wrt. NAP m]
3
2
1
0
-1
-2
-3
0
15000
30000
44700
t [sec]
1
2, 3
4
1 BRANCH 1 x=4 km
2 BRANCH 2 x=8 km
3 BRANCH 3 x=8 km
4 BRANCH 4 x=2 km

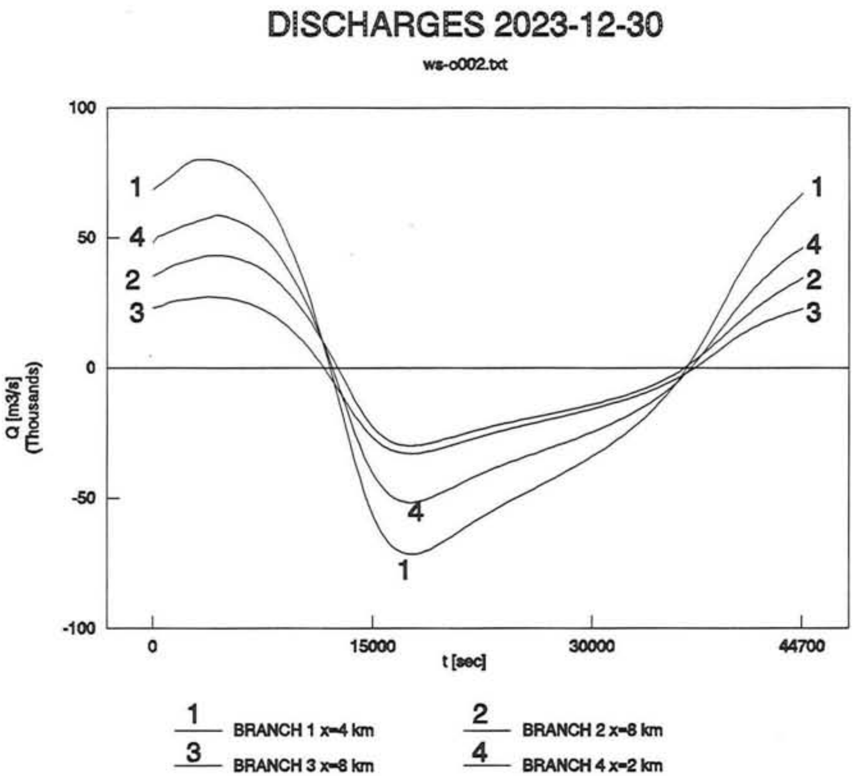
DISCHARGES 2023-12-30
ws-o002.txt
Q [m3/s]
(Thousands)
100
50
0
-50
-100
0
15000
30000
44700
t [sec]
1
4
2
3
1 BRANCH 1 x=4 km
2 BRANCH 2 x=8 km
3 BRANCH 3 x=8 km
4 BRANCH 4 x=2 km

Annex 12: SOBEK computations: scenario 6

	Vflood $\cdot 10^6\ m^3$	Vebb $\cdot 10^6\ m^3$	Vflood-Vebb $\cdot 10^6\ m^3$
BRANCH 1 x = 4000 m			
1992-02-16	1061	1052	9
2013-05-16	1060	1052	8
2023-12-30	1060	1051	9
BRANCH 2 x = 8000 m			
1992-02-16	537	384	153
2013-05-16	559	408	151
2023-12-30	576	425	151
BRANCH 3 x = 8000 m			
1992-02-16	393	537	-144
2013-05-16	370	512	-142
2023-12-30	353	495	-142
BRANCH 4 x = 2000 m			
1992-02-16	765	756	9
2013-05-16	764	756	8
2023-12-30	764	756	8

Table I: Volumes of water that passes a channel during the ebb and flood period

	a0 [m]	h1 [m]	alfa1 [°]	h2 [m]	alfa2 [°]	h3 [m]	alfa3 [°]
BRANCH 1 x=4 km							
1992-02-16	-0.002	2.047	90.069	0.213	142.335	0.015	-52.689
2013-05-16	-0.002	2.047	90.241	0.214	142.535	0.015	-55.084
2023-12-30	-0.002	2.047	90.333	0.214	142.712	0.015	-55.016
BRANCH 2 x=8 km							
1992-02-16	-0.015	2.165	96.064	0.267	161.866	0.054	-54.483
2013-05-16	-0.009	2.164	95.609	0.266	159.632	0.052	-54.812
2023-12-30	-0.008	2.164	95.774	0.266	159.828	0.053	-54.734
BRANCH 3 x=8 km							
1992-02-16	-0.010	2.155	94.904	0.259	158.421	0.049	-52.683
2013-05-16	-0.010	2.154	94.893	0.262	157.751	0.049	-54.887
2023-12-30	-0.009	2.153	94.846	0.261	157.503	0.049	-54.357
BRANCH 4 x=2 km							
1992-02-16	-0.030	2.299	101.402	0.344	173.035	0.091	-55.833
2013-05-16	-0.024	2.301	101.533	0.345	171.843	0.091	-57.292
2023-12-30	-0.024	2.301	101.689	0.346	171.897	0.091	-57.172

Table II: Results of the harmonic analysis

	a0 [m]	h1 [m]	alfa1 [°]	h2 [m]	alfa2 [°]	h3 [m]	alfa3 [°]
BRANCH 1 x=4 km							
1992-02-16	-0.002	2.047	0.000	0.213	-37.803	0.015	-322.896
2013-05-16	-0.002	2.047	0.000	0.214	-37.946	0.015	-325.806
2023-12-30	-0.002	2.047	0.000	0.214	-37.954	0.015	-326.015
BRANCH 2 x=8 km							
1992-02-16	-0.015	2.165	0.000	0.267	-30.262	0.054	-342.674
2013-05-16	-0.009	2.164	0.000	0.266	-31.587	0.052	-341.640
2023-12-30	-0.008	2.164	0.000	0.266	-31.721	0.053	-342.056
BRANCH 3 x=8 km							
1992-02-16	-0.010	2.155	0.000	0.259	-31.386	0.049	-337.395
2013-05-16	-0.010	2.154	0.000	0.262	-32.036	0.049	-339.567
2023-12-30	-0.009	2.153	0.000	0.261	-32.188	0.049	-338.895
BRANCH 4 x=2 km							
1992-02-16	-0.030	2.299	0.000	0.344	-29.769	0.091	-0.039
2013-05-16	-0.024	2.301	0.000	0.345	-31.223	0.091	-1.891
2023-12-30	-0.024	2.301	0.000	0.346	-31.482	0.091	-2.240

Table III: The following table shows the phase difference between the M4 and M2, and M6 and M2 component at that point.

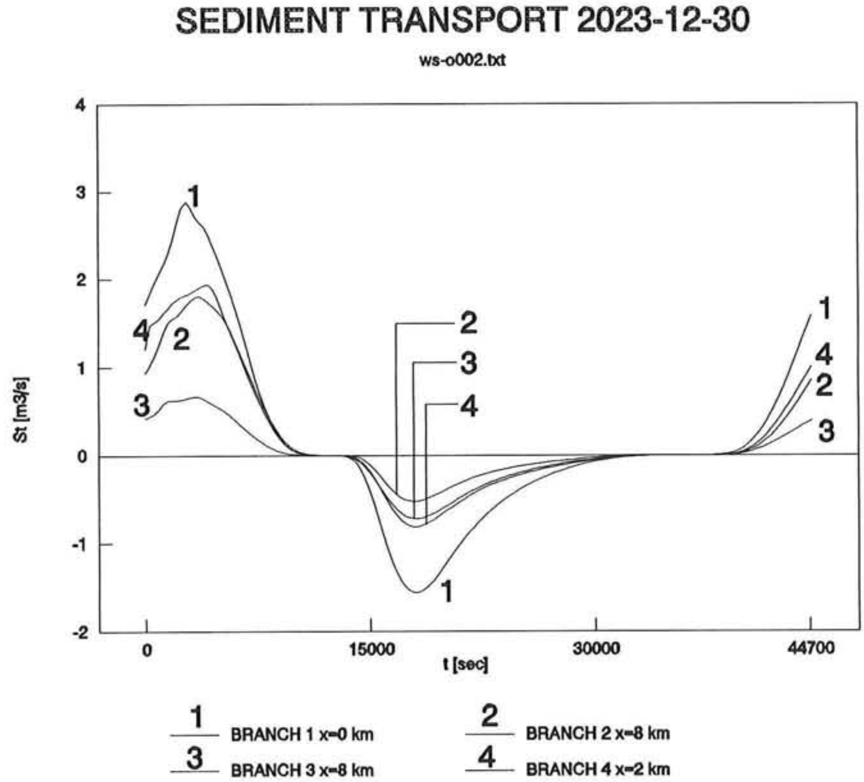

	S_{flood} [m^3]	S_{ebb} [m^3]
BRANCH 1 x=0 km	20254	11376
BRANCH 2 x=8 km	13290	3671
BRANCH 3 x=8 km	4967	5498
BRANCH 4 x=2 km	14566	6042

Table VI: Sediment transport during the flood and ebb period at the end of the calculation (2023-12-30)